A Pilot-scale Evaluation of Soluble Manganese Removal Using Pyrolucite Media in a High-Rate Adsorptive Contactor

Archana Subramaniam

Thesis submitted to the faculty of the Virginia Polytechnic Institute and State University in partial fulfillment of the requirements for the degree of

Master of Science

In

Environmental Engineering

William R. Knocke
John C. Little
Daniel L. Gallagher

February 1, 2010
Blacksburg, VA

Keywords: manganese, adsorption, pyrolucite media, MnO_x(s)-coated media, water treatment

A Pilot-scale Evaluation of Soluble Manganese Removal Using Pyrolucite Media in a High-Rate Adsorptive Contactor

Archana Subramaniam

ABSTRACT

Soluble manganese (Mn) is a common water contaminant which can cause discoloration of water and staining if not treated properly in a water treatment plant. The "natural greensand effect" is one of the proven methods for efficient removal of Mn from water. Therefore, research is ongoing to develop different ways to effectively create the natural greensand effect in a post-filtration sorptive contactor for application at water treatment facilities.

The research reported by Zuravnsky (2007) focused on the use of oxide-coated media in a post-filtration contactor and served as a starting point for the research reported in this thesis. As a part of the work conducted by Zuravnsky (2007), a preliminary model was formulated to predict soluble Mn removal via adsorption and oxidation onto large-size MnO_x(s)-coated media. A major part of the current research was to calibrate the proposed model in predicting the soluble Mn removal performance by incorporating a statistical non-linear regression method to estimate a best-fit value for the fitting parameter k_r, the rate constant associated with Mn oxidation by free chlorine.

The research work included an 18-week pilot-plant study conducted at a water treatment facility in Newport News, VA. A contactor column loaded with 27" of pyrolucite media was operated at varying applied water conditions. Hydraulic loading rate (HLR), temperature, pH and influent free chlorine concentration were the operational parameters that were varied and their effect on the Mn removal performance evaluated. The resulting data were then used in the model to aid in its calibration and to obtain the best-fit k_r values corresponding to effective Mn removal for the various operating conditions.

Soluble Mn removal in the contactor column was directly dependent on solution pH and initial free chlorine concentration. The applied water temperature and HLR also had a small impact on the Mn removal profiles observed. On analyzing the results obtained from the model, it was noted that the best-fit k_r values for the pilot plant data increased with increasing solution pH (When temperature = 20^0C and the initial Cl levels were below 1.5mg/L). Also, the Mn uptake capacity of the pyrolucite media increased with both an increase in initial Mn concentration and solution temperature. Long-term operation of the contactor also resulted in significant head loss accumulation in the upper portion of the contactor column, most probably due to MnOx(s) deposition on the media and partial blockage of contactor void spaces. Media fluidization was necessary to address this operational issue.

ACKNOWLEDGEMENTS

I would like to thank my advisor Dr. William Knocke for his valuable guidance and support throughout this research work and my graduate study. His encouragement and enthusiasm inspired me to strive better. I am also extremely grateful to him for funding me and keeping me financially stable throughout my study at Virginia Tech.

I would also like to thank my committee members, Dr. John Little and Dr. Daniel Gallagher, for their valuable inputs and timely guidance.

I am grateful to Mr Randall Hawkins and Mr Scott Dewhirst for their invaluable help with the pilot plant setup and sample collection. Without their assistance, I may not have had any data for my research.

Thank you to Ms Athena Tilley in the soils testing lab for helping me out with the ICP-MS analysis for my water samples.

I would like to acknowledge the Edna Bailey Sussman Foundation for providing funding for this research.

Special thank you to Ying Xu and Zhe Liu for helping me understand the working of the model by sharing their astute knowledge of MatLab and numerical analysis.

Thank you to Julie Petruska and Jody Smiley for their advice and help in lab. I would also like to thank Betty Wingate and Beth Lucas for their invaluable assistance in administrative issues. My special acknowledgement goes to Roberta Niemietz for her help and guidance in setting up the ultra filtration.

Special thanks to my family and friends for their constant love and unwavering support.

Table of Contents

List of Tables

List of Figures

CHAPTER 1 INTRODUCTION

Soluble manganese (Mn) is a common water contaminant and can be a nuisance in a water supply. Soluble Mn is not a health hazard but can cause offensive taste, discoloration of water and staining. The soluble manganese concentration can reach and exceed the Secondary Maximum Contaminant Level (SMCL) of 0.05 mg/L in the water distribution system, without proper removal at a water treatment facility(Sly *et al.* 1990). At this level, soluble Mn can be oxidized to solid Mn-oxide particulates, leading to water discoloration events and potentially resulting in numerous consumer complaints. One of the treatment methods available for removal of soluble Mn in drinking water is the "natural greensand effect". The greensand is naturally occurring sand which is made of calcium, manganese, iron oxide, marine potash and over thirty other trace elements. Greensand works to retain moisture because each grain of it is coated with naturally occurring $MnO_{2(s)}$. This $MnO_{2(s)}$ coating reacts with the soluble Mn present in the water and precipitates it. The Mn which precipitates is then filtered out by the naturally occurring greensand. Currently, there is no other treatment alternative available that can remove soluble Mn with the high efficiency of the "natural greensand effect".

Therefore, research is ongoing to develop different ways to effectively create the natural greensand effect in a post-filtration sorptive contactor for application at water treatment facilities. Based on the results obtained from previous research, the process of adsorption and oxidation of Mn onto oxide-coated media grains in the contactor were used for the removal of soluble Mn (Knocke *et al.* 1988; Knocke *et al.* 1990; Knocke *et al.* 1991) in the research conducted by Zuravnsky (2007). Different media configurations have been evaluated for improved head loss and Mn removal (Coffey *et al.* 1993). However, small media grains, such as sand or anthracite, could produce prohibitive head loss in a sorptive contactor because of the desired hydraulic loading rates.

The research reported by Zuravnsky (2007) focused on the further development of the "natural greensand effect" with application as a post-filtration contactor. In her research project, Zuravnsky (2007) aimed to show that Mn could be effectively removed via adsorption onto larger media (2.0-6.4 mm) at hydraulic loading rates of 16-24 gpm/ft^2, thus producing less head loss and furthering the development of soluble Mn sorptive contactors to be implemented in water treatment facilities. The continuous regeneration mode was implemented and it required an oxidant which provided rapid and effective oxidation at the media surface without oxidizing the soluble Mn in solution. Free chlorine was determined to be the most effective oxidant for this situation (Knocke *et al.* 1987).

Modeling of the adsorption and surface oxidation processes can be helpful for practical application of the Mn removal system to treatment situations. Previous models have been developed (with certain limitations) that attempt to predict soluble Mn removal profiles across oxide-coated media beds (Coffey *et al.* 1993; Merkle *et al.* 1997b). Zuravnsky (2007) developed a preliminary model to predict the soluble Mn removal via adsorption and oxidation onto large-size $MnO_{x(s)}$-coated media in a post-filter contactor concept. The main focus of the research reported on in this thesis is to calibrate the model developed by Zuravnsky (2007) and also to study the sensitivity of the model to various parameters such as temperature, pH and Freundlich Isotherm constants. The specific research objectives that are addressed in this thesis are as stated below:

1. To evaluate the contactor concept for an extended period of time by collecting data at the pilot-scale level. The tests were conducted at varying pH, temperature and hydraulic loading rates (HLR).

2. To enhance the modeling work of Zuravnsky (2007) by incorporating statistical methods and to study the impact of the various operational parameters (temperature, HLR, free chlorine concentration, pH, k_f and Freundlich isotherm constants) on the oxidation rate constant (k_r) value, which in turn, would impact the model prediction capability.

.

CHAPTER 2 BACKGROUND AND LITERATURE REVIEW

This chapter presents a brief summary of previous research conducted by prior researcher Zuravnsky (2007) who worked on the removal of soluble Mn from drinking water using oxide-coated media which was employed as a post-filter contactor. A literature review of previous research is important for development of successful experimental methods and progressive research objectives to further enhance knowledge of the subject. This chapter includes sections on experimental setup and methods employed by Zuravnsky (2007), the results observed by her and the development of the model for Mn removal via sorption and oxidation.

EXPERIMENTAL SETUP

Contactor Column Design

Based on the results obtained from previous research, the process of adsorption and oxidation of Mn onto oxide-coated media grains in the contactor were used for the removal of soluble Mn (Knocke *et al.* 1988; Knocke *et al.* 1990; Knocke *et al.*1991). Different media configurations were evaluated for improved head loss and Mn removal (Coffey *et al.* 1993). However, small media grains, such as sand or anthracite, could produce prohibitive head loss in a sorptive contactor. The focus of the research project conducted by Zuravnsky (2007) was to show that Mn could be effectively removed via adsorption onto larger media (2.0-6.4mm) at hydraulic loading rates of 16-24 gpm/ft^2, thus producing less head loss and furthering the development of soluble Mn sorptive contactors to be implemented in water treatment facilities. Research was conducted by executing laboratory- and pilot-scale experiments using columns packed with oxide-coated media. Contactor columns were the main focus of the laboratory experiments conducted by Zuravnsky (2007) and the experimental set up is as shown in Figure 2.1.

Tap water was used as the main water source in the laboratory experiments performed by Zuravnsky (2007). The local water treatment facility practiced chloramination for disinfection purposes. The tap water characteristics are shown in Table 2.1.

In the lab experiment, influent soluble Mn concentration was controlled by the addition of a $MnCl_2$ solution. The concentration of this solution was varied as necessary while the pumping rate was held constant. The pH of the column feed water was controlled by sulfuric acid addition to the $MnCl_2$ solution. The media bed within the column was constructed by placing approximately two inches of each of the three support gravel sizes obtained from the Blacksburg-Christiansburg-VPI Water Authority into the bottom of the pipe. Twenty inches of the active oxide-coated media were placed over the support gravel. This depth of oxide-coated media will be referred to as the media bed.

Measurements of soluble Mn concentrations at different depths in the media bed were required to determine the soluble Mn removal profile.

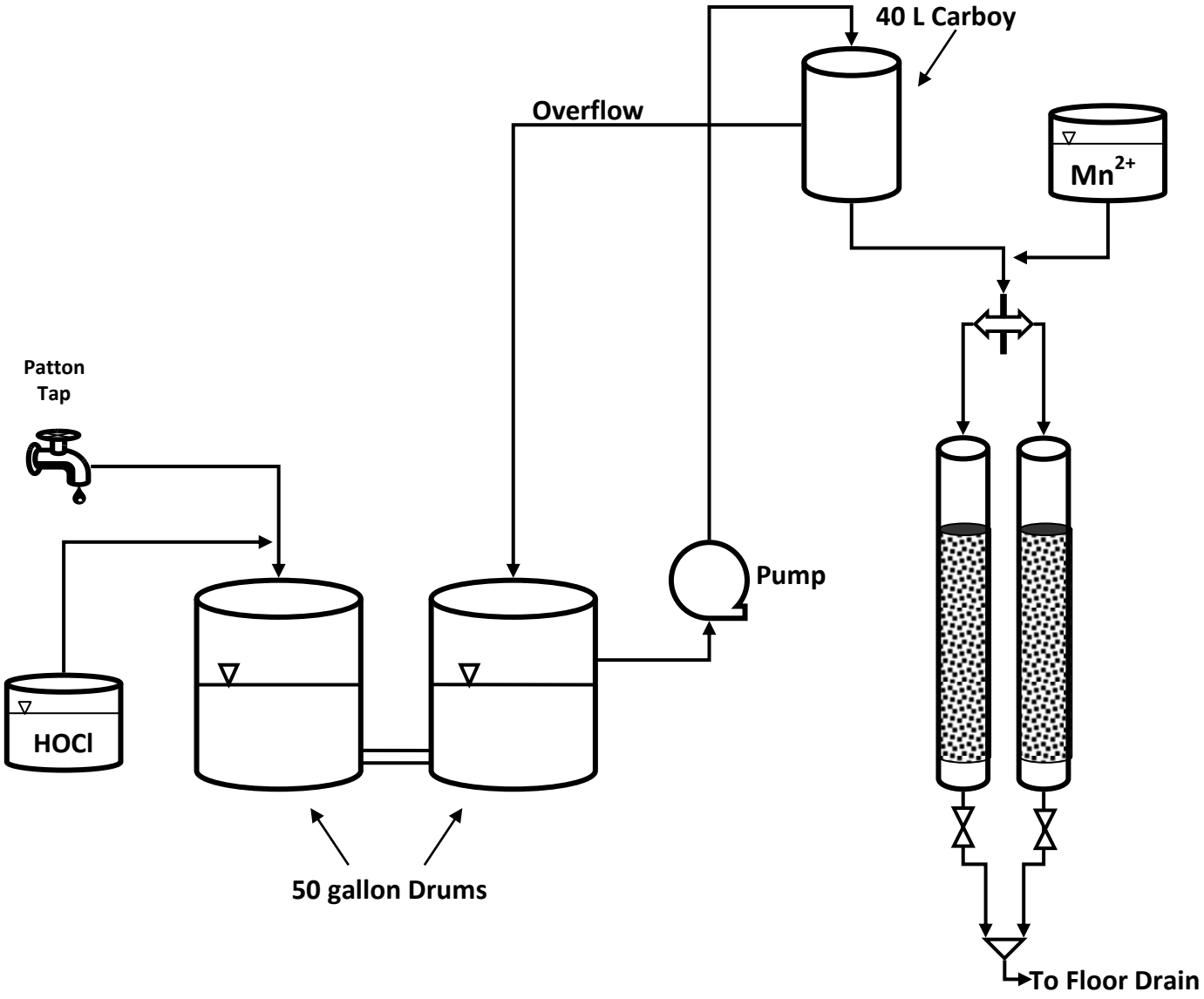

Figure 2.1 Flow diagram of lab-scale contactor column experimental setup (Reprinted with permission from Zuravnsky (2007))

Table 2.1
Summary of tap water characteristics
(Adapted from Zuravnsky (2007))

Parameter	Value
Free Chlorine Concentration	Less than 0.2 mg/L
Total Chlorine Concentration	1.8 – 2.2 mg/L
pH	7.4 – 8.1
Alkalinity	34 mg/L as $CaCO_3$

Sample points for water collection were placed at 0", 3", 9", 15", and 20" as measured from the top of the media bed (Figure 2.2). A detailed description of the contactor column design and the experimental procedure can be obtained from Zuravnsky (2007).

Contactor Media Selection

Previous research has been conducted on filter sand grain media (Coffey *et al.* 1993; Knocke *et al.* 1988; Knocke *et al.* 1987; Knocke *et al.* 1990; Knocke *et al.* 1991). Larger sized media was selected for this study to determine the effectiveness of the process under conditions that included decreased media surface area (9-18 cm^2/cm^3 as compared to 34 cm^2/cm^3) and increased hydraulic loading rate (16-20 gpm/ft^2 as compared to 2-5 gpm/ft^2). Sorptive contactors with large media grains provide a more practical design for use in water treatment plants as a tertiary treatment step after filtration since such contactors could be implemented without a large disruption in the plant hydraulic grade line. Zuravnsky (2007) evaluated three types of media: large grain "torpedo sand", pyrolucite granules, and small gravel. Table 2.2 shows the properties of each media and Table 2.3 gives the operational parameters of the influent water.

Pyrolucite was particles of solid manganese oxide (MnO_2) which required activation with an oxidant prior to use. Pyrolucite media was LayneOx™ brand material obtained from the Layne Christensen Co. (Mission Woods, KS); received at 8x20 mesh size and then sieved to obtain the 8x10 mesh size used in the columns. Gravel and torpedo sand had to be coated to develop the required oxide coating. Gravel media with a size range of ⅛ - ¼ inches was obtained from the Roberts Filter Group (Darby, PA). Torpedo sand media with a size range of 2.0 – 2.5 mm was obtained from R.W. Sidley, Inc. (Painesville, OH). The procedure for depositing a MnOx(s)-coating on the gravel and torpedo sand is presented in detail in Merkle *et al.* (1997b).

Soluble Manganese Adsorption Capacity Determination

In the research study conducted by Zuravnsky (2007), the short-term soluble Mn adsorption capacity of the media was determined by a four-hour recycle method developed by Bouchard (2005). The details of this experiment can be obtained from the thesis document prepared by Zuravnsky (2007) and is also described in Chapter 3.

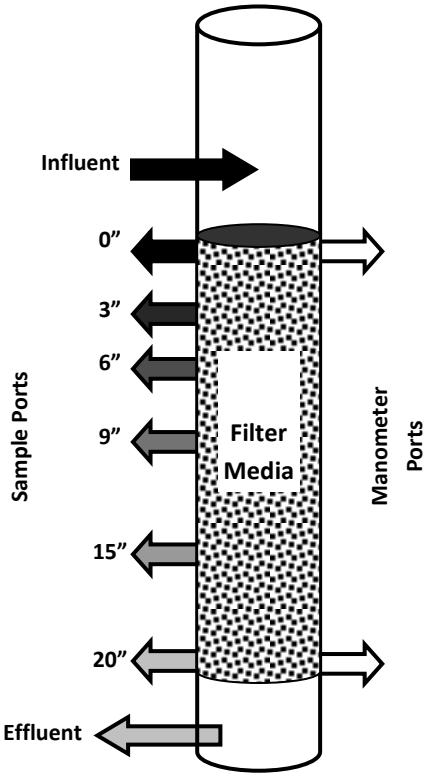

Figure 2.2 Diagram of column port detail
(Reprinted with permission from Zuravnsky (2007))

Table 2.2
Summary of contactor media properties
(Adapted from Zuravnsky (2007))

Contactor Media Properties	**Gravel**	**Sand**	**Pyrolucite**
Specific gravity (g/cm^3)	2.42	2.67	4.15
Porosity (ε)	0.35-0.39	0.43-0.44	0.51-0.53
Particle size (mm)	3.2-6.4	2.0-2.5	2.0-2.4

Table 2.3
Summary of operational parameters of experimental influent water
(Adapted from Zuravnsky (2007))

Operational parameter	Numerical value
Hydraulic loading rate	16 – 20 gpm/ft^2
Mn^{2+} concentration	Routine values: 0.05 – 0.10 mg/L
	Maximum value: 0.25 mg/L
Free chlorine concentration	0.2 – 4.0 mg/L
pH	6.5 – 7.5

Based on the results obtained from Zuravnsky's (2007) experiment, the Mn uptake capacity of oxide-coated media was found to be dependent on the extractable surface MnO_x coating level. The soluble Mn adsorption capacity experiments were also conducted as part of the AWWARF studies and some of the trends observed as a result of those studies are plotted in the figures below (Figures 2.3 & 2.4). Figure 2.3 and 2.4 show the relationship between the Mn uptake capabilities and the Mn coating levels.

Figure 2.3 shows the measured regenerated Mn uptake capabilities as a function of the extractable Mn coating on the media surface (expressed as mg Mn/g media). Figure 2.4 is a plot of regenerated Mn uptake capability per milligram of Mn oxide coating as a function of Mn coating level (per g media). The results show a clear decreasing trend of Mn uptake on a per mg of coating basis with increasing coating level, especially beyond a coating level of 15 mg Mn/g media. This phenomenon also supports the hypothesis that as coating level increases, some of the adsorption sites may be deep within the media and not readily accessible for soluble Mn adsorption.

MODELING EFFORTS

Development and Description of a Model to Predict Soluble Manganese Removal via Adsorption and Oxidation

A basic model was developed as part of the research study conducted by Zuravnsky (2007), to predict the soluble Mn removal via adsorption and surface oxidation onto MnOx(s)-coated media. This model was developed from first principles for the prediction of soluble Mn removal and fitted to the experimental data (Equation 2.1). The development of the model began with the application of first principles to a mass balance of soluble Mn across an incremental bed depth and is shown conceptually in Figure 2.5.

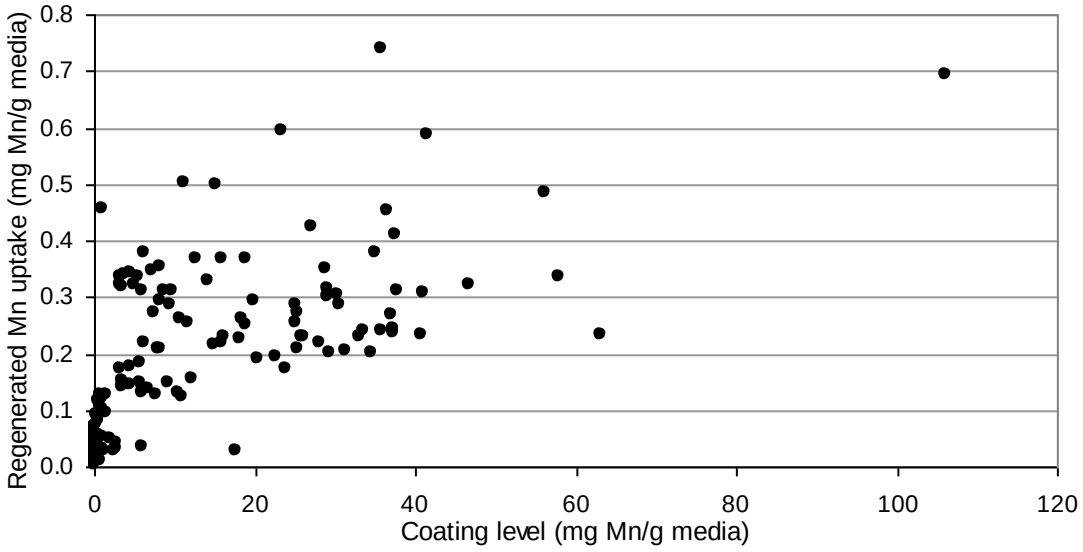

Figure 2.3 Regenerated Mn uptake (mg Mn/g media) versus Mn coating level (Source: Tobiason, J.E,. W.R. Knocke, J. Goodwill, A.A. Islam, P. Hargette, R. Bouchard, and L. Zuravnsky. 2008. *Characterization and Performance of Filter Media for Manganese Control.* ©2008 Awwa Research Foundation. Reprinted with permission)

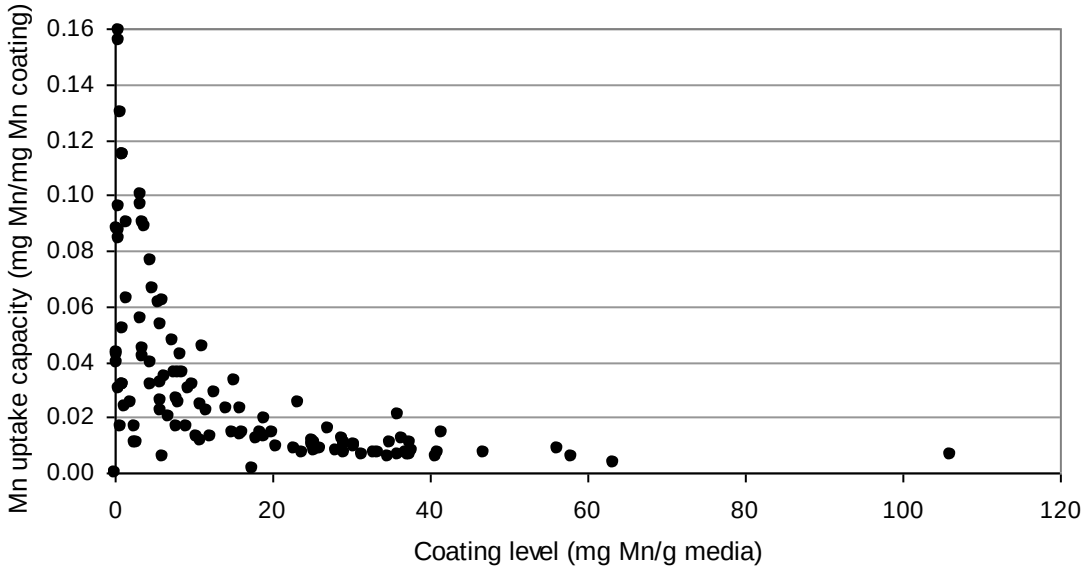

Figure 2.4 Regenerated Mn uptake (mg Mn/ mg Mn coating) versus Mn coating level (Source: Tobiason, J.E,. W.R. Knocke, J. Goodwill, A.A. Islam, P. Hargette, R. Bouchard, and L. Zuravnsky. 2008. *Characterization and Performance of Filter Media for Manganese Control.* ©2008 Awwa Research Foundation. Reprinted with permission)

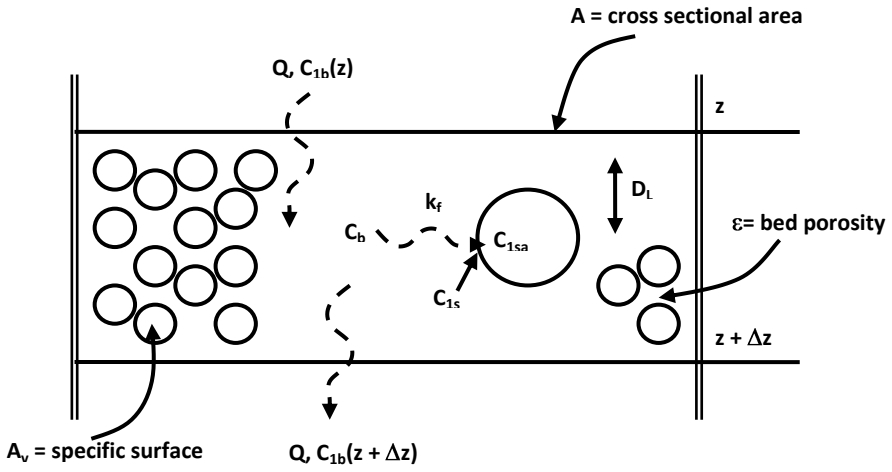

Figure 2.5 Representation of the flow of Mn across an incremental depth of media (Reprinted with permission from Zuravnsky 2007)

$$Q\,C_{1b}(z) = k_f\,(C_{1b}-C_{1s})\,A_v\,(1-\varepsilon)\,A\,\Delta z + Q\,C_{1b}(z+\Delta z) \qquad (2.1)$$

where: Q = volumetric water flow rate (m^3/s)
C_{1b} = bulk aqueous-phase Mn concentration (mol/m^3)
k_f = liquid to solid mass transfer coefficient (m/s)
C_{1s} = aqueous-phase Mn concentration at the liquid-solid interface (mol/m^3)
A_v = specific surface of media (m^2 media/m^3 media)
e = fractional pore volume (m^3 water/m^3 bed)
A = cross sectional area of bed (m^2)

The Freundlich equilibrium isotherm was then applied at the media surface to describe the relationship between the aqueous-phase soluble Mn concentration at the surface and the adsorbed Mn concentration on the surface (Equation 2.2).

$$C_{1s} = \left[\frac{C_{1sa}}{K}\right]^n \qquad (2.2)$$

where: C_{1sa} = adsorbed-phase Mn concentration on the media surface (mol/kg)
K, n = Freundlich isotherm constants

Manipulation of the soluble Mn mass balance equation provided a group of three solvable steady-state equations as shown in Equations 2.3-2.5. The change in soluble Mn concentration across the media depth is defined by Equation 2.3. The change in free chlorine concentration over depth can also be described by a mass balance approach and was manipulated into the form shown in Equations 2.4-2.5. In addition, an overall balance yields Equation 2.6.

$$0 = -U\frac{\partial C_{1b}}{\partial z} + D_L\frac{\partial^2 C_{1b}}{\partial z^2} - k_f A_v\left(\frac{1-\varepsilon}{\varepsilon}\right)\left[C_{1b} - \left[\frac{C_{1sa}}{K}\right]^n\right] \quad (2.3)$$

$$0 = -U\frac{\partial C_{2b}}{\partial z} + D_L\frac{\partial^2 C_{2b}}{\partial z^2} - \rho_b k_r C_{1sa} C_{2b} \quad (2.4)$$

$$0 = \frac{k_f A_v}{\rho_b}\ 1-\varepsilon\ \left[C_{1b} - \left[\frac{C_{1sa}}{K}\right]^n\right] - k_r \varepsilon C_{1sa} C_{2b} \quad (2.5)$$

$$C_{1b(in)} - C_{1b(out)} = C_{2b(in)} - C_{2b(out)} \quad (2.6)$$

where: C_{1b} = bulk aqueous-phase manganese concentration (mol/m^3)

C_{2b} = bulk aqueous-phase free chlorine concentration (mol/m^3)

ρ_b = bulk density of media (kg media/m^3 bed)

U = pore water velocity (= Q/Aε) (m/s)

D_L = axial dispersion coefficient (m^2/s)

The model equations were solved for the soluble Mn concentration and free chlorine concentration per unit depth using numerical methods described in Chapter 3; the step size used across the contactor bed depth was 0.5 inches. The solution was then coded into a statistical software called R (Press *et al.* 2002) . The required input parameters (Table 2.4) were modified in the file editor. The output from the model was a best estimate for the unknown parameter, oxidation rate constant (k_r) along with a plot of soluble Mn concentration over media depth and a plot of free chlorine concentration over media depth.

Results and Future Direction of Work

Based on the results from the research study conducted by Zuravnsky (2007), it was observed that as compared to the oxide-coated gravel and torpedo media, the pyrolucite media provided the best Mn removal of 80-90% of the initial Mn concentration (Figure 2.6).

The predictive model plots (Figure 2.7, 2.8) obtained from the research conducted by Zuravnsky (2007) indicated that removal performance depended on the specific surface area of the contactor media and the porosity (ε). Experimental data presented in Zuravnsky's (2007) thesis has also shown that HLR affects the Mn removal profile. Data plotted in Figure 2.9 shows that the model reflects this relationship appropriately. Owing to lack of time, the model could not be tested extensively for the effect of all the operational parameters in her research study but it nevertheless served as a starting point for further research in this area which is dealt with in detail in the next chapter.

Table 2.4
Characteristic parameters for each of the three media types - pyrolucite, gravel and torpedo sand (Adapted from Zuravnsky 2007)

Parameter	Pyrolucite	Gravel	Torpedo Sand
Fractional pore volume (ε)	0.52	0.37	0.44
Bulk density (kg media/m^3 bed)	1992	1525	1495
Specific surface area (m^2 media/m^3 media)	7260	2937	6895
Particle diameter (m)	0.0022	0.0048	0.0023
Freundlich isotherm constant (K), new media (pH = 7.5)	0.441	0.00034	0.00042
Freundlich isotherm constant (1/n), new media (pH = 7.5)	0.944	0.055	0.0795
Freundlich isotherm constant (K), used media (pH = 7.5)	0.108	0.0034	0.0245
Freundlich isotherm constant (1/n), used media (pH = 7.5)	0.722	0.371	0.595

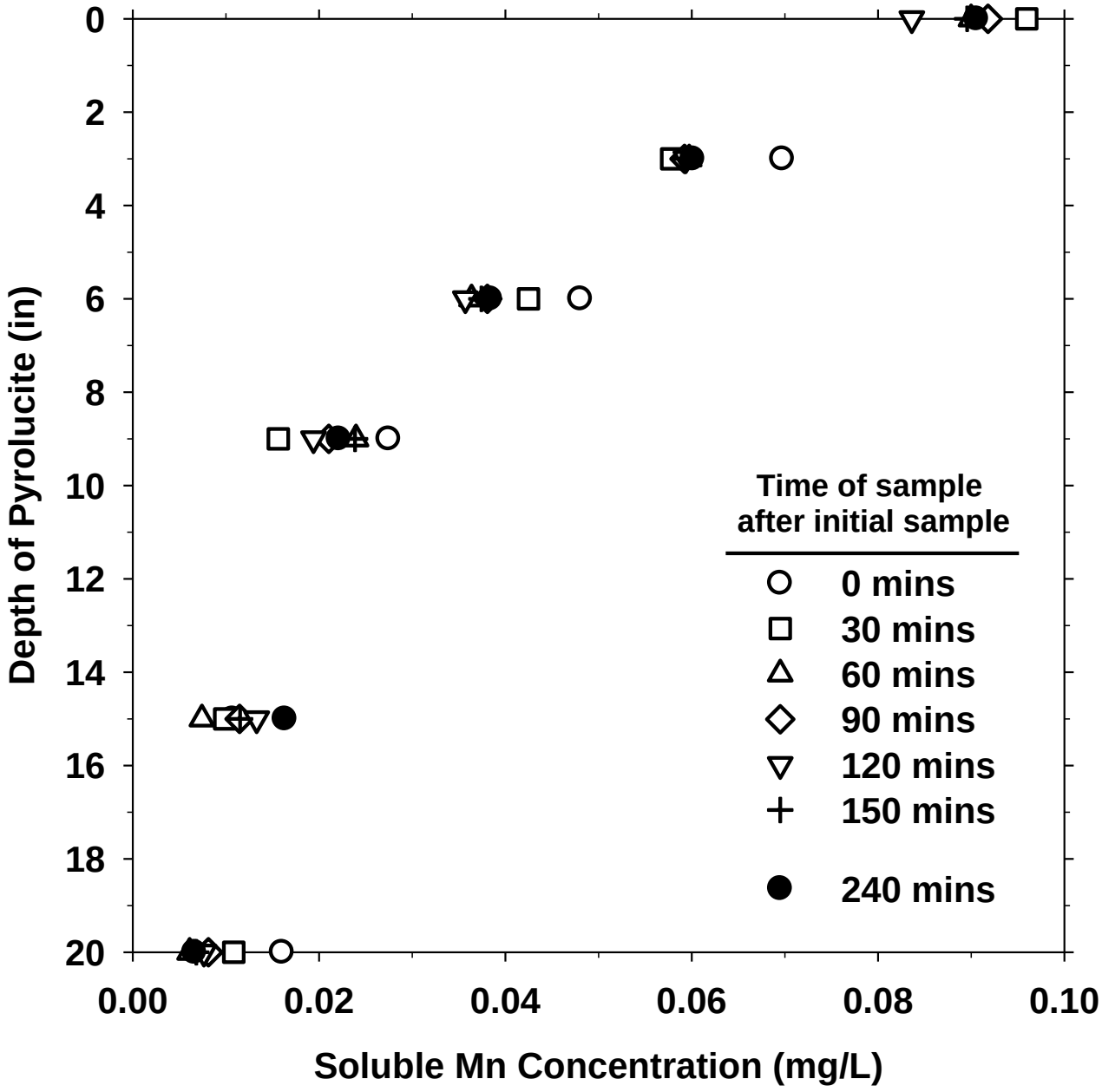

Figure 2.6 Soluble Mn removal profiles over depth of pyrolucite as a function of time (Influent water: HLR=16 gpm/ft^2, free chlorine conc =1.3-1.9 mg/L, pH=7.6)

(Reprinted with permission from Zuravnsky 2007)

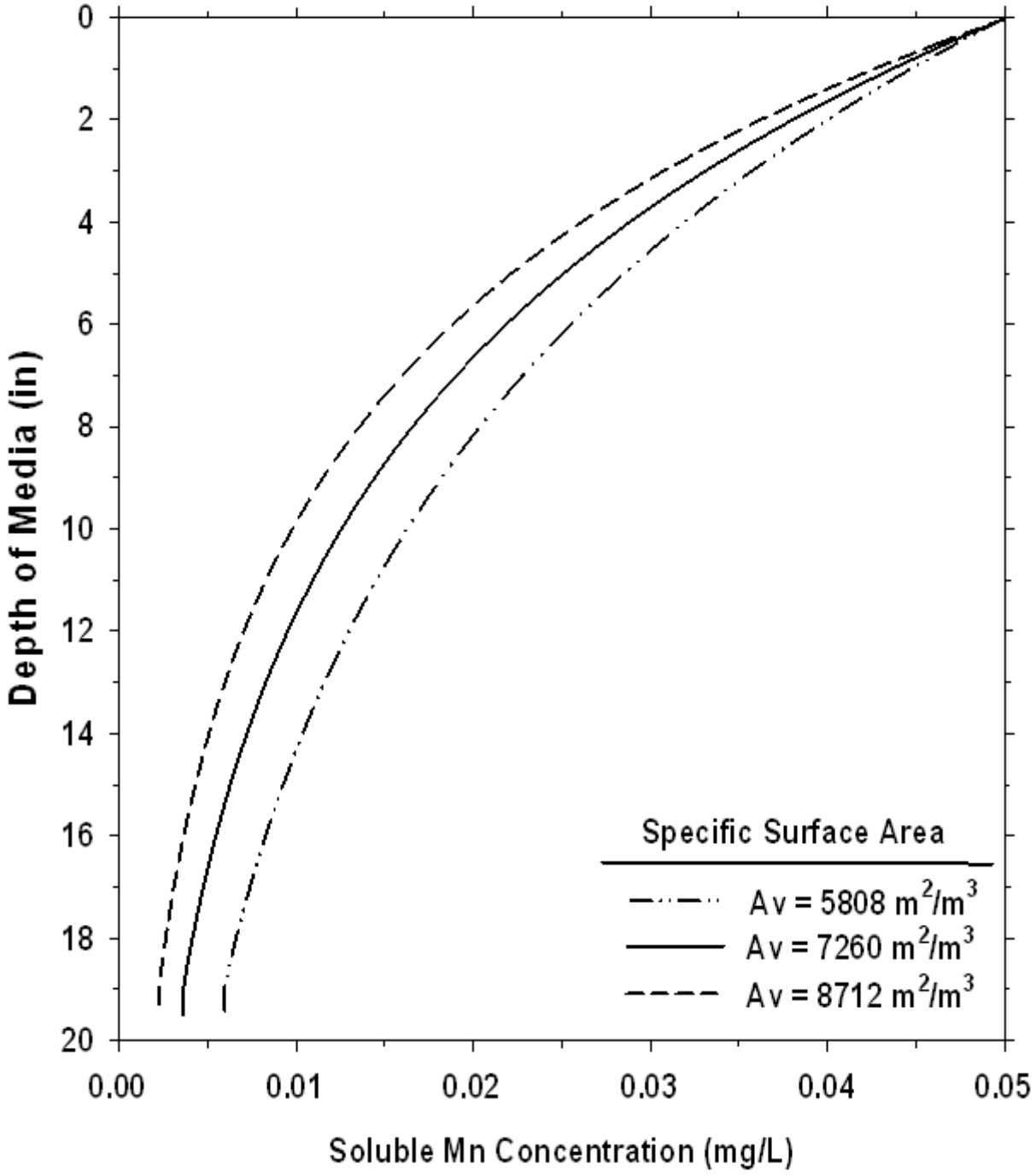

Figure 2.7 Sensitivity analysis: effect of specific surface area on model output

(Reprinted with permission from Zuravnsky 2007)

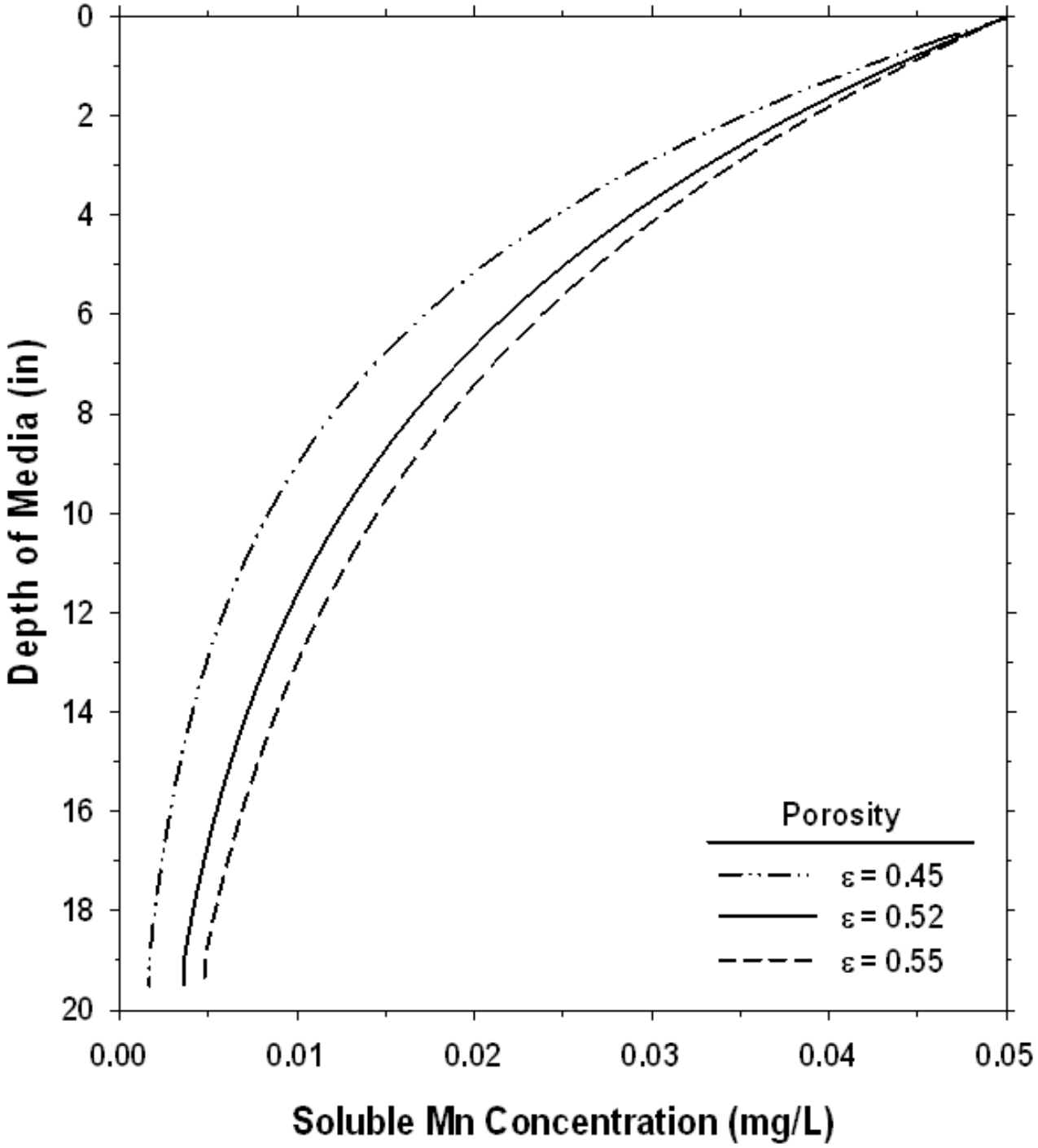

Figure 2.8 Sensitivity analysis: effect of porosity on model output

(Reprinted with permission from Zuravnsky 2007)

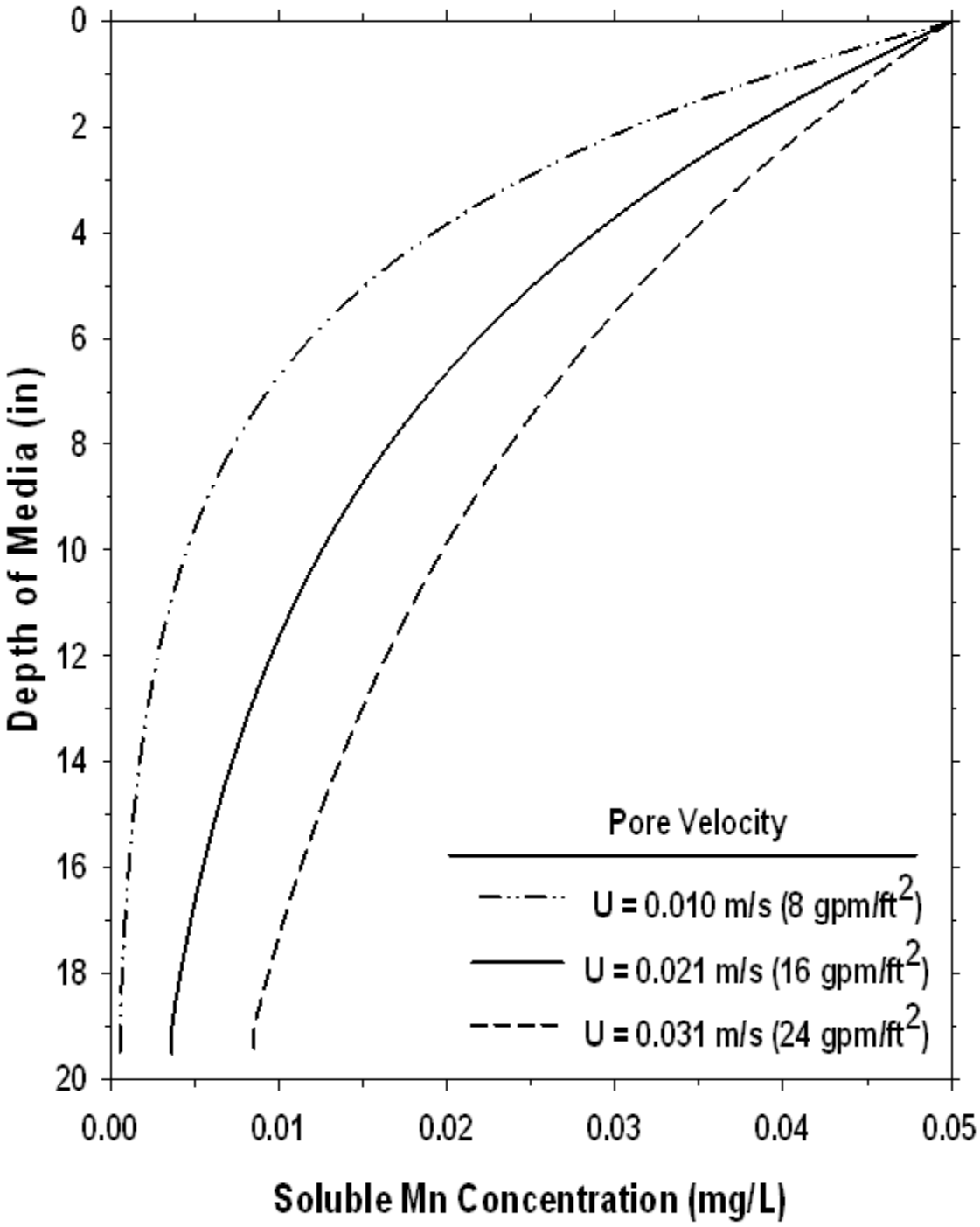

Figure 2.9 Sensitivity analysis: effect of pore velocity on model output
(Reprinted with permission from Zuravnsky 2007)

CHAPTER 3 PILOT PLANT SET-UP

The purpose of this chapter is to describe the pilot plant setup and methods used to achieve the research objectives stated in Chapter 1. The entire discussion in this chapter is broadly divided into two major parts, namely, the description of the mathematical modeling efforts followed by a detailed description of the pilot plant set up in Newport News. In the later part of this chapter, there is also a brief discussion about the experimental set up for the Mn adsorption capacity determination.

Extension of Modeling Efforts

The development of the basic model by Zuravnsky (2007), and the equations employed in it are described in detail in chapter 2. The model equations were then solved for the soluble Mn concentration and free chlorine concentration per unit depth, using numerical methods. As described in Chapter 2, the three solvable steady-state equations involve a second order derivative. Four boundary conditions were required to solve the steady-state equations. The influent Mn and free chlorine concentrations accounted for two of the boundary conditions and the other two conditions are as shown in Equations 3.1 and 3.2. A brief description of the numerical method employed for solving the model equations are described below.

$$C_{1,b}(n) = C_{1,b}(n-1) \tag{3.1}$$

$$C_{2,b}(n) = C_{2,b}(n-1) \tag{3.2}$$

Where C_{1b} = bulk aqueous-phase manganese concentration (mol/m^3)

C_{2b} = bulk aqueous-phase free chlorine concentration (mol/m^3)

n = representative point of depth in the contactor

The steady-state equations were solved by initially assigning a guess value of 0.001 mg/L for the soluble Mn concentration at the bottom of the contactor. The free chlorine concentration at the same depth was then calculated using Equation 2.6. Then with the help of the boundary conditions (Equations 3.1, 3.2) and an iterative process, the Mn and HOCl concentrations at the various depths of the contactor column were calculated. The error between the influent Mn concentration (corresponding to the media depth of 0") obtained by the above calculation and the actual influent Mn concentration for the particular experimental scenario was calculated and accordingly the initial guess value for the Mn concentration at the bottom of the contactor was adjusted. The numerical process was then repeated till the error between the calculated influent Mn concentration and the actual influent Mn concentration was eliminated. Solving the steady-state equations yielded the soluble Mn concentration per unit depth of the contactor. The model solution was then coded into the statistical software, R. The required input parameters as tabulated in Table 2.4 were modified in the file editor. The main objective of the model is to

optimize the fitting parameter, k_r, for a given set of conditions using the experimental data points collected from the pilot study as a base line.

The model is coded using a statistical software R and the input parameters are modified in a file editor. The major input parameters used in the model coding are the sampling depths, the observed Mn concentration at each of these depths, initial Mn concentration, initial Cl concentration, HLR and pH. Based on the HLR and pH which are used as input, the code will appropriately use the relevant values for the other parameters such as Freundlich Isotherm constants, pore-water velocity, mass transfer coefficient and axial dispersion coefficient. In the current research, certain modifications were made to the existing model setup developed by Zuravnsky (2007), and the sensitivity analyses of the model with respect to various operational parameters were checked. Also, the stability and robustness of the model were tested by incorporating certain statistical methods into the model setup. The statistical method used for optimizing k_r is non-linear regression. The details are described below.

In the model developed by Zuravnsky (2007), an error was observed in the calculation of the liquid to solid mass transfer coefficient (k_f). This was resolved and the data modeled by Zuravnsky (2007), were re-evaluated. The Mn plots obtained as a result of the modeling indicated that removal performance depended on the specific surface area of the contactor media, hydraulic loading rate (HLR), and the mass transfer coefficient. As a part of the current research study, an attempt was made to study the stability and effectiveness of the developed model by varying the different model parameters such as k_f (liquid-solid mass transfer coefficient), Freundlich isotherm constants and k_r (Oxidation rate constant) and studying their effects on the model output. The relevant data were obtained from prior experiments done in the water treatment plants in Blacksburg and Newport News, VA respectively (Zuravnsky 2007). In addition to the existing data, more relevant Mn uptake data were obtained from a pilot plant setup in the Newport News, VA water treatment plant. Further details of the pilot plant setup in Newport News, VA are discussed in detail in the next section.

Also, based on the experimental results obtained from the research study conducted by Zuravnsky (2007), it was observed that as compared to the oxide-coated gravel and torpedo media, the pyrolucite media provided the best Mn removal of 80-90% of the initial Mn concentration. In addition, pyrolucite is a commercially available media and is also economically viable. Hence in the model, only the data corresponding to pyrolucite media were used.

Pilot Plant Setup

A pilot plant was setup in the Newport News Waterworks' water treatment plant in Virginia in early summer 2008, to obtain Mn uptake data for the mathematical model. The entire experimental set up in the pilot plant was as shown in Figure 3.1.

Newport News Waterworks is a regional water provider, owned and operated by the City of Newport News, which serves over 400,000 people in Hampton, Newport News, Poquoson, and

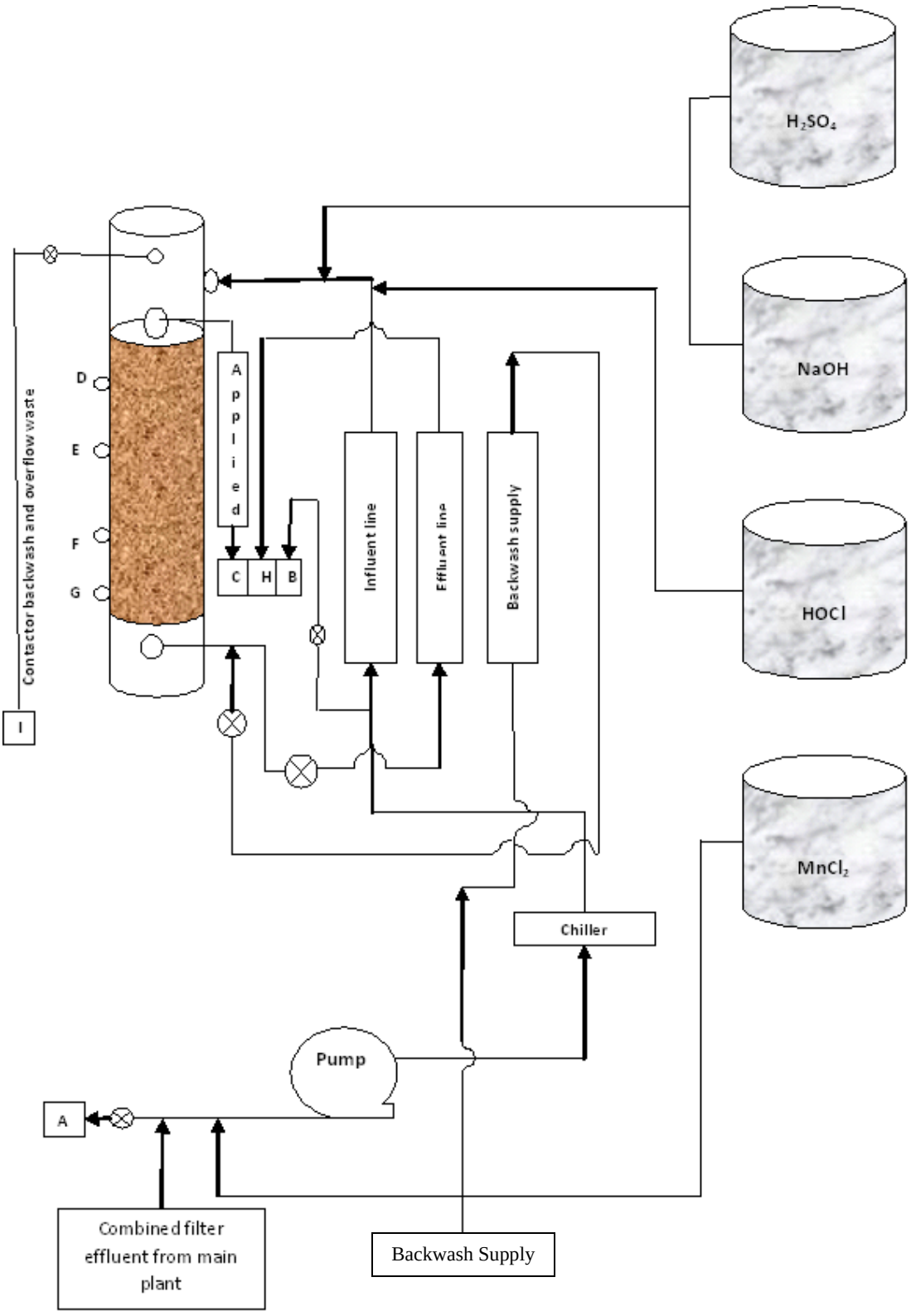

Figure 3.1 Pilot-plant setup in Newport News, VA

portions of York County and James City County. Waterworks treats both surface water and brackish groundwater.

The surface water is pumped from their reservoirs to their treatment plants. The water passes through screens and then alum and polymer are added as coagulants. After the water is clarified, ozone or chlorine is added to kill microorganisms such as bacteria and viruses. After the disinfection process, the water is then sent through dual media filters comprising of anthracite and coal to remove any remaining particles. Lime is added to adjust the pH to around 6 and zinc orthophosphate is added to control corrosion inside the pipe system.

The brackish groundwater is pumped to a desalination plant and is then treated by the reverse osmosis process, where in water is forced by high pressure through membranes that can remove the salt and most other contaminants to produce very high-quality water. This water is then blended with their treated surface water.

For the pilot plant experiments, the combined filter effluent from the Lee Hall treatment plant in Newport News was used as the main water source as it was low in turbidity and alkalinity. In the pilot plant set up, the contactor column was constructed from a 3" ID clear PVC pipe. A PVC cap was attached to the bottom of the pipe and at the top. The media bed within the column was constructed by placing pyrolucite media on top of the media support disc, there was no support media used. Twenty-seven inches of the pyrolucite media was placed over the filter screen. For the purpose of this discussion, this depth of oxide-coated media will be referred to as the media bed depth. Bulk media was added or removed from the column through the top of the PVC pipe.

The holes drilled into the pipe walls were named ports D, E, F and G in Figure 3.2. Influent water was applied to the column at point C above the top of the media bed, while effluent water flowed from the column at point H below the media bed. Influent and effluent lines were made of clear vinyl tubing. A manometer was constructed from two lengths of glass tubing attached to the column through short sections of clear vinyl tubing and plastic elbow joints. One glass tube was connected to the column 0" from the top of the media bed, while the other glass tube was connected at 27" from the top of the media bed. The head loss across the media bed was measured as the difference in inches between the water levels in the two glass tubes. Later, manometers were also constructed across each of the ports D, E, F and G enabling the measurement of head loss as a function of media depth in the contactor.

Measurements of soluble Mn concentrations at different depths in the media bed were required to determine the soluble Mn removal profile. Sample points for water collection were drilled at 0", 3.5", 9.5", 15.5", 21.5" and 27.5" as measured from the top of the media bed. The sample points were fitted with a rubber stopper, through which a narrow, 3" long glass tube was positioned to reach the approximate centerline of the column. On the exterior of the column, a flexible tube was connected to the glass tube and clamped. Water samples for soluble Mn determination were collected by loosening the clamp to allow water flow through the tubing while sample water was captured in 25 mL plastic sample jars with lids. Solid media samples for the purpose of conducting Mn adsorption capacity experiments were collected from the column by removing the rubber stopper and gently extracting media grains from the bed. The adsorption capacity experiment is dealt in detail in the later part of this chapter. Influent and effluent free chlorine samples were collected and measured from the top (0") sample point and the column effluent tubing, respectively.

Hydraulic flow through the system originated at the influent and ended at the column effluent tubing which led to a floor drain. The hydraulic loading rate of the media bed was ultimately controlled by a clamp on the column effluent tubing. Flow rate was determined by measuring the time required to collect a known volume of effluent water. The clamp was tightened or loosened to generate the desired flow rate.

pH vas varied in each of the experiments by the addition of either a sulfuric acid (H_2SO_4) or a sodium hydroxide (NaOH) solution. These solutions were added to the influent tubing as shown in the Figure 3.1. Clear vinyl tubing of various sizes was used to convey the sulfuric acid and sodium hydroxide solutions to the influent water line.

Free chlorine concentration in each experiment was controlled by the addition of a dilute bleach (NaOCl) solution. A Master-Flex peristaltic pump was used to add the solution from the drum at a location directly in the influent tubing. Clear vinyl tubing of various sizes was used to convey the free chlorine solution to the influent water line.

Influent soluble Mn concentration was controlled by the addition of a stock Mn solution which was prepared by dissolving $MnCl_2$ in water. The concentration of this solution was varied as necessary while the pumping rate was held constant. A Master-Flex peristaltic pump was used to add the solution at the beginning of the influent line. Clear vinyl tubing was used to convey the soluble Mn solution.

The temperature of the column feed water was controlled by the use of a chiller. The chiller was set to ideally provide three target temperatures namely 10^0C, 20^0C and 30^0C and they were calibrated by testing the influent water temperature with the help of a thermometer. At each of these three temperatures samples were obtained at different depths across the media by varying the various parameters such as HLR, pH and residual chlorine concentration as per the experimental matrix. The experimental matrix is described in detail in the next section. Towards the later part of this pilot study, the water temperatures in the plant actually decreased to less than 10^0C and hence some studies were done at values below 10^0C.

In addition to the influent and the effluent lines, there was also a separate tubing line provided for the backwash supply and it joined the effluent line as shown in the Figure 3.1. A typical backwash procedure was done when the headloss across the contactor media bed was greater than 6" and that was roughly once in every 10 days. The flow rate for backwash was maintained at 82 gpm/ft^2 (4 gpm) and the duration of backwash was approximately 5 min. The filter overflow and backwash waste were collected at a port I located above the media top as shown in Figure 3.1.

Towards the end of the pilot study, the accumulation of headloss across the contactor media became an area of research interest. Hence, monometers were inserted at each of the sample ports for water collection throughout the media bed. Two consecutive backwash cycles were performed with intensive backwash protocols. The entire duration of each of those backwash cycles were approximately 15 minutes each. Four different backwash flow rates were used namely 4 gpm/ft^2 (0.2 gpm), 20 gpm/ft^2 (0.98 gpm), 40 gpm/ft^2 (1.96 gpm) and 80 gpm/ft^2 (3.92 gpm) and the approximate duration for each of these flow rates were 3.5 minutes. Various samples were collected during the backwash procedure and were analyzed for Mn, Al and Fe

concentrations using the ICP method. The mass balance of Mn removed during backwash was also calculated. The results are discussed in detail in chapter 4.

Experimental Matrix

The pilot plant setup in Newport News had been done in such a way that it was functioning for a total period of18 weeks (Figure 3.2). The details of the experimental matrix are outlined below.

The total 18 week period was divided into 3 sets of 6 weeks namely period 1, period 2 and period 3. In period 1, the temperature was maintained at 30^0C and it was reduced to 20^0C for period 2 and finally maintained at 10^0C for the period 3. Each of the 3 periods was further divided into 3 smaller subsets of 2 weeks each namely a, b, c and the HLR was kept constant across each of these 2 weeks. In period 1a, the HLR was kept constant at 16 gpm/ft^2, followed by an HLR of 20 gpm/ft^2 during period 1b and then finally the HLR was incremented to 24 gpm/ft^2 for the period 1c. During each week, the pH of the water was varied between 5.5 and 7.5 with a 0.5 increment each day. In order to ensure that the pH variation in the water is never drastic, the pH over the first week was incremented from 5.5 to 7.5 and then in the following week the pH was decremented from 7.5 to 5.5. This pattern was followed for each of the 3 periods. A typical pH routine in the pilot plant over any 2 week period is shown below in Table 3.1.

Table 3.1
Typical pH rotation over 2 weeks in the pilot-plant

Day	pH
Week 1	
Day 1	5.5
Day 2	6.0
Day 3	6.5
Day 4	7.0
Day 5	7.5
Day 6,7	Maintain at pH 7.5
Week 2	
Day 1	7.5
Day 2	7.0
Day 3	6.5
Day 4	6.0
Day 5	5.5
Day 6,7	Maintain at pH 5.5

At a specified time every day, the Mn adsorbed by the filter media across each of the six depths (0", 3.5", 9.5", 15.5", 21.5", and 27.5") was collected in small 25 mL sample bottles. The Mn concentrations were immediately measured onsite using the HACH kit and the data was sent across to Blacksburg by email. At the end of every week the bottles were then carefully shipped to Blacksburg, where the samples were sent to the lab for analysis of Mn concentrations using a coupled plasma mass spectrometer (ICP). Then, the data were modeled to obtain the best-fit k_r value corresponding to which, the final measured soluble Mn concentration at the various depths of the media matched with the actual experimental data. The k_r values obtained were then compared with respect to the other parameters such as pH, free chlorine concentration and initial

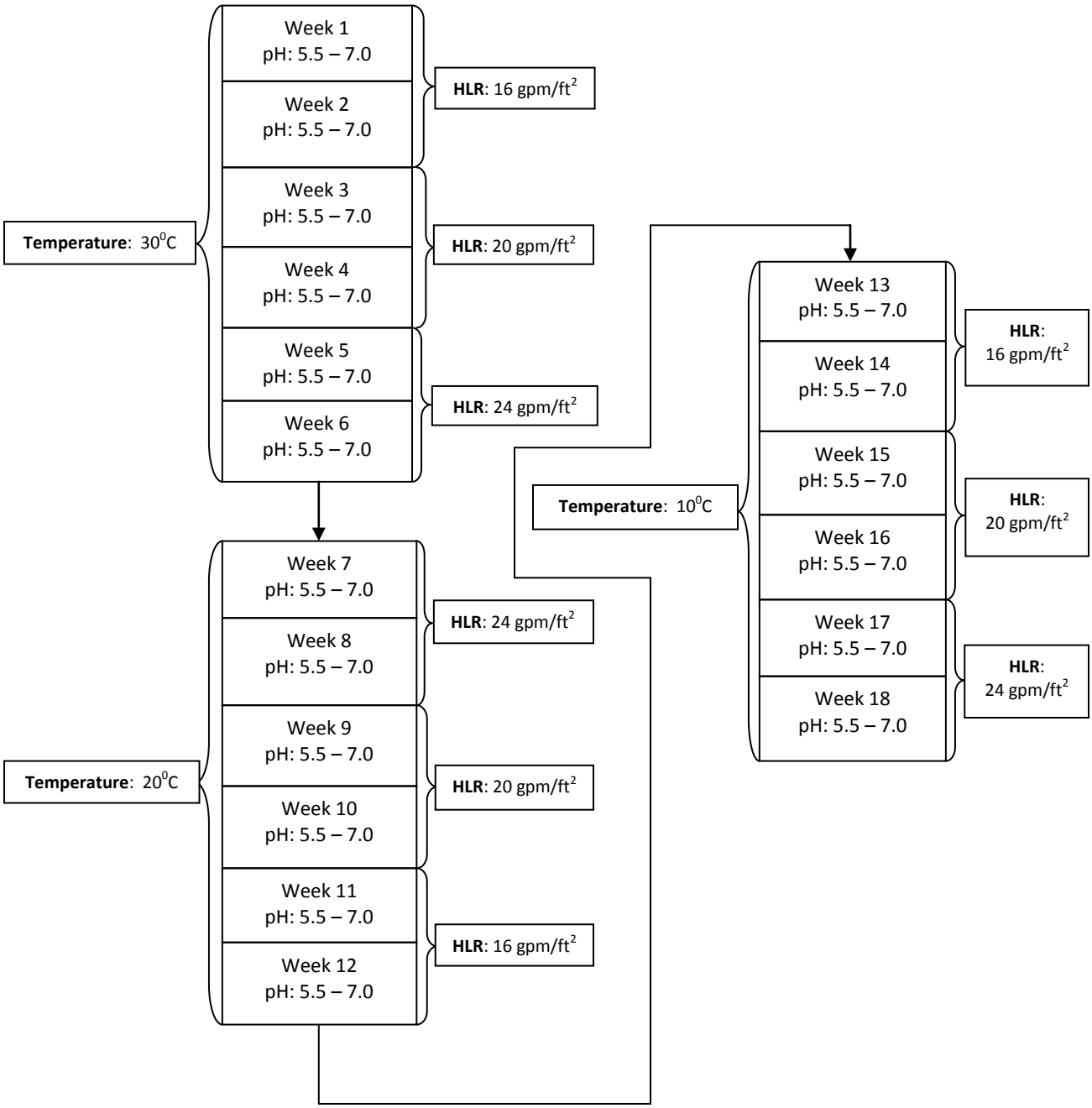

Figure 3.2 Newport News pilot-plant operational matrix

Mn concentration to identify the trends. Figure 3.3 shows the distribution of the soluble Mn concentration data obtained from the pilot-plant study when analyzed by both the HACH and ICP methods. From the Figure 3.3 it can be observed that the data plot has an R^2 value which is close to 1(~ 0.93), which indicates that during the course of the pilot-plant study, the values obtained for the soluble Mn concentration of a sample by both the HACH and ICP method tend towards linearity. The HACH method over predicted the Mn concentration values by 10 %. In other words, based on the R^2 value as well as the equation of the trend line, it can be noted that the soluble Mn concentration values of the samples measured on-site using the HACH kit were very close to the "true" concentrations obtained by the ICP method. However, since the ICP method is a more detailed and accurate method for estimating the soluble Mn concentrations, all the data plots represented in this thesis have utilized the soluble Mn concentration values obtained by using an ICP. All soluble Mn concentration measurements analyzed by the ICP were determined to be above the instrument's detection limit of 0.02 ppb.

Soluble Manganese Adsorption Capacity Determination

Towards the later part of the research study, short-term soluble Mn adsorption capacity of the media was determined by a four-hour recycle method developed by Bouchard (2005). A bed depth of 2.5 cm of media with a known weight was supported by glass wool in a 1.5 cm diameter glass tube as shown in Figure 3.4. A dilute bleach solution (2 mL of 6% bleach in 5 L tap water) was pumped by a Master-Flex peristaltic pump from a continuously mixed (100 rpm) reservoir through tubing at a rate of 4 gpm/ft^2. The solution circulated through the media for four hours, after which the media was rinsed, removed, and allowed to air dry. This regeneration step was to ensure that all available sorption sites were oxidized before the short-term capacity was measured.

The media was returned to the glass tube once dry. A prepared solution containing specified properties was placed in the continuously mixed reservoir and pumped through the media at a rate of 4 gpm/ft^2. An initial and final sample of the solution reservoir were collected and filtered for soluble Mn concentration analysis using the ICP. Only the initial and final measurements were used in the capacity calculation. Additional samples were taken at 30, 60, 90, 120, 150, 180 and 210 minutes to be filtered and analyzed by the HACH method for soluble Mn analysis. Since sorption capacity is related to bulk Mn concentration, the additional samples were taken to monitor the soluble Mn concentration in the reservoir. If more than 10% of the initial concentration was adsorbed during the four-hour period, soluble Mn was added at each of the sampling times as required to keep the concentration within the desired range. Short-term soluble Mn adsorption capacity was calculated from the difference of initial and final soluble Mn concentrations using Equation 3.3.

$$\text{Capacity} = [(C_i - C_f) * V_{solution}] / M_{media} \qquad (3.3)$$

where:
- C_i = initial concentration of Mn^{2+} in the reservoir (mg/L)
- C_f = final concentration of Mn^{2+} in the reservoir (mg/L)
- $V_{solution}$ = volume of solution in reservoir (L)
- M_{media} = mass of media in glass tube (g)

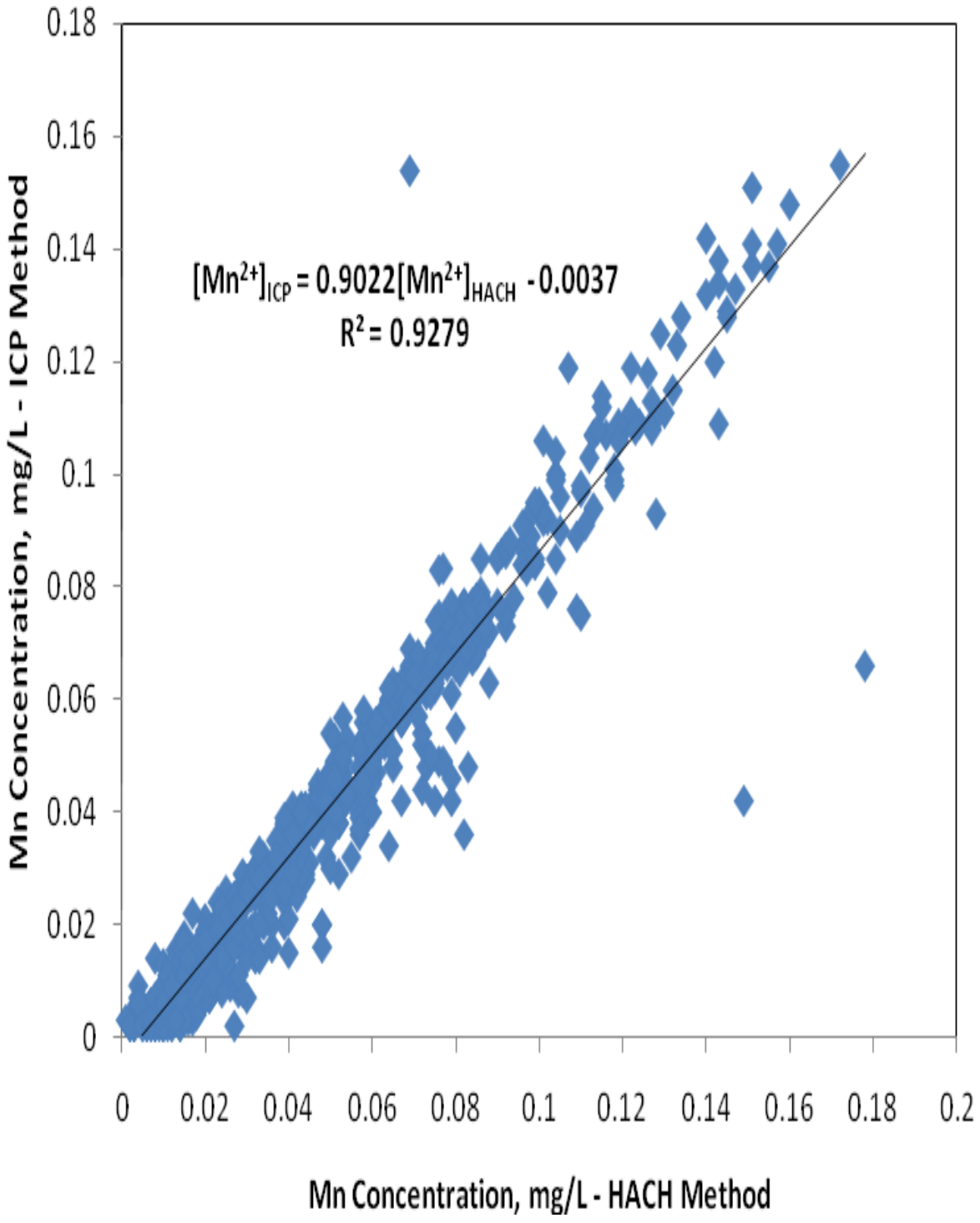

Figure 3.3 Distribution of pilot-scale soluble Mn concentration values analyzed by HACH and ICP

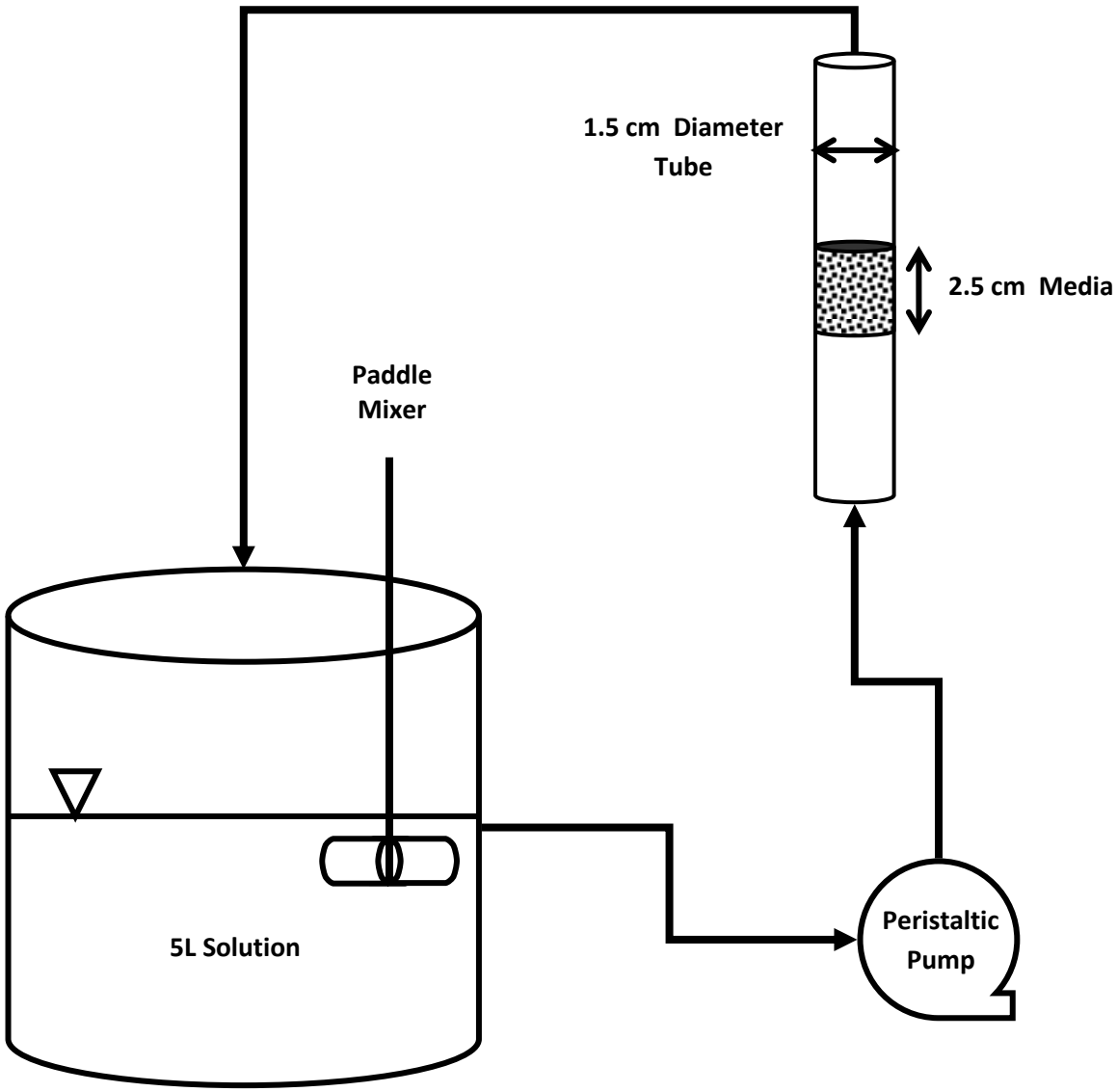

Figure 3.4 Schematic of short-term recirculating Mn uptake experiment

(Reprinted with permission from Zuravnsky 2007)

Method for Extraction of Manganese Oxide Coating

A method published by Knocke *et al*. (1990) was used to determine the extractable amount of manganese oxide coating on the pyrolucite media. Media samples were air dried, weighed and placed into a 250 mL Erlenmeyer flask with 100 mL of 0.5% Nitric Acid and approximately 300 mg of hydroxylamine sulfate (HAS). The flask was periodically agitated and the solution was allowed a sufficient contact time of six hours. After six hours, the solution was agitated and a sample of the solution was removed and filtered. The soluble Mn concentration was analyzed using the ICP method. This procedure was repeated over a 5-day period and the Mn extracted from the used pyrolucite media across the various sampling ports over 5 days was noted. The extractable manganese (mg/g media) was calculated using Equation 3.4.

$$EMC = [C * V] / W \qquad (3.4)$$

where: EMC = extractable manganese (mg/g media)
C = measured soluble Mn concentration (mg/L)
V = volume of nitric acid (L)
W = mass of media placed in the flask (g)

ANALYTICAL METHODS

Samples collected for soluble Mn concentration determination were acidified with the addition of 0.1% concentrated nitric acid for sample preservation and were shipped across from Newport News to Blacksburg via 2-3 day delivery.

The Hach Low Range Method (0.006 – 0.700 mg/L) for soluble Mn analysis (Method 8149, 1-(2-Pyridylazo)-2-Naphthol PAN Method) was used to obtain immediate results at the pilot plant site before the samples were shipped to Blacksburg. Reagents were obtained from the Hach Company and a Hach DR/2400 was used for analysis. The machine was zeroed with a blank cell, which was prepared with 10 mL of deionized water and reagents. The samples were prepared by placing 10 mL of filtered sample in a sample cell. An ascorbic acid pillow was added to each cell. Fifteen drops of alkaline-cyanide solution were added, followed by 21 drops of PAN indicator. The cell was inverted multiple times after the addition of each reagent. The sample cell was allowed to rest for two minutes before analysis.

Once the samples reached Blacksburg, an inductively coupled plasma mass spectrometer (ICP-MS) was also used for soluble Mn analysis. The calibration curve was created using five standard solutions (1, 10, 50, 100, 1000 ppb). A quality assurance check of a blank (zero Mn) and a 50 ppb standard solution was evaluated after every nine unknown samples.

Free chlorine was measured using the Hach Method 8021 (DPD Method) with a detection range of 0.02 – 2.00 mg/L Cl_2. Reagents were obtained from the Hach Company and a Hach DR/2400 was used for the analysis. The machine was zeroed with a blank cell, which was prepared by placing 10 mL of sample to the sample cell. Samples were prepared by placing 10 mL and a DPD Free Chlorine Powder Pillow in a sample cell. The cell was inverted to mix the reagent and allowed to rest for 30 seconds before analysis. Samples containing chlorine level which were greater than 2mg/L were diluted to achieve the desired range of the HACH method.

Temperature was measured with a Fisher Scientific Ever-Safe™ Thermometer with a range of -5°C – 110°C. The solution pH was measured with a portable Fisher Scientific Accumet Model AP62 meter with an Accumet Liquid Electrode. The meter was calibrated with pH 7 buffer solution.

All plastic sample containers and glassware were cleaned before use in the following manner. Items used for soluble Mn analysis (sample containers) were double rinsed with de-ionized water and placed in a 10% nitric acid bath for at least nine hours. After the acid bath, containers and syringes were double rinsed with de-ionized water and allowed to dry. All other glassware was rinsed before and after each use and acid washed prior to their use in an experiment and for sample collection.

Model code was developed and executed using open source statistical software called R (Version 2.6.1). Data collected from the ICP-MS output and from the R code were stored in Microsoft Excel and a hardcopy version was also maintained in a laboratory notebook. Data collected in the laboratory were stored in a notebook as well as in Microsoft Excel. Microsoft Excel was also used for data organization, comparison and for plotting graphical representations of data. All files were backed up periodically in an external hard disk.

CHAPTER 4 RESULTS AND DISCUSSION

The purpose of this chapter is to describe the characteristic experimental and modeling results obtained from the pilot-plant contactor experiments and contactor media Mn uptake capacity experiments. This chapter is arranged in three broad sections. The first section describes the experimental results of the pilot-scale contactor column experiments. This section includes representative figures showing data from individual experiments showing the effect of pH, temperature, HLR and initial chlorine concentration on soluble Mn removal performance. The second section describes in detail the results obtained from the pyrolucite media Mn uptake capacity tests and also by modeling the data obtained from the pilot-plant study. The third section of this chapter is devoted towards the observations related to headloss buildup across the contactor, the results obtained from the backwash of the pilot-plant contactor column and sieve analysis of the pyrolucite media. Due to the volume of data collected, representative plots were included in this chapter, with supplementary data shown in figures included in Appendix A.

Experimental Results from Pilot-Plant Tests

An increase in bulk solution pH has been shown to have a positive effect on the Mn adsorption capacity of $MnO_{2(s)}$ (Morgan and Stumm 1964) and on $MnO_{x(s)}$-coated filter media (Knocke *et al.* 1991). Figures 4.1 and 4.2 display the soluble Mn removal profiles obtained in the current study over a wide pH range. In both the figures, the pH is varied from 5.5 to 7.5 and the other parameters such as temperature, HLR, initial Mn concentration and initial chlorine concentration were kept constant for each of the data sets. For the data plotted in Figure 4.1, the water temperature was maintained at 20^0C, the HLR constant at 16 gpm/ft^2, the free chlorine concentration which was being fed into the column was maintained between 1.1-1.3 mg/L, and the influent Mn concentration maintained between 0.06 mg/L - 0.08 mg/L. The operating condition for data plotted in Figure 4.2 was very similar to Figure 4.1 except for a higher HLR of 20 gpm/ft^2.

Data presented in both figures demonstrate the important role of pH in defining the Mn uptake onto MnO_x(s) surfaces. The amount of Mn removed by the contactor column increased as the pH was increased from 5.5 (acidic pH condition) to 7.5 (alkaline pH condition). This effect of pH on the soluble Mn removal profiles agreed well with the results observed by Zuravnsky (2007) in her research on MnO_x(s)-coated media in post-filter contactors. Also, on comparing the Mn removal profiles between Figures 4.1 and 4.2, it can be seen that just by increasing the HLR from 16 gpm/ft^2 to 20 gpm/ft^2 (keeping all the other operational conditions the same) the soluble Mn removed across the entire contactor column decreased slightly. This observation was also in agreement with the findings of Zuravnsky (2007). A more complete analysis of the effect of HLR on Mn removal within the contactor is discussed in a later part of this chapter.

The literature review conducted as a part of this research study did not uncover any prior published research dealing with the effects of temperature on the sorption of Mn onto MnO_x(s)-coated filter media, in depth. During the pilot-plant studies, the temperature of the water flowing into the contactor column was varied with the help of a water chiller. The three temperatures used during the course of the study were 10^0C, 20^0C and 30^0C.

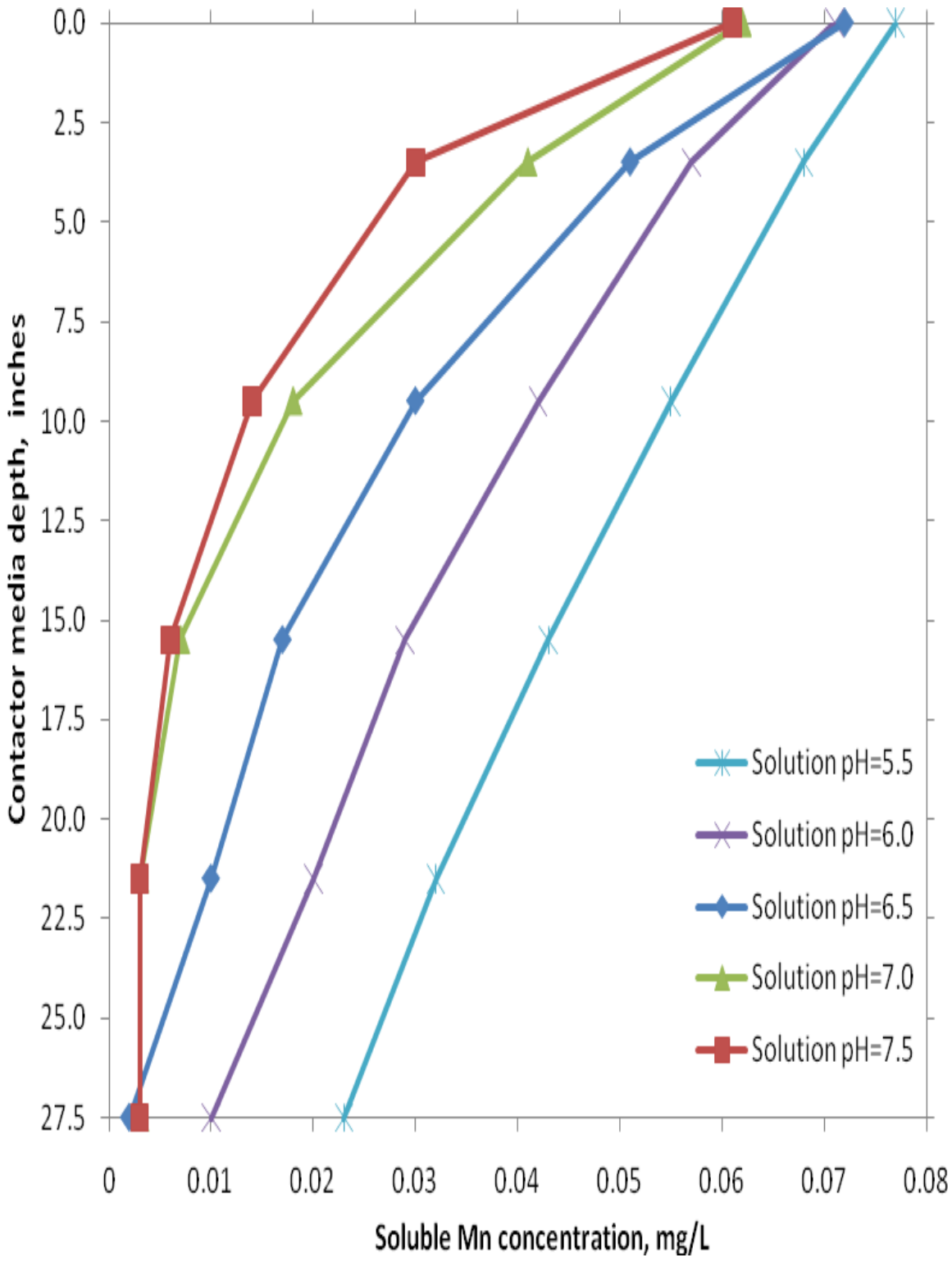

Figure 4.1 Effect of solution pH on the soluble Mn Uptake in contactor column

[Influent water: Mn^{2+} = 0.06-0.08 mg/L, Temp=20^0C, HLR = 16 gpm/ft^2, free chlorine conc = 1.1-1.3 mg/L]

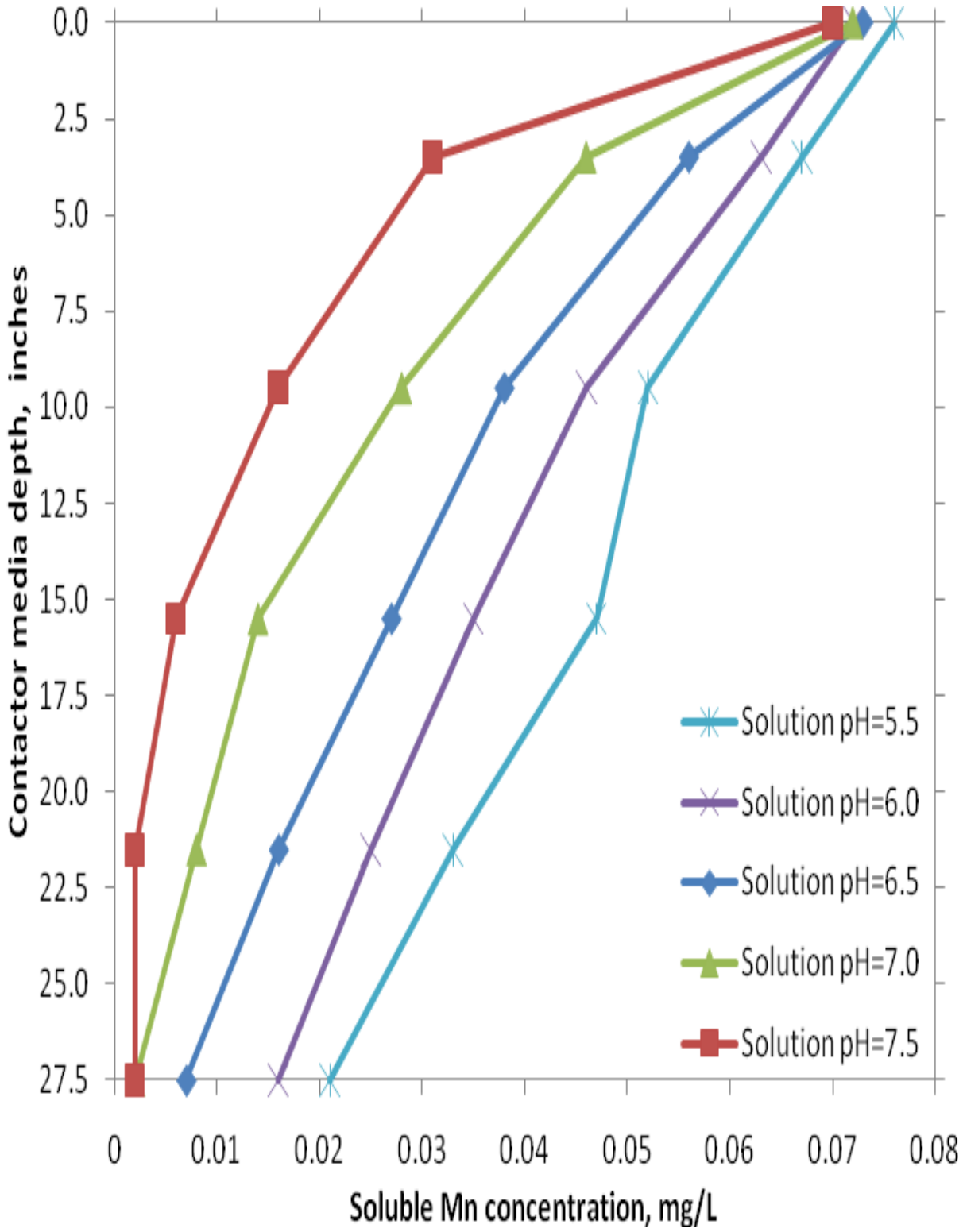

Figure 4.2 Effect of solution pH on the soluble Mn Uptake in contactor column

[Influent water: Mn^{2+} = 0.07-0.08 mg/L, Temp=20^0C, HLR = 20 gpm/ft^2, free chlorine conc = 1.2 mg/L]

Profiles from the pilot-scale experiments were compared to determine the effect of temperature on soluble Mn removal in the pyrolucite contactor. Figures 4.3 and 4.4 show the Mn removal profiles for the three temperature values. Here, the data sets in each of the two plots have been grouped such that they have comparable initial chlorine concentrations, pH and HLR values. However, the initial Mn concentrations for the data sets in Figure 4.3 and 4.4 varied to a significant degree (between 0.04-0.07 mg/L); hence the normalized Mn concentrations have been used in place of the actual Mn concentrations in these two figures. Results shown in Figures 4.3 and 4.4 correspond to an applied water pH of 6.5 and 7.0 respectively.

Data presented in Figures 4.3 and 4.4 indicate that temperature did not have any major impact on the overall Mn removal performance of the contactor media. However, it was noted that at the lowest water temperature of 10^0C, there was a slight worsening in the Mn uptake at any given media depth. Considering the practical implications of this observed detrimental effect of very low temperatures on the soluble Mn removal profile, it can be said that Mn related complaints in the finished water have typically been observed by water treatment utilities more during the summer and fall seasons and less during the winter months. Based on the interpretation of data plotted in Figures 4.3 and 4.4, it was noted that the Mn removal performance of the contactor media was not affected drastically during higher temperatures which typically correspond to the summer and fall periods.

Profiles from the pilot-scale experiments were also compared to determine the effect of HLR on soluble Mn removal in the pyrolucite contactor; representative data are shown in Figures 4.5 and 4.6. The various conditions under which the contactor column was operated are specified below each of the plots, and it can be noticed that the data corresponding to the Figures 4.5 and 4.6 had comparable initial Mn and Cl concentrations. The influent water temperature was also maintained at 20^0C for the data used in both the plots. The only operating condition which was different in both the plots is the pH; for data in Figure 4.5, the pH of the influent water was maintained at 6.5, whereas for the data plotted in Figure 4.6, the influent water pH was 7.0.

On detailed analysis of the trends in the plot, it was observed that when the water temperature was maintained at 20^0C (data in Figure 4.5) there was a slight decrease in the amount of soluble Mn removed across the column as the HLR was increased from 16 gpm/ft^2 to 20 gpm/ft^2. However as the HLR was increased to 24 gpm/ft^2, the Mn removal profile overlapped with the profiles corresponding to the HLR values of 16 gpm/ft^2 and 20 gpm/ft^2. Whereas, for data presented in Figure 4.6, when HLR was varied from 16 gpm/ft^2 to 20 gpm/ft2, the Mn removal profiles overlapped with each other but as the HLR was further increased to 24 gpm/ft^2, there was a slight decrease in the amount of soluble Mn removed across the column. Overall, an increase in HLR had a very slight negative effect on the Mn removal profiles, an observation in agreement with the results obtained by Zuravnsky (2007).

Previous research (Knocke *et al.* 1988) has indicated that adequate free chlorine (HOCl) concentration was required to oxidize the adsorbed soluble Mn on the MnO_x(s) surface of the media. Although the rate of oxidation was considered rapid, the concentration of available oxidant could have an effect on the shape of the adsorption profile. The authors noted that the presence of free chlorine at a concentration of 1-2 mg/L was sufficient for maintaining soluble Mn removal on MnO_x(s)-coated media.

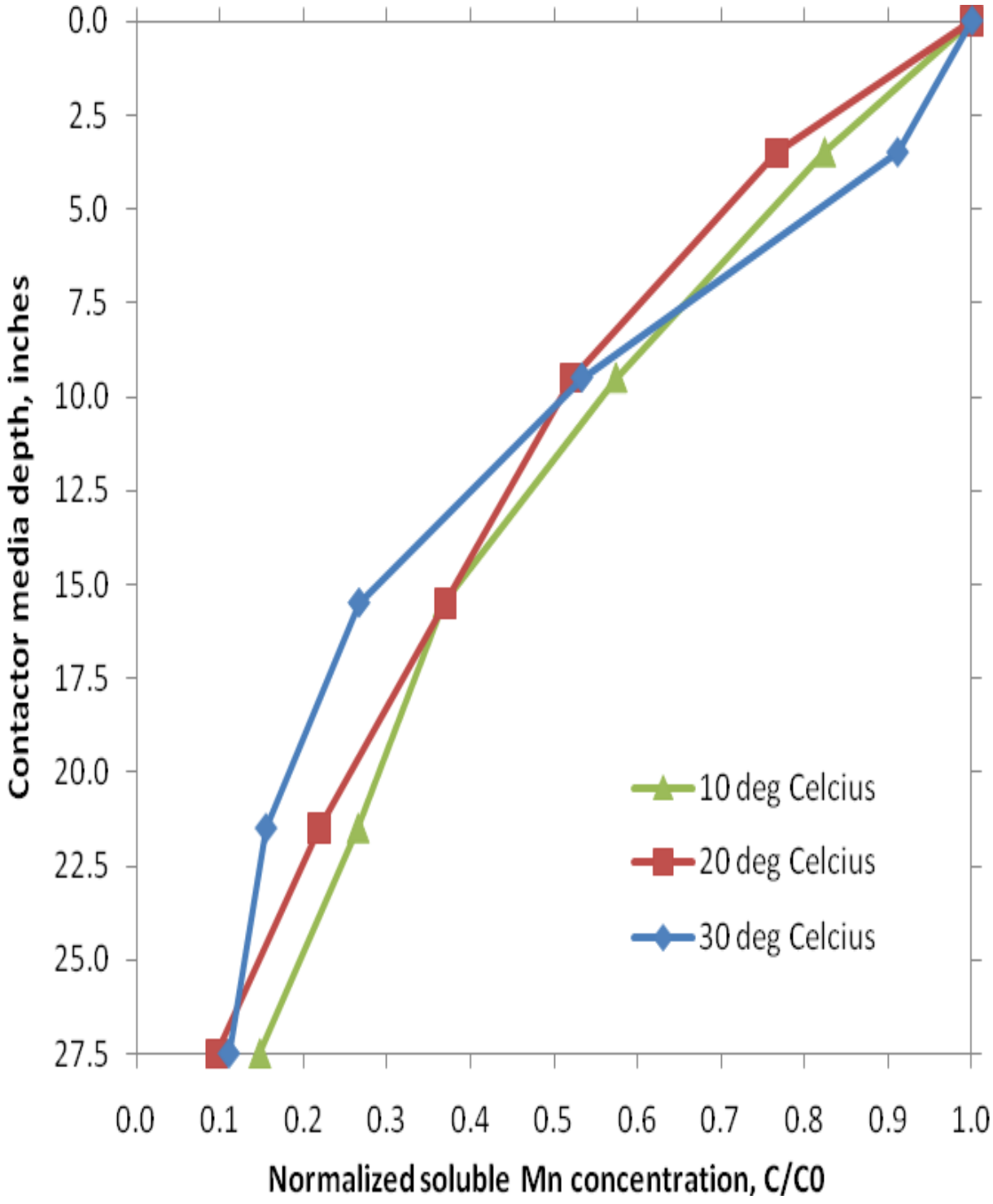

Figure 4.3 Effect of temperature on soluble Mn uptake in contactor plotted in terms of normalized Mn concentration, C/C_0

[Influent water: Mn^{2+} = 0.04-0.07 mg/L, pH = 6.5, HLR = 20 gpm/ft^2, free chlorine conc = 1.2-1.3 mg/L]

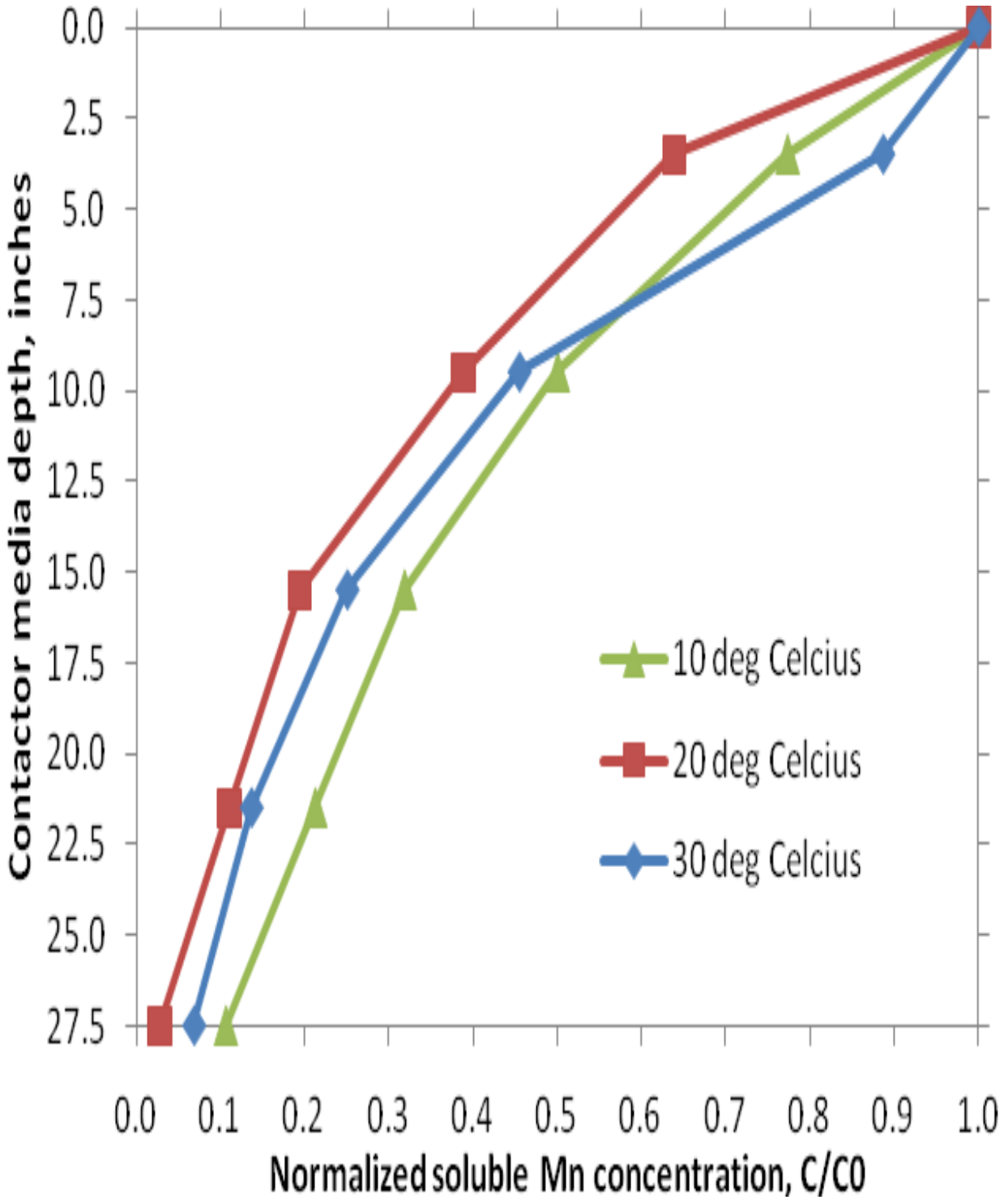

Figure 4.4 Effect of temperature on soluble Mn uptake in contactor plotted in terms of normalized Mn concentration, C/C_0

[Influent water: Mn^{2+}= 0.04-0.07 mg/L, pH = 7.0, HLR = 20 gpm/ft^2, free chlorine conc = 1.1-1.2 mg/L]

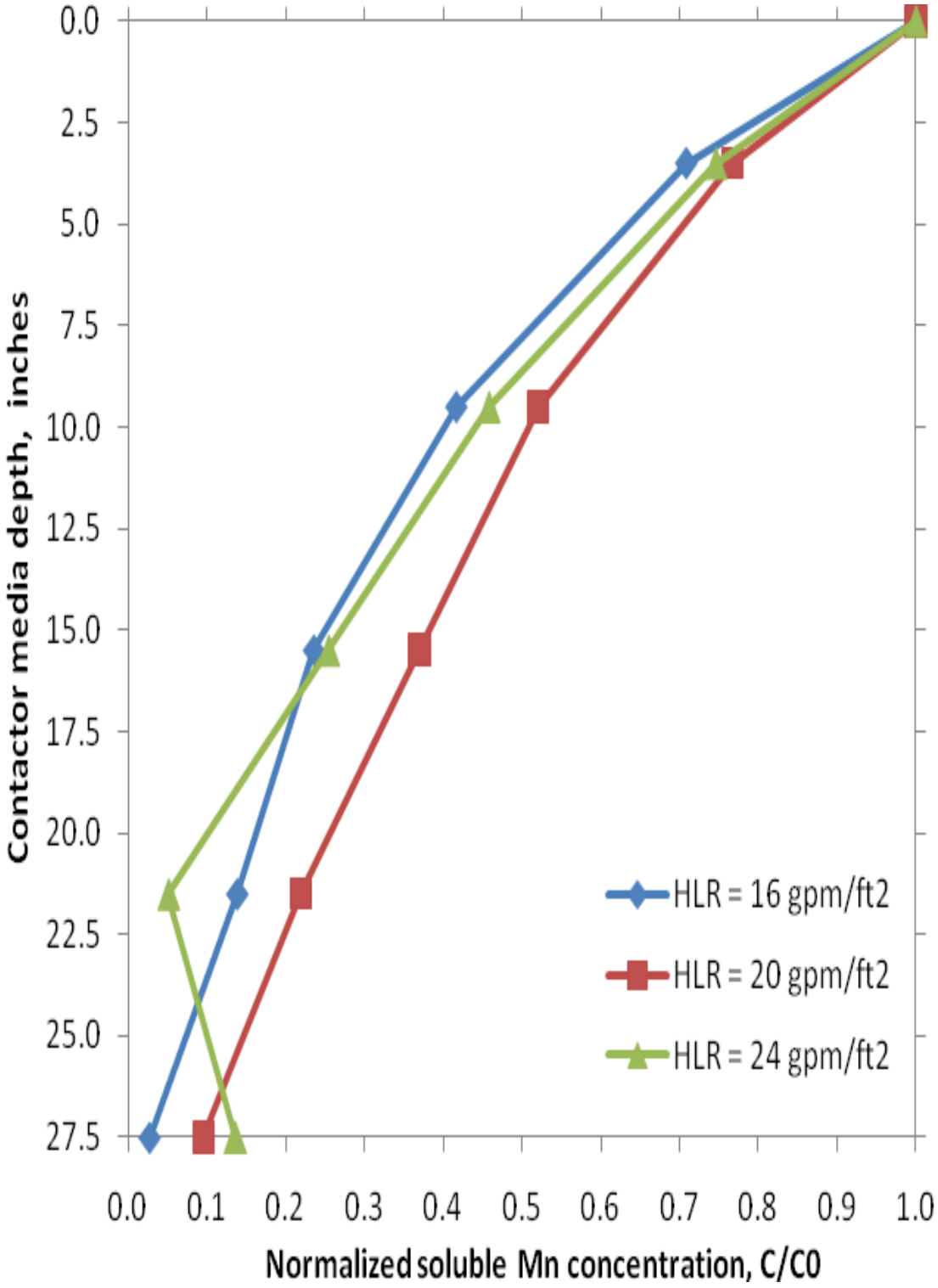

Figure 4.5 Effect of HLR on Mn Uptake in contactor in terms of normalized Mn concentration, C/C_0

[Influent water: Mn^{2+}= 0.06-0.07 mg/L, pH = 6.5, Temp = 20^0C, free chlorine conc = 1.1-1.2 mg/L]

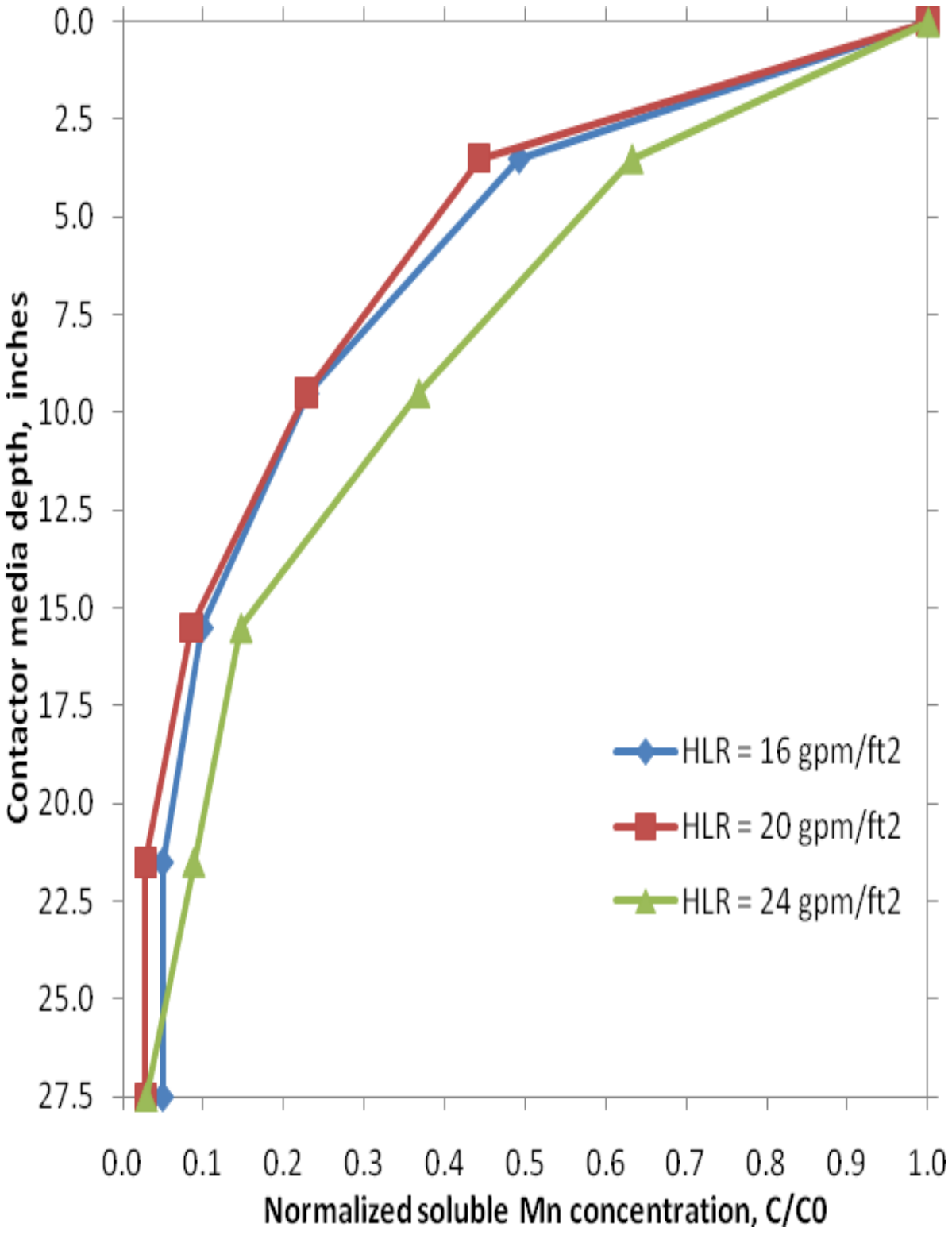

Figure 4.6 Effect of HLR on Mn Uptake in contactor in terms of normalized Mn concentration, C/C_0

[Influent water: Mn^{2+}= 0.06-0.07 mg/L, pH = 7.5, Temp = 20^0C, free chlorine conc = 1.1-1.3 mg/L]

The vast majority of the contactor studies were conducted using an free chlorine feed concentration ranging between 1.2-1.3 mg/L. However, Mn removal profiles from a few pilot-plant experiments were compared to determine the effect of free chlorine concentration on soluble Mn removal across the pyrolucite contactor. Representative results are shown in Figures 4.7 and 4.8. The applied water condition for data plotted in Figure 4.7 was an initial soluble Mn concentration of 0.055 mg/L, an HLR of 16 gpm/ft^2, temperature of 30^{0}C and a pH of 6.5. The applied water condition for data plotted in Figure 4.8 was quite similar to that in Figure 4.7 except for an elevated pH of 7.5.

Data plotted in Figures 4.7 and 4.8 showed a slight improvement in the soluble Mn removal profile as the influent free chlorine concentration was increased from 1.3 mg/L to 5 mg/L. This observation was in accordance with the results obtained from previous research by Zuravnsky (2007) that, increased free chlorine concentrations generally improved the soluble Mn removal profile by more rapidly regenerating the available Mn sorption sites at the media surface.

One item of concern is that very high free chlorine concentrations in the feed water could result in an increase in the disinfectant by product (DBP) concentrations in the treated water. Hence, water treatment utilities would have to strike a fine balance between achieving improved Mn removal profiles in the contactor and potentially increasing the DBP concentrations in the finished water. The data plotted in Figures 4.7 and 4.8, demonstrate that very effective Mn uptake can be obtained in a contactor without having to use very high free chlorine feed concentrations that could increase DBP concerns.

Media Uptake Capacity Studies & Modeling Results

As described in detail in Chapters 2 and 3, the soluble Mn uptake model was developed by applying first principles to a mass balance of soluble Mn across an incremental bed depth. The model incorporates use of input parameters such as the initial concentrations of Mn and free chlorine, the Freundlich isotherm constants describing Mn uptake onto the media surface (K and 1/n), the mass transfer coefficient (k_f) and the rate constant associated with the oxidation of Mn by HOCl (k_r).

The main objective of the model developed was to predict the soluble Mn removal performance of the adsorptive contactor when it was subjected to different applied water conditions. However, in order to ensure that the model functioned effectively in predicting the soluble Mn removal, it had to be calibrated for the various water conditions that might be encountered in a water treatment plant. The experimental data collected from the pilot-plant study served as a good baseline for the model calibration.

The input parameters for the model were determined for individual experiments since they were affected by applied water conditions and media characteristics. The influent Mn and Cl concentrations were known for each experimental scenario. The values for pore water velocity, axial dispersion coefficient and specific surface area of the pyrolucite media were calculated in detail for each of the HLR values based on the equations used by Zuravnsky (2007).

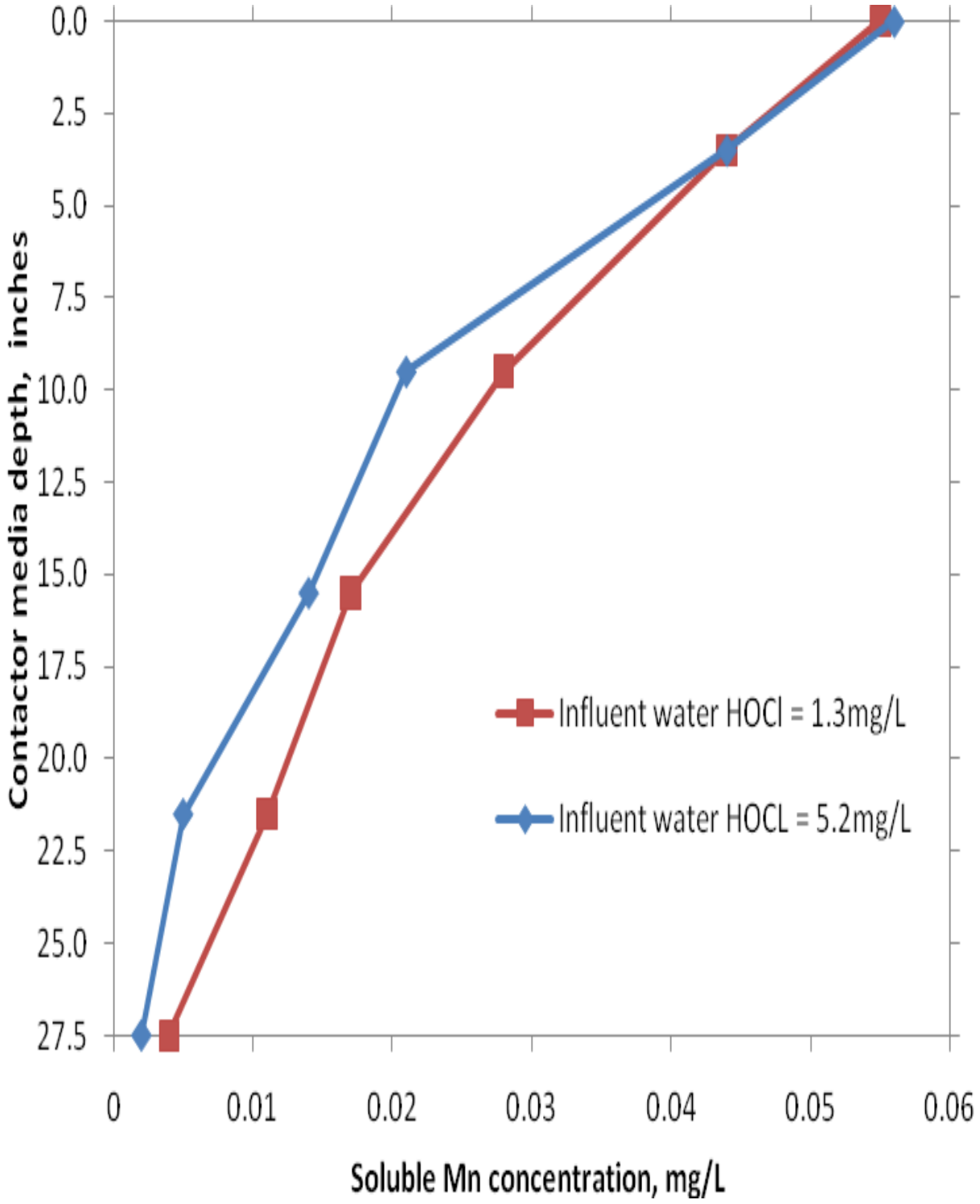

Figure 4.7 Effect of free chlorine on Mn Uptake in contactor in terms of normalized Mn concentration, C/C_0

[Influent water: Mn^{2+}= 0.055 mg/L, pH = 6.5, Temp = 30^0C, HLR = 16 gpm/ft^2]

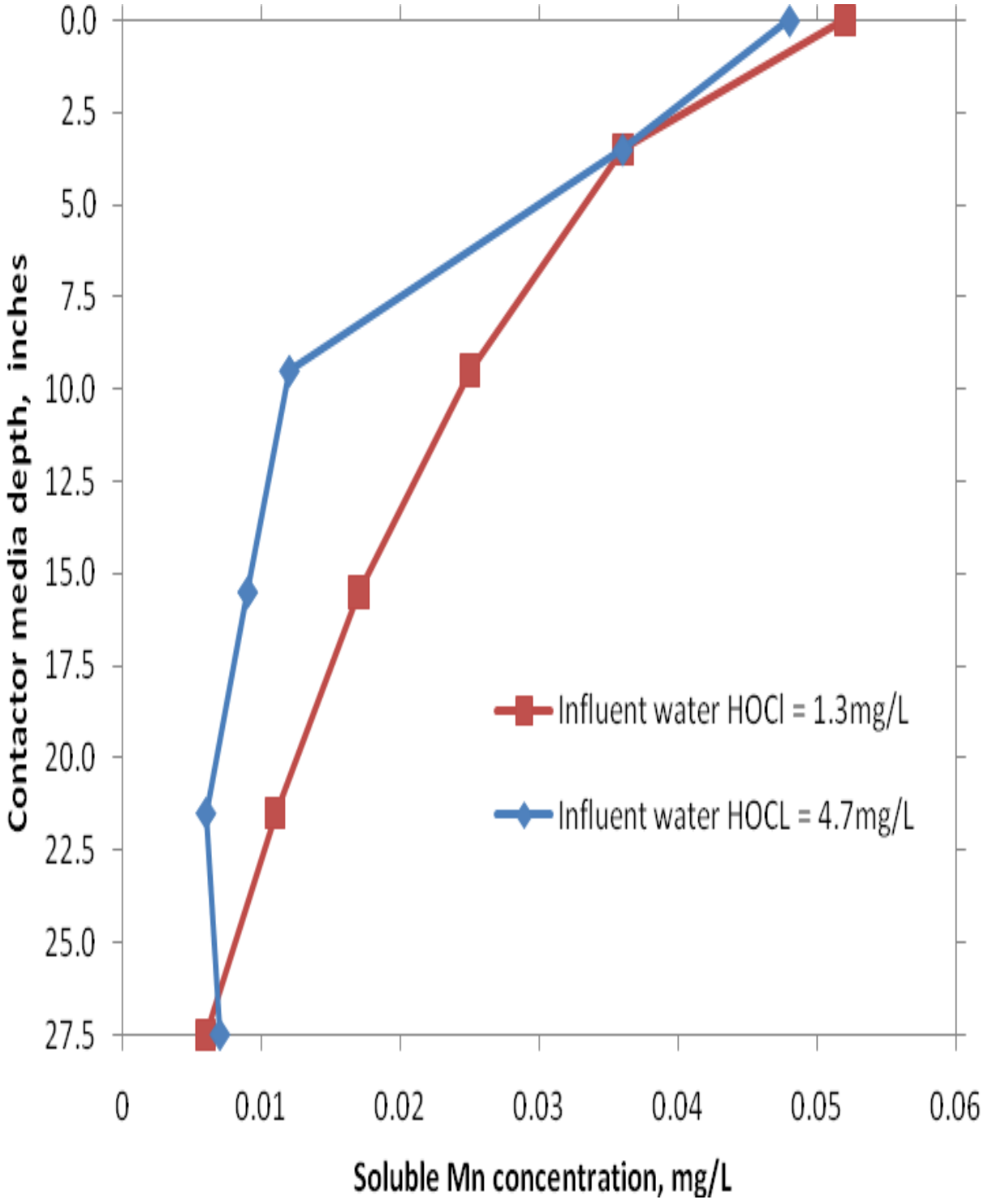

Figure 4.8 Effect of free chlorine on Mn Uptake in contactor in terms of normalized Mn concentration, C/C_0

[Influent water: Mn^{2+}= 0.05 mg/L, pH = 7.5, Temp = 30^0C, HLR = 16 gpm/ft^2]

The value of k_f was calculated by using a correlation proposed by Ohashi *et al.* as shown in Equation 4.1 (Roberts *et al.* 1985). This correlation was valid over the range of Reynolds numbers calculated (5.8<R<500) for pyrolucite media under the experimental HLR conditions from 16-24 gpm/ft^2. The units were then converted for use in the model.

$$Sh \approx \frac{k_f d_p}{D_{L,diff}} \approx \left(2 + 1.21 R^{1/2} Sc^{1/3} \right) \tag{4.1}$$

where:
Sh = Sherwood number
k_f = liquid to solid mass transfer coefficient (m/s)
d_p = particle diameter (m)
$D_{L,diff}$ = bulk liquid diffusivity (m^2/s) = $1x10^{-9}$ m^2/s @ 20°C
R = Reynolds number (= Ud_p/υ)
Sc = Schmidt number (= $\upsilon d_p/D_{L,diff}$)
υ = kinematic viscosity = $1.004x10^{-6}$ m^2/s @ 20°C

The Freundlich isotherm constants (K and 1/n) were calculated using the soluble Mn uptake capacity experimental data for conditions corresponding to pH values of 6.5 and 7.5. The short-term soluble Mn uptake capacity of the media was determined by the four-hour protocol method developed by Bouchard (2005), previously discussed in detail in Chapter 3. The media used for the uptake capacity study was removed from the Newport News (NN) pilot plant column at the end of the contactor study. The water used for the test was also obtained from the NN water treatment facility. Pyrolucite media Mn uptake capacities were measured over a range of soluble Mn concentrations from 0.05-0.5 mg/L. Estimates for K and 1/n (shown in Table 4.1) were then made for the media from a log-log (Freundlich isotherm) plot of the appropriate uptake capacity data.

An interesting observation within this research was related to the changes in the Mn uptake capacity of the pyrolucite media during the course of its usage in the contactor; relevant data to the issue are shown in Figure 4.9. As mentioned previously the pyrolucite media in the NN contactor was tested for Mn uptake capacity following several months of usage in the pilot-plant study. Zuravnsky (2007) had also evaluated the uptake capacity of pyrolucite media, when it was fairly new and had not been exposed to the level of Mn and hydraulic loading seen in the NN pilot-plant study. On a comparative basis the Mn uptake capacity of pyrolucite media increased rather substantially over the extended period of usage, most likely due to the deposition of additional MnO_x(s) coating on the media surface that generated additional Mn uptake sites. It should be noted that the results labeled "UMASS Water" in Figure 4.9 relate to Mn uptake tests conducted in the University of Massachusetts using very similar dissolved major ion makeup as the NN water, with the exception being the lack of DOC present in the UMASS water in comparison to the 3.5-4.0 mg/L of DOC typically present in the NN water samples used in this study.

The Mn uptake results from Zuravnsky (2007) and additional Mn uptake testing of new pyrolucite media allowed for an estimate of Freundlich isotherm constants K and 1/n to be made that might characterize the uptake performance of this media when relatively new or unused.

Using Mn uptake data for pH 7.5 studies allowed for estimates of K and 1/n for newer pyrolucite media to be developed as 0.34 mg Mn/g media and 0.89 respectively.

The adsorption capacity of the media was affected not just by pH but also by temperature changes. Hence, in order to study the effects of temperature on the uptake capacity of the pyrolucite media, the media uptake capacity tests were also done at three different temperatures (10^0C, 20^0C and 30^0C) for an initial Mn concentration of 0.5 mg/L. Data presented in Table 4.2 show the effect of temperature on the adsorption capacity of the contactor media. Results demonstrated that as the temperature increased from 10^0C to 30^0C for a particular pH, the Mn adsorption capacity of the pyrolucite media also increased.

The estimation of Freundlich isotherm constants for Mn uptake onto the pyrolucite media was key to the modeling efforts. With the K and 1/n values available and other model information being directly provided as input or calculated (e.g., k_f calculated by Ohashi correlation) the only unknown parameter in the model was k_r, which related to the rate of surface oxidation of Mn by HOCl. As such it was possible to use the soluble Mn removal profiles from the pilot-plant contactor studies (conducted under defined experimental conditions of pH, initial Mn and free chlorine concentration, temperature and HLR) and allow the model to generate appropriate estimates of k_r.

Table 4.1
Freundlich isotherm constants for "used" pyrolucite media from Newport News pilot-plant

pH/Temperature Range	6.5/ 20-25 ^{0}C	7.5/ 20-25 ^{0}C
K (mg Mn/g media)	0.72	0.88
1/n	1.20	1.19

Table 4.2
Temperature and pH effects on the Mn uptake capacity of "used" pyrolucite media
[Initial Mn concentration = 0.5 mg/L]

Applied Water pH	Mn uptake capacity of pyrolucite media at various applied water temperatures (mg Mn/g media)		
	10^0C	20^0C	30^0C
6.5	0.27	0.30	0.31
7.5	0.29	0.32	0.36

As described in Chapter 2, manipulation of the soluble Mn mass balance equation provided a group of three solvable steady-state equations (equations 2.3-2.5) which were then coded into a statistical software called R. The model was found to be non-linearly dependent on the unknown parameter k_r. Hence, the approach adopted to solve the model was one wherein the best-fit parameter was determined by the process of minimization of the least square vector (χ^2) returned

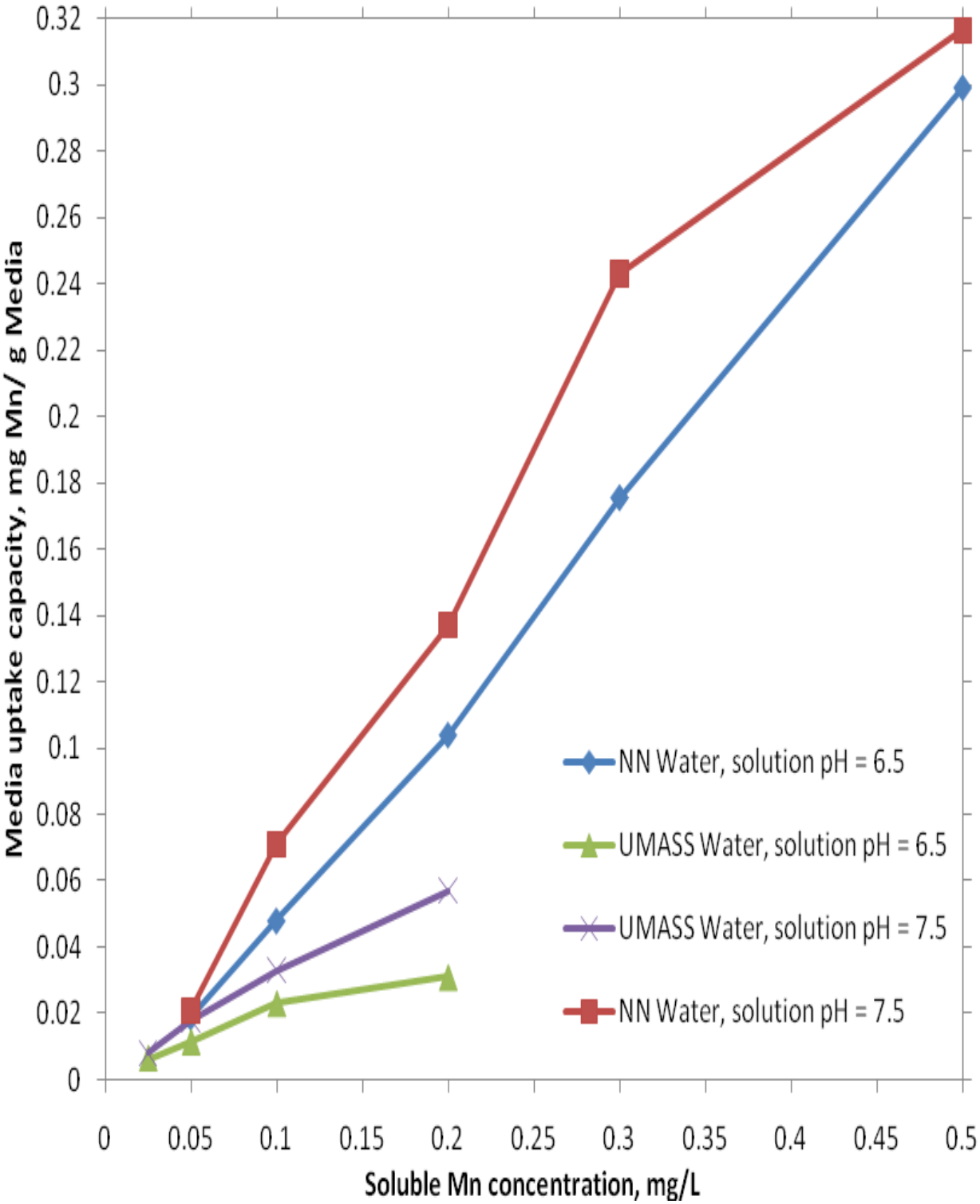

Figure 4.9 Mn Uptake (short-term capacity studies) on pyrolucite Media as a function of pH & Initial Mn Level for Newport News Water & UMASS Water (Temperature = 20^0C)

by the function which predicted the soluble Mn concentration at various depths of the contactor column. However, owing to the non-linear dependence the minimization had to proceed iteratively, i.e. trial values were initially given for the unknown parameter k_r and then a procedure was developed that improved the trial solution. The procedure was then repeated until χ^2 value effectively stopped decreasing.

The method used for solving the non-linear model was a variation of the Levenberg-Marquardt method (Press *et al.* 2002). The best-fit estimate of k_r obtained was one which resulted in a close match between the actual Mn removal profiles and the model predicted Mn removal profiles across the contactor depth. Figures 4.10 and 4.11 show a comparison of the Mn removal profiles obtained from the NN pilot-study and as predicted by the model. In both figures "Soluble Mn removal profile – pilot-plant data" refers to the actual data obtained from the pilot studies at NN and "Soluble Mn removal profile – model output" refers to the data predicted by the model for the same operating conditions.

The applied water conditions in Figure 4.10 correspond to a temperature of 20^0C, pH value of 6.5, initial Mn concentration of roughly 0.087 mg/L, free chlorine concentration of 5.1 mg/L and HLR value of 24 gpm/ft^2. The applied water conditions for data in Figure 4.11 are similar to the ones in Figure 4.10 with the exception of a lower free chlorine concentration and HLR value of 1.2 mg/L and 20 gpm/ft^2 respectively. In both the figures it was seen that the model predicted Mn removal profile was a good fit to the actual data obtained from the pilot-study.

In addition to modeling the pilot plant data, sensitivity of the model to changes in the parameter k_r were studied. The knowledge of parameter sensitivity was important for identifying the effect parameter estimation may have on the model output. The value of k_r was varied by approximately 0.5 and 1.5 times the original estimation predicted by the model for a particular set of operating conditions. The resulting Mn removal profiles were plotted with the original model predicted profile and also the actual pilot-plant data for comparison (Figure 4.12). The applied water conditions for data in Figure 4.12 are similar to those in Figure 4.11. At the specified operating conditions, the best-fit k_r value as estimated by the model was 1.45E-02 and it resulted in a Mn removal profile which was a good fit to the actual data obtained from the pilot-plant study. However it was observed that in Figure 4.12, varying the k_r value by 0.5 and 1.5 times the model estimated value, had a large effect on the model predicted Mn removal profiles. This indicates that the model is quite sensitive to changes in k_r.

The pilot-plant data were modeled for pH values of 6.5 and 7.5 and temperature corresponding to 20^0C. The modeling was not implemented for the temperatures of 10^0C and 30^0C due to a lack of the freundlich isotherm constants for those temperatures. The results for the best-fit k_r obtained from the model for the above conditions are tabulated in Table 4.3. Based on the results, it was observed that for data where the initial Cl concentration was approximately 1.2-1.3 mg/L, the k_r values increased with an increase in pH. For the last two sets of data in Table 4.3 which have a higher initial Cl concentration over the rest of the data, the best fit k_r value as predicted by the model decreased when pH increased from 6.5 to 7.5. On comparing the first two sets of data in Table 4.3 with the last two sets, it was noticed that there was a slight decrease in the k_r values as the feed free chlorine values increased from 1.3 to 5.1. This seems to indicate that the model may be sensitive to the initial Cl concentration in the water feed. However, this observation cannot be

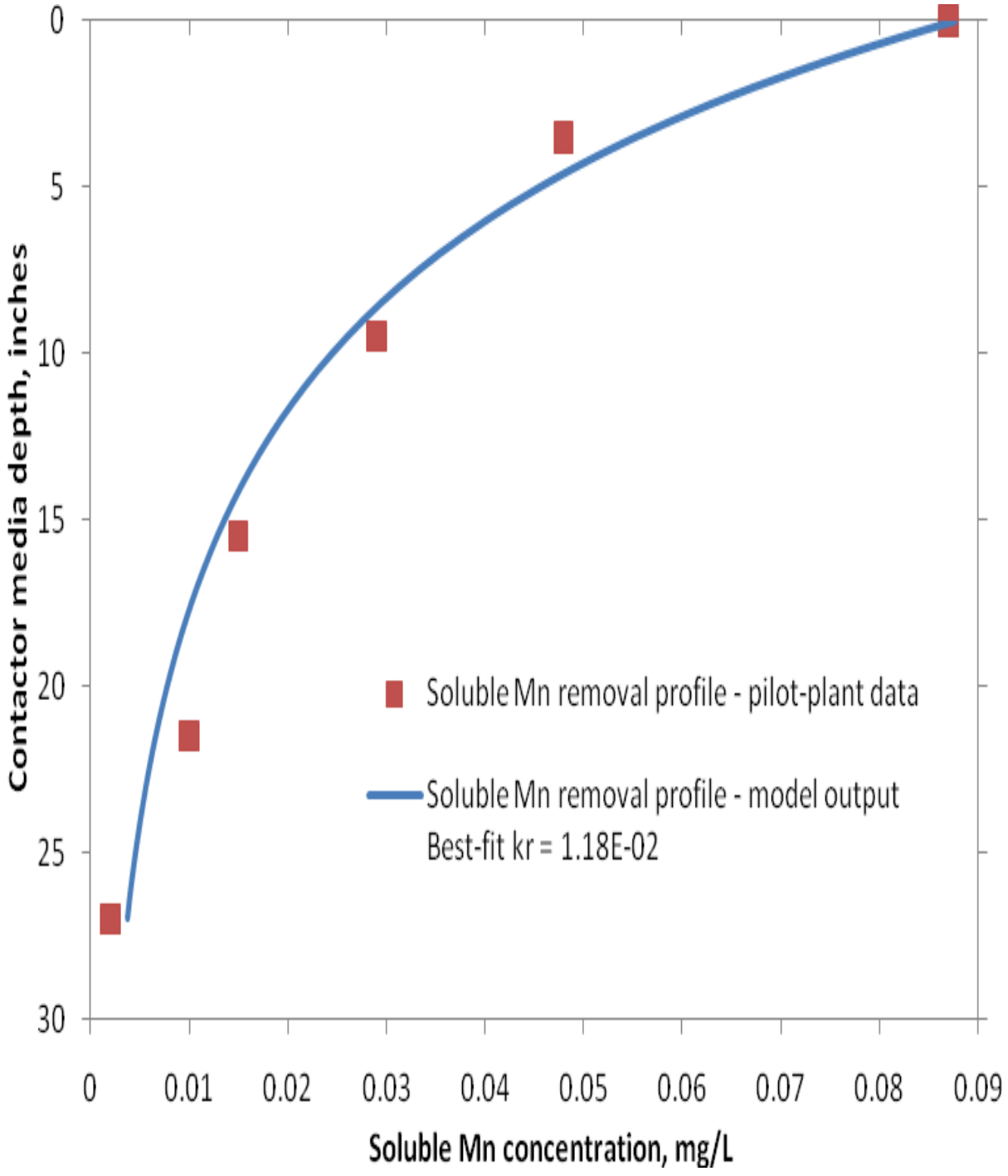

Figure 4.10 Comparison of Mn removal profiles over depth of contactor media obtained from pilot-plant studies and as predicted by the model

[Influent water: Mn^{2+}= 0.087 mg/L, free chlorine conc = 5.1 mg/L, pH = 6.5, Temp = 20^0C, HLR = 24 gpm/ft^2]

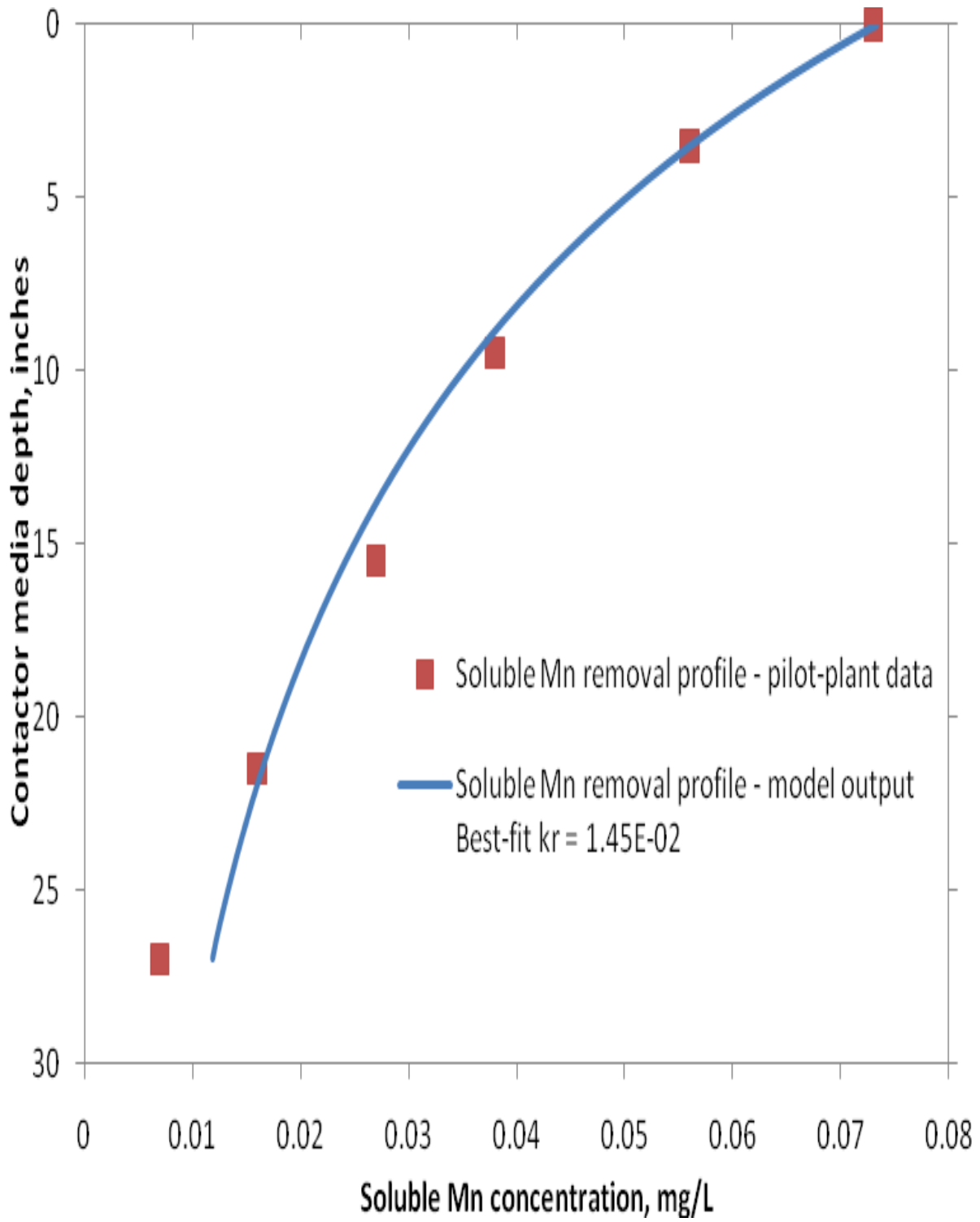

Figure 4.11 Comparison of Mn removal profiles over depth of contactor media obtained from pilot-plant studies and as predicted by the model

[Influent water: Mn^{2+}= 0.073 mg/L, free chlorine conc = 1.2 mg/L, pH = 6.5, Temp = 20^0C, HLR = 20 gpm/ft^2]

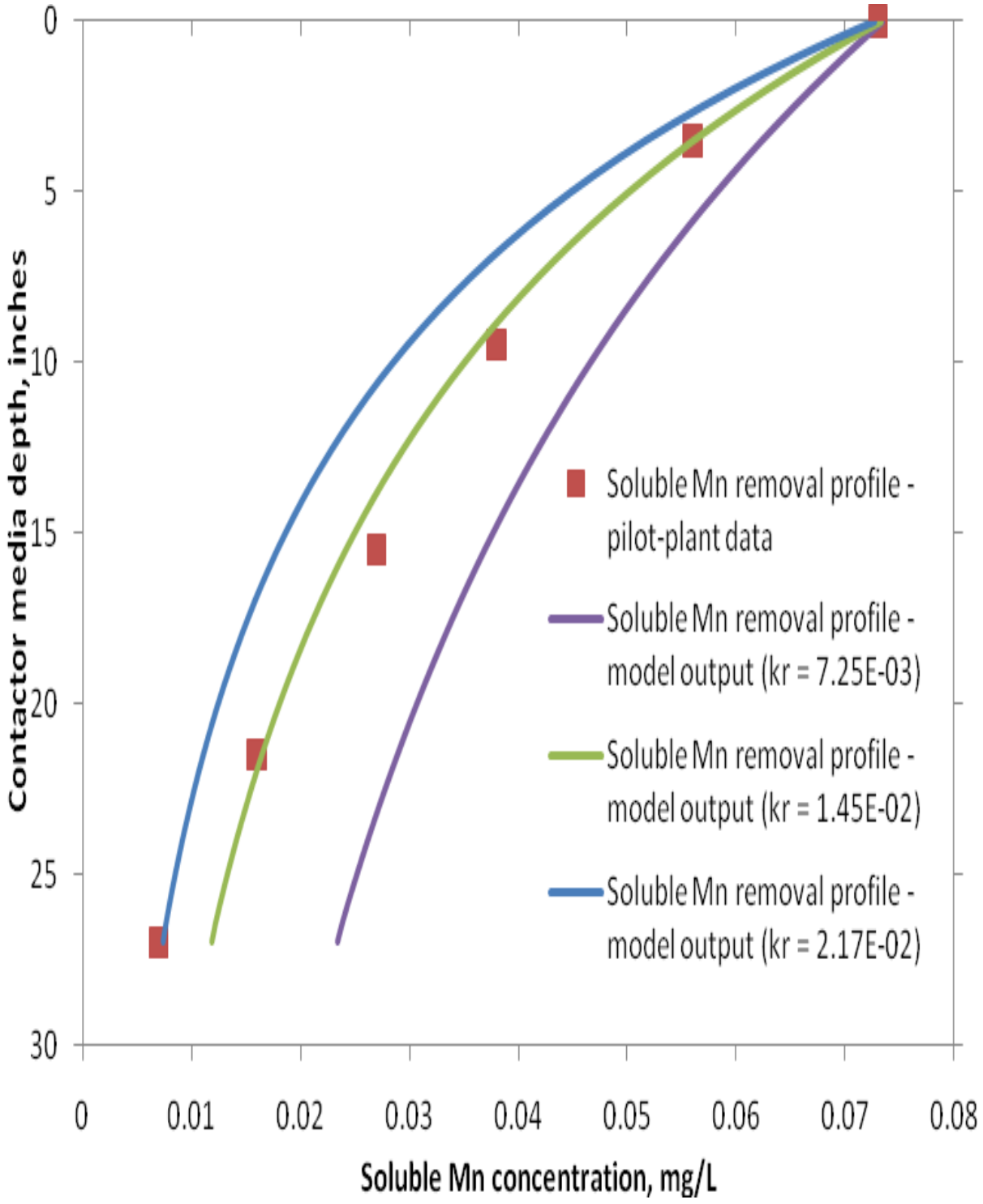

Figure 4.12 Sensitivity analysis: effect of k_r on model output

[Influent water: Mn^{2+}= 0.073 mg/L, free chlorine conc = 1.2 mg/L, pH = 6.5, Temp = 20^0C, HLR = 20 gpm/ft^2]

Table 4.3
Model results for data obtained from Newport News pilot-plant for temperature = 20^0C

Initial Mn Concentration, mg/L	Initial Free Cl Concentration, mg/L	pH	HLR, gpm/ft^2	Best-fit k_r estimation by model	Standard Error
0.06	**1.3**	**6.5**	**24**	**2.63E-02**	**0.0041**
0.07	1.3	7.5	24	3.23E-02	0.0033
0.07	**1.2**	**6.5**	**20**	**1.45E-02**	**0.0012**
0.07	1.2	7.5	20	9.76E-02	0.0397
0.07	**1.1**	**6.5**	**16**	**1.96E-02**	**0.0017**
0.06	1.3	7.5	16	3.87E-02	0.0068
0.09	**5.1**	**6.5**	**24**	**1.18E-02**	**0.0024**
0.09	5.2	7.5	24	7.78E-03	0.0013

confirmed unless more tests are done at varying influent chlorine concentrations and those data are modeled.

Column Head-loss, Media Backwash & Sieve Analysis Results

During the pilot-plant study at the NN facility, a significant amount of head loss was observed to develop across the contactor column. Figure 4.13 shows the headloss buildup across the contactor column as a function of time. The data plotted in Figure 4.13 indicate that there was visible headloss accumulation across the column over the period of the pilot plant study. This observation was quite contrary to the expected behavior across the column since the water that was being fed into the contactor column was post-filtration water obtained from the Lee Hall water treatment plant. As mentioned in detail in Chapter 3, the feed water had already passed through a dual-media filter comprised of anthracite and coal in the treatment plant and hence did not contain any particulate matter (which was quite evident by its low turbidity of < 0.1 NTU).

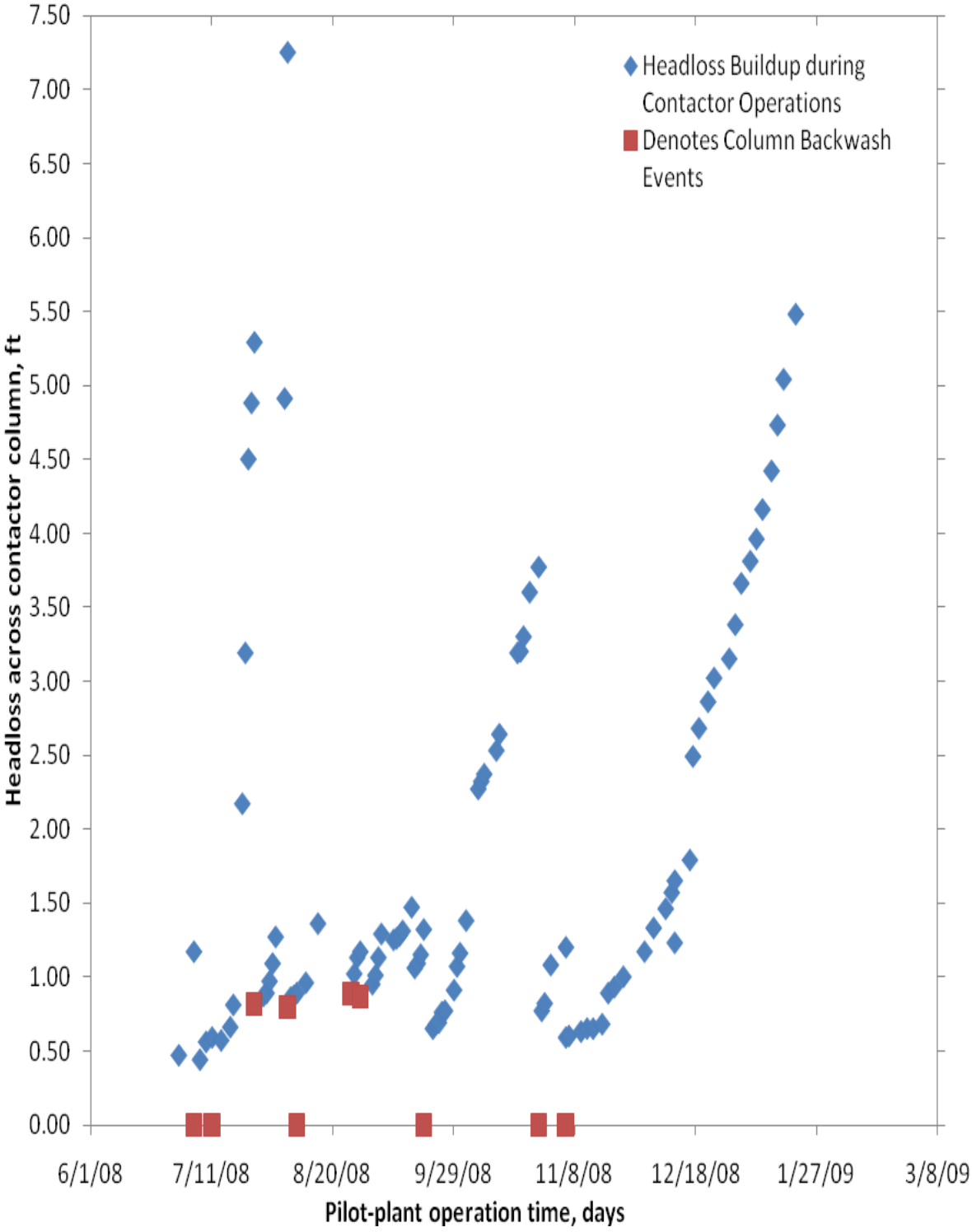

Figure 4.13 Headloss buildup across contactor column as a function of time

Further, the water was being loaded to the contactor at high HLR values. Coupled with the large pyrolucite media size and the absence of any coagulant in the contactor feed water it was felt that the feed water would not promote any kind of direct deposition of particles within the contactor.

Explanations were considered as to why such large head loss values (up to 6-7 feet) were occurring between backwash events. This head loss could have been due to the soluble Mn uptake and subsequent oxidation on the media surface, resulting in a direct deposition of $MnO_x(s)$ onto the surface of the pyrolucite media. Another possible explanation could be the bonding together or "cementation" of the media particles due to $MnO_x(s)$ formation, resulting in a partial blocking of the available sites or pore spaces. The decreased void spaces within the media bed would then result in the generation of additional head loss across the column as water was required to travel at higher flow velocities in order to maintain the HLR.

In order to better understand the headloss buildup pattern and to also identify the depths across the column where there was significant particle depositions occurring, manometers were added in the later part of the pilot study at each of the sampling ports in the contactor (ports D, E, F, G). The addition of manometers provided the opportunity to collect cumulative head loss readings at each of the sampling ports in the contactor column. The plot of total head loss accumulation at each sampling port as a function of the bed volume of feed water that flowed through the contactor column is shown in Figure 4.14. A substantial amount of the head loss build-up (up to 2 feet) occurred at the top part of the contactor media (across port D) and that head loss across each of the other sampling ports reduced significantly on proceeding down the depth of the contactor media. The phenomenon of more soluble Mn uptake being concentrated in the upper portion of the filter bed consisting of a $MnO_x(s)$-coated media has been noted by Bouchard (2005) and by Hargette and Knocke (2001). This accounts for the increased deposition of Mn in the upper part of the pyrolucite column observed in Figure 4.14, thereby resulting in increased inhibition of flow regime in the upper portion of the contactor media as compared to the lower portion of the contactor.

In Figure 4.14, the data plot corresponding to the total head loss across contactor column show a head loss build-up up to 5.5 feet. The data values in this plot corresponded to the headloss which was built between the last sampling port of the contactor (21.5") and the sampling port which was 0.5" below the contactor column (27.5"); a visual inspection of the support disc was conducted and showed evidence of substantial precipitate accumulation on the screen. The precipitate which was observed on the screen was assumed to be MnOx(s), however owing to lack of time; it was not tested in the lab. This buildup of deposits on the screen would have blocked the available openings in the support disc for the feed water to pass through, thereby resulting in the observed head loss accumulation at the lowest layer of the contactor column where there was not much Mn uptake. It was also observed that around 100,000 gallons of water flowing through the contactor column resulted in a head loss of about 5.5 feet across the column. Towards the end of the pilot study, water samples were collected while the contactor column was backwashed. This procedure was conducted in order to identify a loading rate that was suitable for column backwash and also to analyze the amounts of soluble Mn that was retained in the column. The backwash procedure consisted of washing the contactor column with water at four different HLR values: 4 gpm/ft^2, 20 gpm/ft^2, 40 gpm/ft^2 and 80 gpm/ft^2. Here, except for 80 gpm/ft^2, the remaining loading rates were all sub-fluidization rates. The purpose of having the

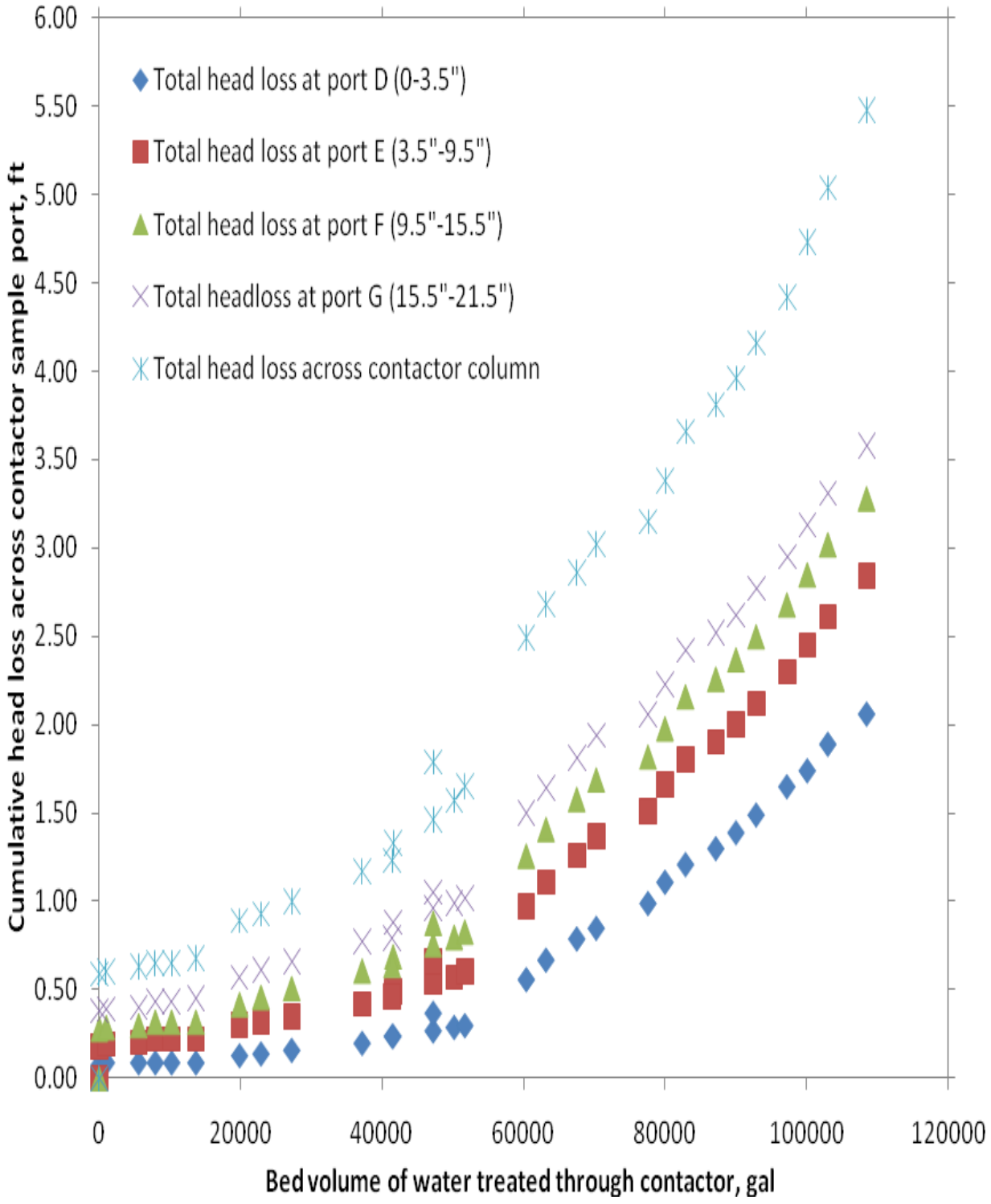

Figure 4.14 Total head loss buildup at each sampling port of the contactor as a function of bed volumes of water flowing through the contactor column

backwash procedure done at four different hydraulic loading rates was mainly to study the effect of loading rates on the release of Mn during backwash. The water was maintained at each of the specified HLR values for approximately four minutes and the backwash samples collected were analyzed for Mn concentration. Two complete backwash cycles were analyzed and the percentage of Mn released as a function of backwash HLR calculated; results are tabulated in Table 4.4. It was observed that a total of 8.6 and 14.1 g of Mn were removed during the backwash cycles 1 and 2 respectively. The data presented in Table 4.4 shows the percentage split-up of the Mn removed across each of the loading rates. In addition, mass balance calculations were done to calculate the amount of Mn that were adsorbed onto the pyrolucite media in the contactor operating cycle prior to each of these two backwash cycles. It was noted that 12.2 and 38.3 g of soluble Mn were loaded onto the contactor prior to backwash cycles 1 and 2 respectively. Based on these calculations it can be seen that approximately 71% and 37% of the Mn loaded onto the contactor were removed during the backwash cycles 1 and 2 respectively. Data presented in Figures 4.15 and 4.16 show the comparative log plots for the amount of Mn released for each of the four HLR's in the first and second backwash cycles respectively as a function of backwash time.

Table 4.4
A comparison of Mn released during each of the four backwash periods

Backwash Cycle 1 – 10/27/2008		**Backwash Cycle 2 – 01/21/2009**	
Backwash Flow Rate, gpm/ft^2	**% Manganese Released**	**Backwash Flow Rate, gpm/ft^2**	**% Manganese Released**
4	0.002	4	0.002
20	0.206	20	0.056
40	1.181	40	7.920
80	98.611	80	92.022
TOTAL	**100**	**TOTAL**	**100**

Visual observation during the two backwash cycles showed that the pyrolucite media bed expanded and moved about only when the HLR was maintained at 80 gpm/ft^2. The other three HLR values were all sub-fluidization rates, yielding no observed media movement. The sub-fluidization velocities were used to assess if any of the deposition of mass in the contactor would be easily released (hence, not strongly bound in some manner to the media). Data in Figures 4.15 and 4.16 indicate that most of the Mn was released only when the HLR was 80 gpm/ft^2, and that hardly any Mn was released during the sub-fluidization rates. This would indicate that most of the Mn adsorbed onto the media surface did not exist as individual particles. Instead, the observed behavior during backwash would support a hypothesis that Mn precipitation taking place on the surface of the media was causing a "cementation" of the media particles and that it required a high HLR in order to expand the bed and break down the precipitated material,

thereby releasing particulate forms of Mn into the backwash water. The observed effect of the backwash rate on the amount of Mn released during filter backwash was in agreement with the findings of Hargette and Knocke (2001), who reported that media dislodgement during backwash resulted in particulate, oxidized Mn solids being released from the media coating.

Since the cycle of Mn adsorption and oxidation theoretically add layers of $MnO_x(s)$ to the filter media grains, a physical test was conducted as a part of the research to analyze if the size of the pyrolucite media had increased over time. For this purpose, a sieve analysis of both new and "used" pyrolucite media was conducted to quantify the changes in the size distribution, if any, of the contactor media. The procedure consisted of passing approximately 500 g of the required media sample through various sieves having openings ranging between 0.59 mm to 4.76 mm (U.S Standard Sieve Numbers – 4, 6, 8, 10, 16 and 30). The weight of the media retained on each sieve was recorded and used to generate a media size distribution. Data presented in Figure 4.17 show the comparative percent finer by weight plots for the "used" and the new pyrolucite media. From the data plotted in Figure 4.17 it was clear that the size distribution of both the used and new media were pretty comparable except for a minor variation in the plot between sieve sizes of 2.3 mm and 3.3 mm. This indicated that there was no major shift in the size distribution of the contactor media, an outcome in agreement with the work of Knocke et al. (1990) who reported no significant impacts on the anthracite and sand media size and specific gravity due to $MnO_x(s)$ coatings.

The above observation can be explained better with the help of an example theoretical calculation as described below. The average particle size of the pyrolucite media used in the NN pilot-plant contactor was 2 mm. For ease of calculation, the media particles were assumed to be uniformly spherical and the volume of each particle was calculated to be approximately $4.19*10^{-3}cm^3$ (Volume of a sphere = $4\pi r^3/3$). As noted in Table 2.2, the specific gravity of pyrolucite is 4.15 g/cm^3. Hence using the values of specific gravity and volume, the weight of a 2mm diameter pyrolucite media particle can be calculated to be 0.017g. From Figure 4.17, it was noted that roughly 80mg of MnO_2/g media was retained at sieve size of 2mm. The additional weight of the $MnO_x(s)$ coating on the original media particle is calculated as $1.36*10^{-3}g$ (= $0.017*0.08$). Hence the new weight of the media particle would be 0.018g (=$0.017+1.36*10^{-3}$). Dividing the new weight by the specific gravity of pyrolucite would result in the new volume of the media particle to be $4.43*10^{-3}cm^3$. Based on the new volume obtained, the new estimated diameter of the coated media particle was calculated to be 2.01 mm. It was observed that the new diameter of the pyrolucite media particle was only 0.5% more than the original diameter of 2mm, an inconsequential size increase. This supports the findings from the sieve analysis that over time there was no major shift in the size distribution of the contactor media.

In addition to the sieve analysis, tests were conducted for extraction of Mn from the used pyrolucite media in the pilot plant at the various sampling ports. The HAS extraction method published by Knocke *et al*. (1990) described in detail in Chapter 3, was used to determine the extractable amount of manganese oxide coating on the media. After the six-hour contact period, roughly 50-55 mg Mn/g of used media was extracted across the contactor media. The observed value of extractable Mn coating was much higher than the new pyrolucite and "used" pyrolucite values of 10-11mg/g and 25-26mg/g respectively, reported by Zuravnsky (2007). The higher value of extractable Mn could be attributed to the long term accumulation of $MnO_x(s)$ solids on

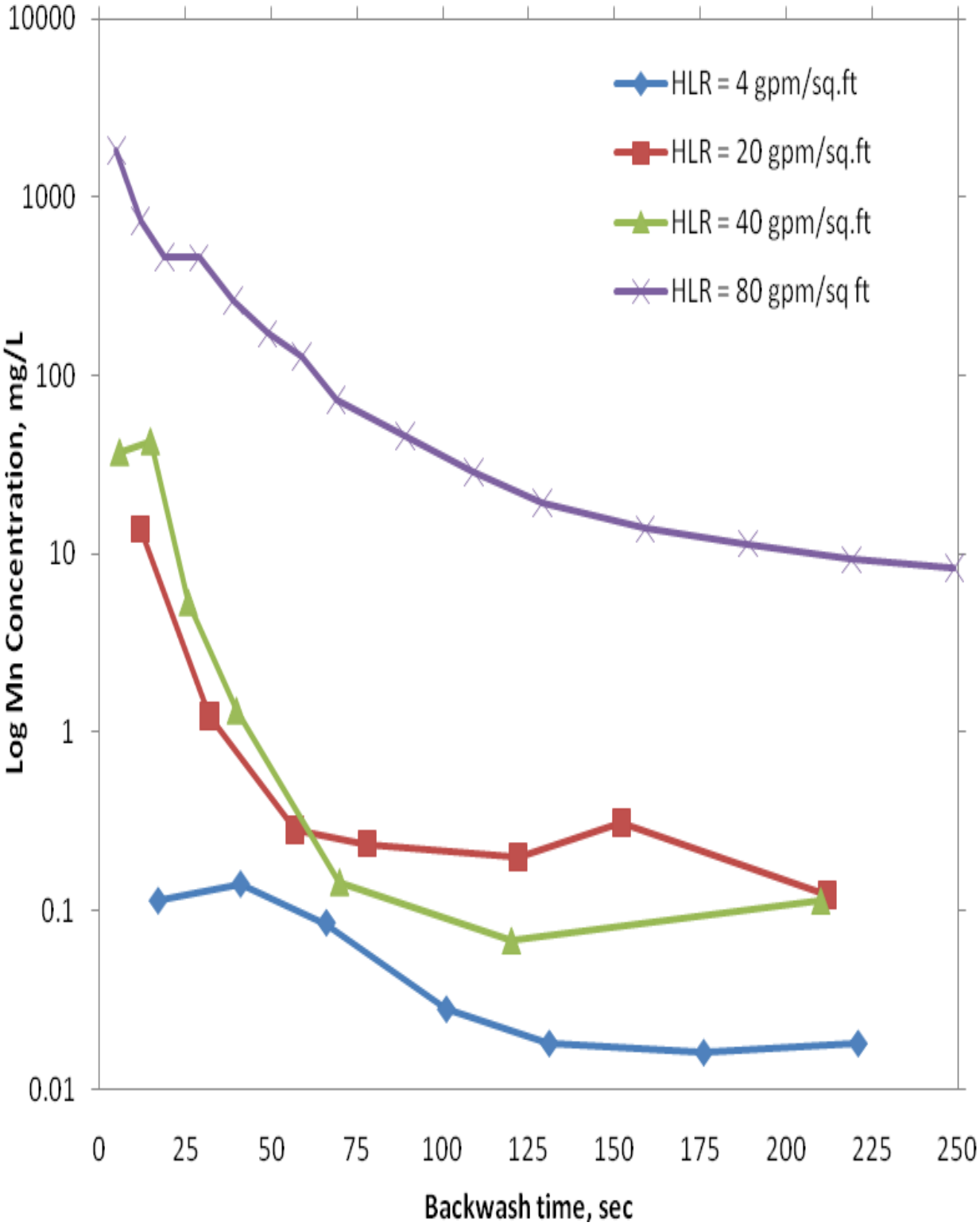

Figure 4.15 Amounts of Mn released during backwash as a function of time (backwash cycle: 10/27/2008)

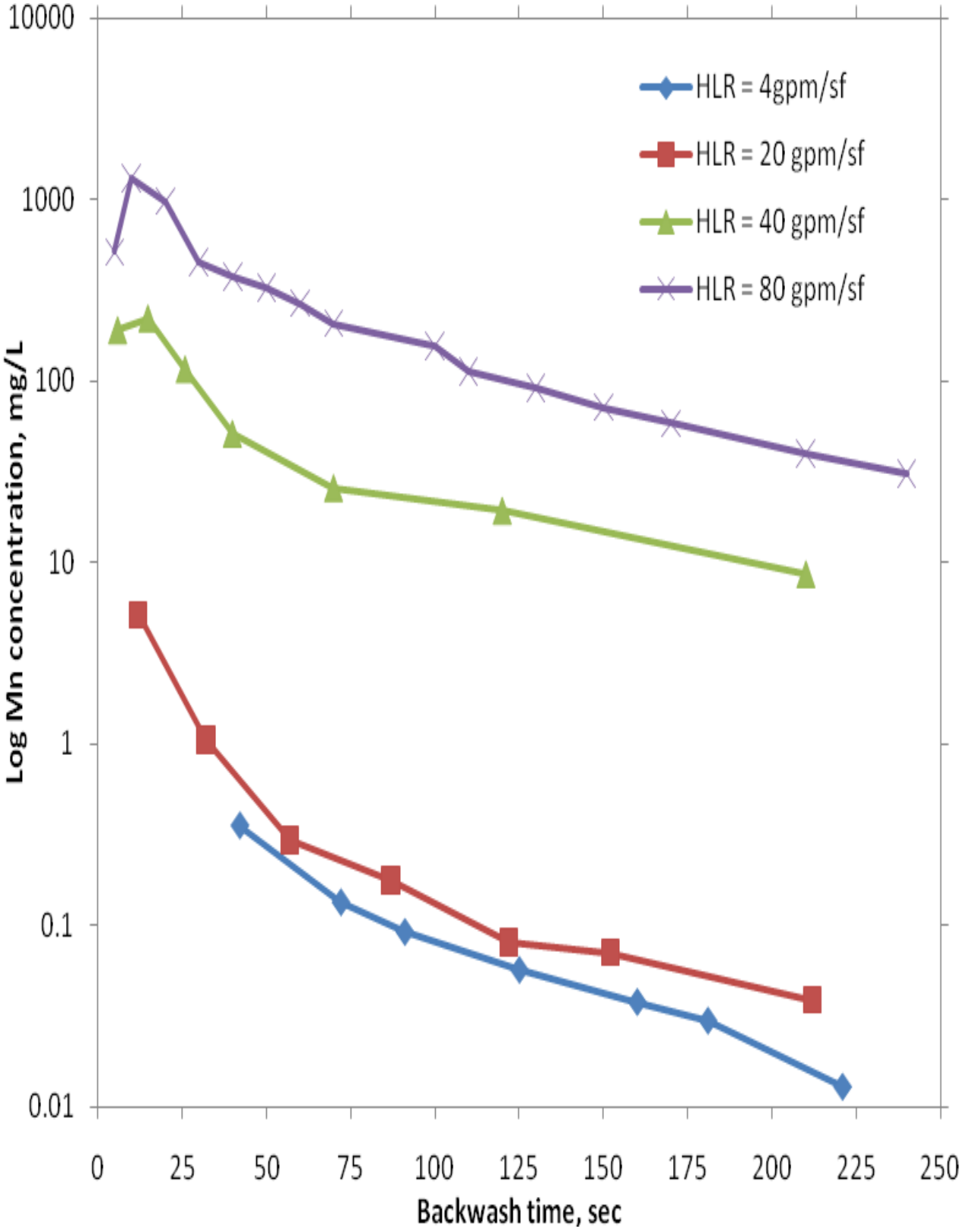

Figure 4.16 Amounts of Mn released during backwash as a function of time (backwash cycle: 1/21/2009)

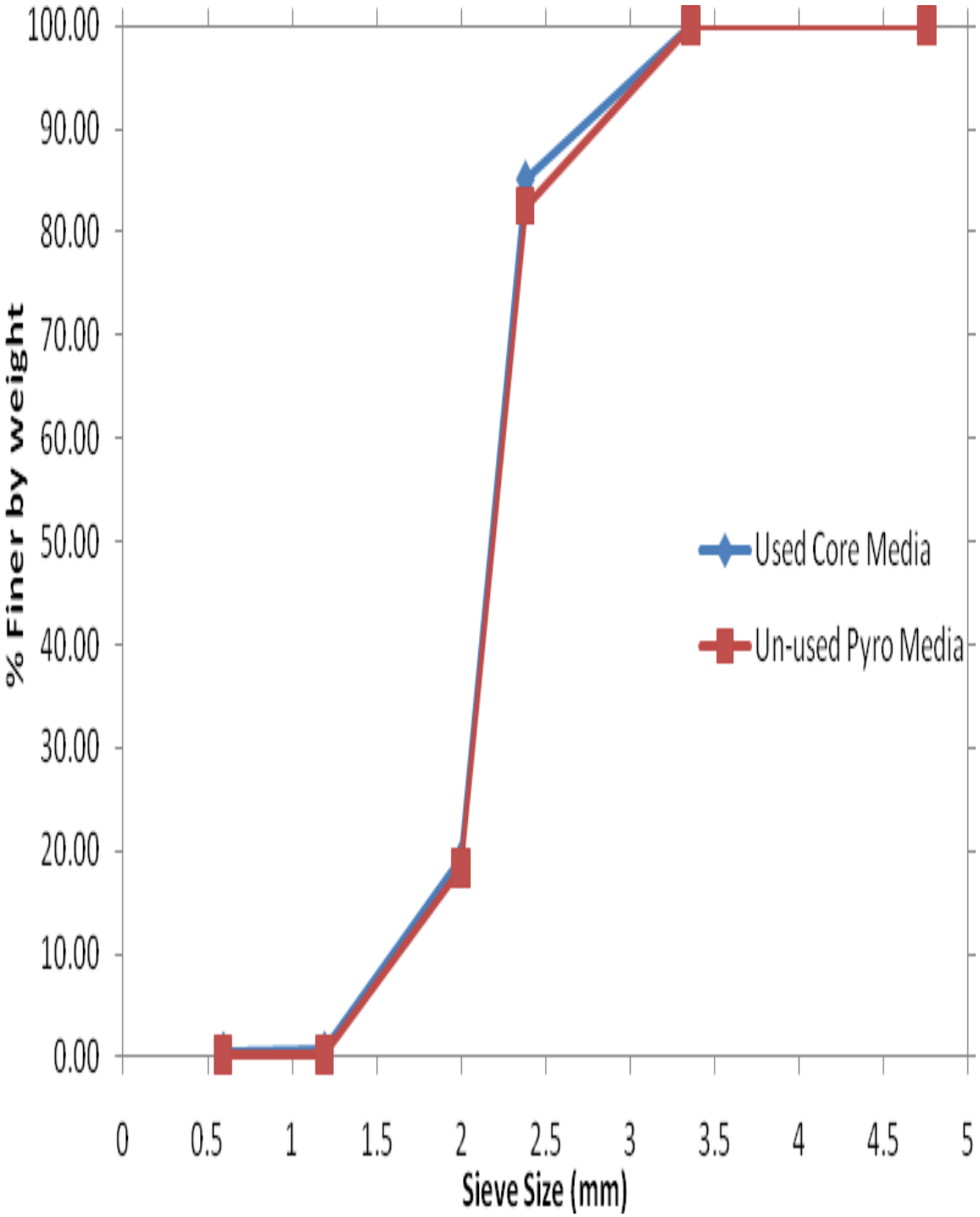

Figure 4.17 Comparative plot of % finer by weight as a function of sieve size for new and used pyrolucite media

the pyrolucite media surface due to the loading of the contactor column at high HLR values for many months in the presence of both soluble Mn and free chlorine which promoted Mn uptake and subsequent $MnO_x(s)$ formation on the media.

In addition it was also noted that the extractable Mn concentrations increased when the contact period of the media in the HAS solution was increased from one to five days. Visual observation of the solution indicated that the pyrolucite media itself was disintegrating over this longer contact period. As such media extraction tests on pyrolucite media should limit the HAS exposure to no more than 4-6 hours at a maximum.

Limitations of Research Study

During the course of this research study one of the challenges encountered was the change in the Mn uptake capacity of the media over time. As discussed earlier in this chapter, a substantial increase in the uptake capacity of the pyrolucite media was noted over time, which was caused most likely due to the generation of additional Mn uptake sites on the media by the deposition of $MnO_x(s)$ coating on the media surface. Backwashing the contactor column did result in some of this coating getting washed away. However, over the period of the pilot-plant study, the backwash cycles were not uniformly regulated, resulting in the time period of operation of the contactor column between any two backwash cycles not being the same. This might have caused varying amounts of $MnO_x(s)$ coating to build up between the backwash cycles.

The amount of $MnO_x(s)$ coating that is present on the media initially is a very important aspect to be considered while modeling data to predict the soluble Mn removal across the contactor column. Hence the general buildup of $MnO_x(s)$ coating on the media surface combined with the varying amounts of $MnO_x(s)$ coating on the pyrolucite media inbetween backwash cycles did pose some challenges while modeling the pilot-plant data. The amount of $MnO_x(s)$ coating on the media surface varying over time resulted in scenarios wherein two sets of pilot-plant data collected under similar operating conditions of temperature, loading rate, pH, initial Mn and free chlorine concentrations could still be different regarding Mn removal owing to the fact that they may vary in terms of the amount of $MnO_x(s)$ coating present on their surfaces at the time the data were collected. This in turn could have some impact on the modeling results. Hence, this could be considered as a limitation of this study. Future research should consider how the $MnO_x(s)$ coating level (and the associated Mn uptake capacity of the media) varies as a function of contactor operating cycle. The model used in the current study would be most applicable to predicting contactor performance with newer media as it would be easier to quantify media Mn uptake capacity (the Freundlich isotherm) with new media. This model would then be a conservative predictor of contactor performance since subsequent $MnO_x(s)$ deposition would only enhance Mn uptake.

CHAPTER 5 CONCLUSIONS

The objectives of this research involved evaluating the contactor concept by studying the impact of the various operational parameters on the soluble Mn performance of the adsorptive contactor and also enhancing the implementation of the model developed by Zuravnsky (2007). Pilot-scale Contactor experiments were conducted at the Lee Hall Water Treatment Plant in Newport News, VA to determine the impact of important operational parameters such as temperature, hydraulic loading rate and pH on overall Mn removal performance. These parameters were tested on a contactor column where the media used was commercially available pyrolucite. The selection of the pyrolucite media was based on Mn removal results obtained from prior research conducted by Zuravnsky (2007) and also due to the commercial availability of the pyrolucite, an important consideration related to future implementation of the process. In addition, the data from the pilot plant acted as input to a first-principles model which was developed to predict the contactor performance for soluble Mn removal under various applied water conditions.

Based upon the results obtained in this research effort, the following conclusions were formulated:

1. Increases in solution pH improved the Mn removal profiles across the pyrolucite media. This observation was in accordance with the results noted by Zuravnsky (2007) and Morgan and Stumm (1964) who saw that alkaline pH conditions promoted Mn adsorption by increasing the amount of available Mn adsorption sites on $MnO_x(s)$.

2. Temperature did not have any significant impact on the overall Mn removal performance of the pyrolucite contactor media though a slight worsening in the Mn uptake was noted at lower temperatures. This is important, as Mn related complaints are typically observed by water treatment utilities more during the summer months when the Mn removal performance of the contactor media was not affected much than in the winter months. In addition, temperature increases resulted in proportionate increases in the soluble Mn uptake capacity of the pyrolucite media (based on short-term media uptake studies).

3. Overall, an increase in HLR had a very slight negative impact on the soluble Mn removal across the contactor column. This observation plays an important role for the commercial implementation of pyrolucite media in an adsorptive contactor and was also in agreement with the findings of Zuravnsky(2007).

4. There was a slight improvement in soluble Mn removal within the contactor when the influent free chlorine concentration was increased from 1.3 mg/L to 5 mg/L. This improvement was felt to be due to enhanced kinetics of Mn oxidation in the pyrolucite surface, thereby increasing the soluble Mn removal (Zuravnsky 2007).

5. For a water temperature of 20^0C, at lower influent free chlorine concentrations (~ 1.3 mg/L) the best-fit k_r values obtained from the model increased with increase

in solution pH. However, at higher free chlorine concentrations (~ 5 mg/L) the best-fit k_r values decreased with increases in solution pH.

6. Head loss accumulation across the contactor column was observed to decrease significantly down the depth of the contactor media. This could be explained by the phenomenon of more soluble Mn uptake being concentrated in the upper portion of the filter bed consisting of a MnOx(s)-coated media (reported by Bouchard (2005) and by Hargette and Knocke (2001)).

   Also, during backwash, substantial amounts of Mn were removed at a loading rate of 80 gpm/ft^2 owing to media expansion whereas hardly any Mn were removed during the sub-fluidization rates of 4, 20 and 40 gpm/ft^2. This indicates that, the Mn uptake taking place on the media surface was causing most of the Mn adsorbed onto the media surface to lump up or "cement" together instead of existing as individual particles.

7. The results from the sieve analysis of the used pyrolucite media indicated that there was no significant shift in the size distribution of the media over time and this was in agreement with the work of Knocke et al. (1990) who reported no significant impacts on the anthracite and sand media size and specific gravity due to MnO_x(s) coatings. This seems to show that over time, the cycle of Mn adsorption and oxidation do not add many layers of MnO_x(s) coating to the filter media grains as expected.

REFERENCES

American Water Works Association (AWWA) Research Foundation and US Environmental Protection Agency (2008). Characterization and Performance of Filter Media for Manganese Control. Colarado, AWWA Research Foundation.

Bouchard, R. (2005). Evaluation of Manganese Removal at Aquarion Water Company (AWC) Surface Water Treatment Plants. Department of Civil & Environmental Engineering. Amherst, MA, University of Massachusetts. M.S. in Env. Eng.: 131.

Coffey, B. M., D. L. Gallagher and W. R. Knocke (1993). Modeling Soluble Manganese Removal by Oxide-coated Filter Media. *Journal of Environmental Engineering,* 119(4):679-695.

Knocke, W. R., J. R. Hamon and C. P. Thompson (1988). Soluble Manganese Removal on Oxide-Coated Filter Media. *Journal of the American Water Works Association,* 80(12):65-70.

Knocke, W. R., R. C. Hoehn and R. L. Sinsabaugh (1987). Using Alternative Oxidants to Remove Dissolved Manganese from Waters Laden with Organics. *Journal of the American Water Works Association,* 79(3):75-79.

Knocke, W. R., S. Occiano and R. Hungate (1990). Removal of Soluble Manganese from Water by Oxide-Coated Filter Media, AWWA Research Foundation.

Knocke, W. R., S. Occiano and R. Hungate (1991). Removal of Soluble Manganese by Oxide-coated Filter Media: Sorption Rate and Removal Mechanism Issues. *Journal of the American Water Works Association,* 83(8):64-69.

Merkle, P. B., W. R. Knocke, D. L. Gallagher and J. C. Little (1997b). Dynamic Model for Soluble Mn2+ Removal by Oxide-Coated Filter Media. *Journal of Environmental Engineering* 123(7):650-658.

Morgan, J. J. and W. Stumm (1964). Colloid-Chemical Properties of Manganese Dioxide. *Journal of Colloid Science,* 19:347-359.

Press, W.H., S. A. Teukolsky, W. T. Vetterling and B. P. Flannery, (2002). Numerical Recipes in C++, The Art of Scientific Computing, 2nd ed. *Cambridge University Press*, Chapter 15.

Roberts, P. V., P. Cornel and R. S. Summers (1985). External Mass-Transfer Rate in Fixed-Bed Adsorption. *Journal of Environmental Engineering,* 11(6):891-905.

Sly, L. I., M. C. Hodgkinson and V. Arunpairojana (1990). Deposition of Manganese in a Drinking Water Distribution System. *Applied and Environmental Microbiology,* 56(3):628-639.

Zuravnsky, L. (2007). Development of Soluble Manganese Sorptive Contactors for Enhancing Potable Water Treatment Practices. Department of Civil & Environmental Engineering. Blacksburg, VA, Virginia Polytechnic Institute and State University. M.S. in Env. Eng.

APPENDIX

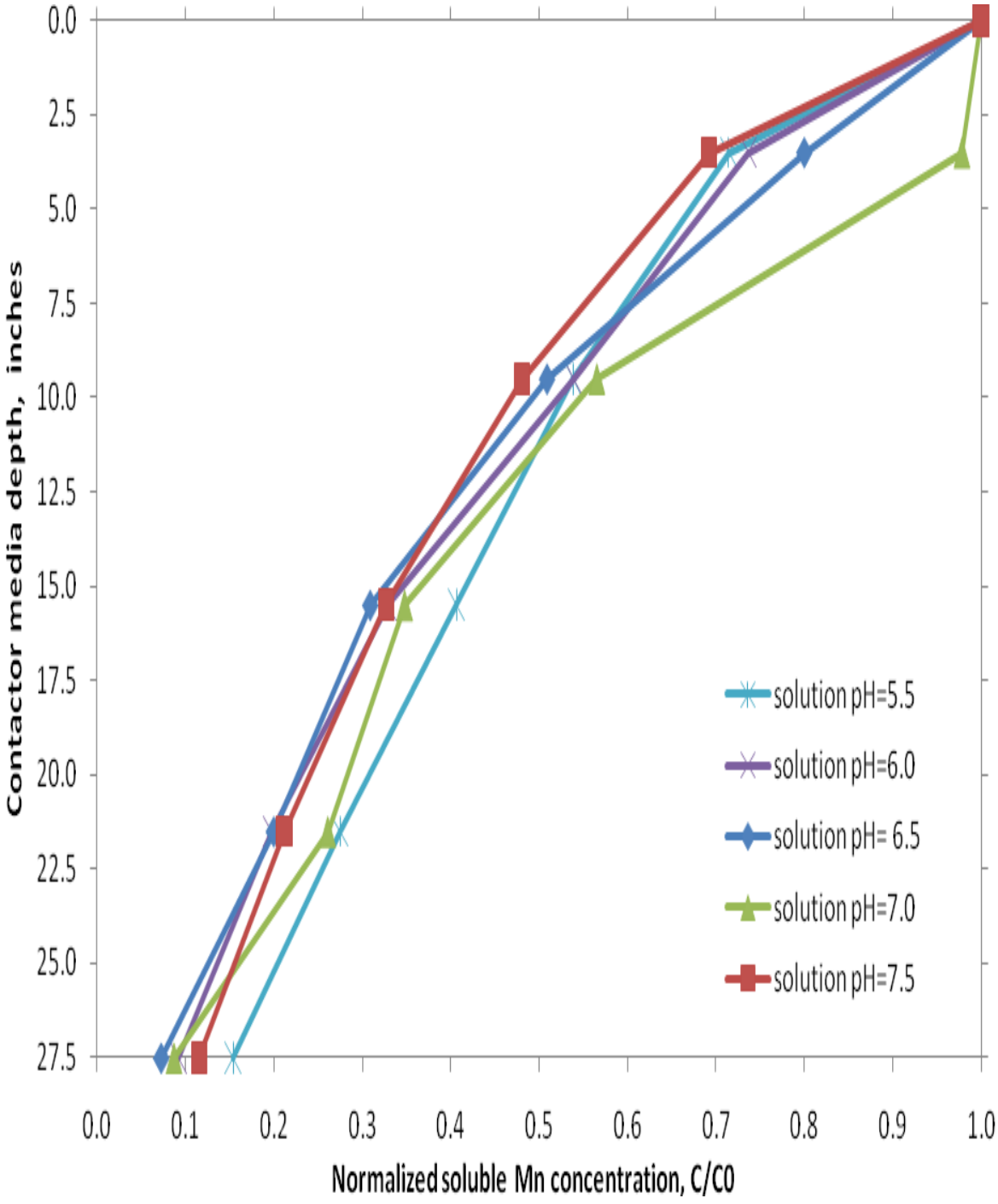

Figure A.1 Effect of pH on soluble Mn Uptake in contactor in terms of normalized Mn concentration, C/C_0

[Influent water: Mn^{2+} = 0.05-0.09 mg/L, Temp=30^0C, HLR = 16 gpm/ft^2, free chlorine conc = 1.3-1.4 mg/L]

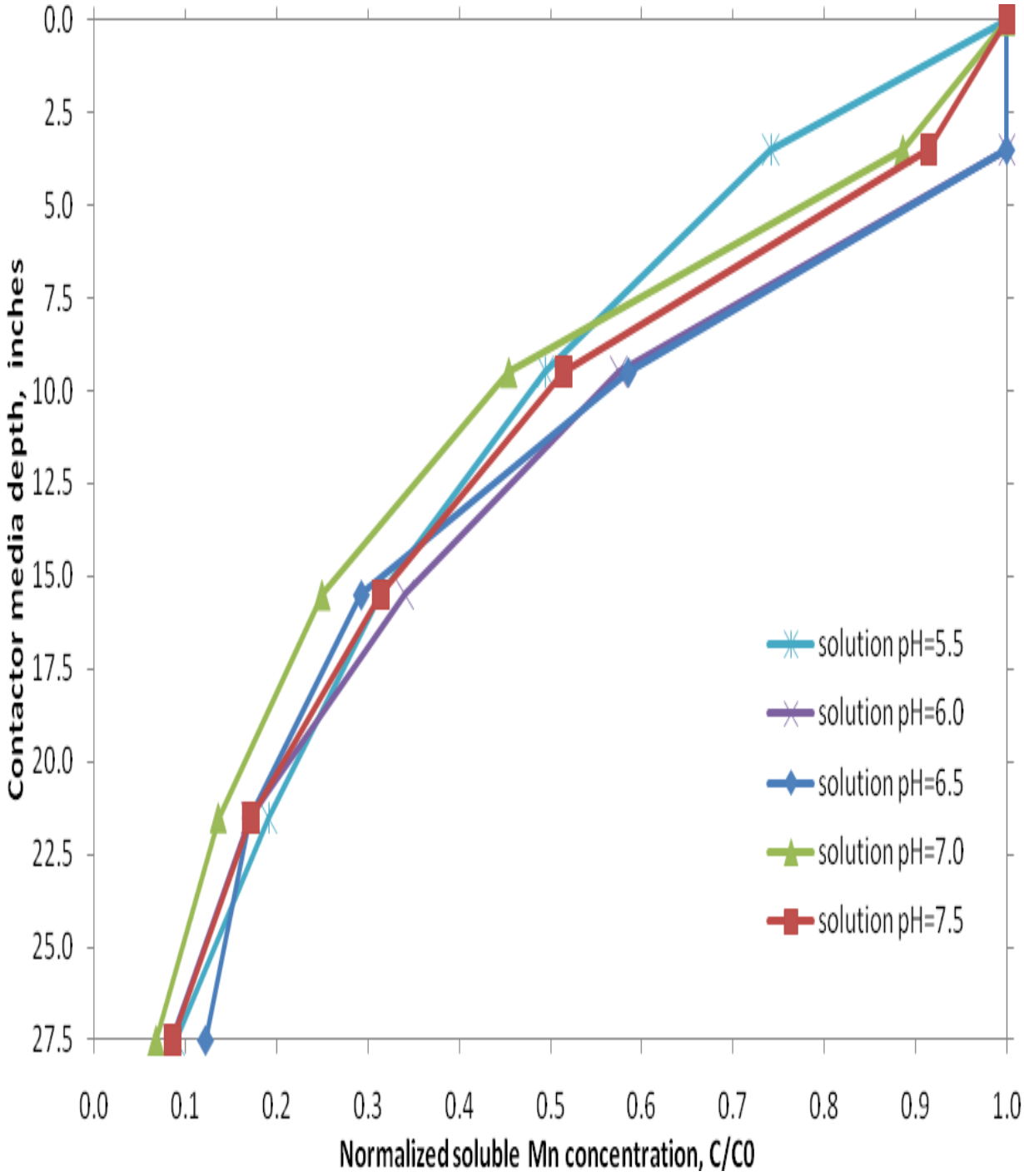

Figure A.2 Effect of pH on soluble Mn Uptake in contactor in terms of normalized Mn concentration, C/C_0

[Influent water: Mn^{2+} = 0.04-0.09 mg/L, Temp=30^0C, HLR = 20 gpm/ft^2, free chlorine conc = 1.2-1.4 mg/L]

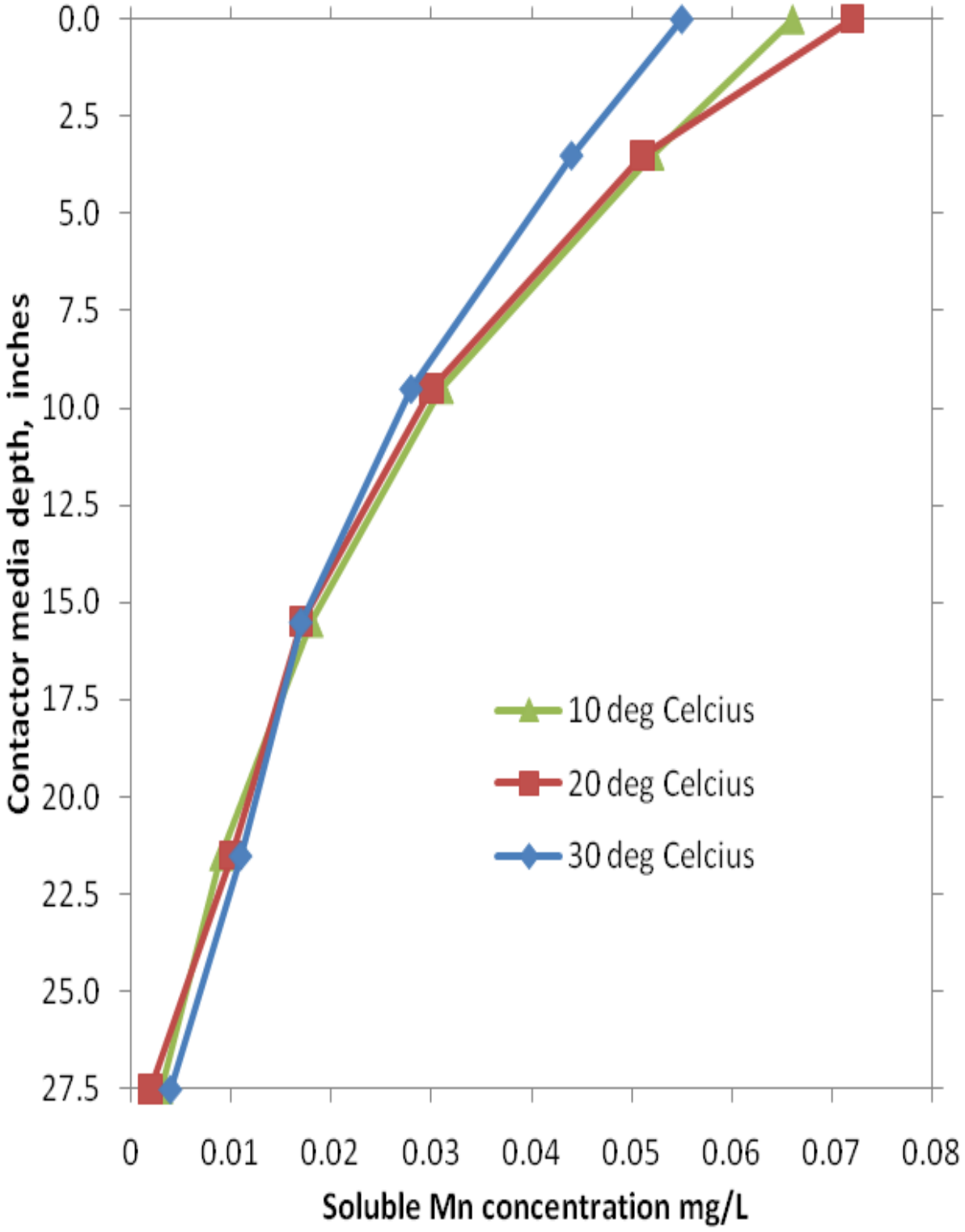

Figure A.3 Effect of Temperature on soluble Mn Uptake in contactor column

[Influent water: Mn^{2+} = 0.05-0.07 mg/L, pH = 6.5, HLR = 16 gpm/ft^2, free chlorine conc = 1.1-1.3 mg/L]

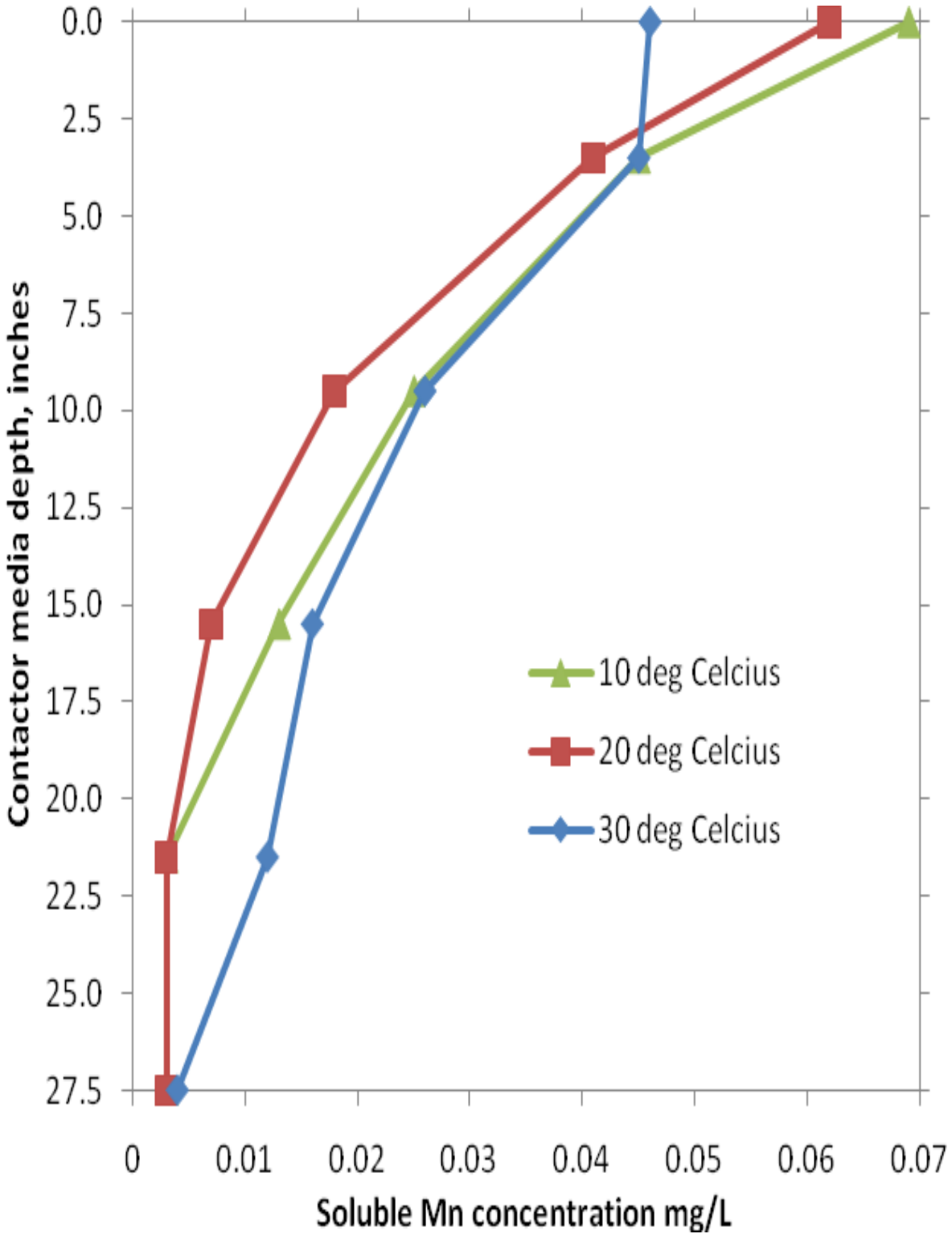

Figure A.4 Effect of Temperature on soluble Mn Uptake in contactor column

[Influent water: Mn^{2+} = 0.075-0.079 mg/L, pH = 7.0, HLR = 16 gpm/ft^2, free chlorine conc = 1.2-1.3 mg/L]

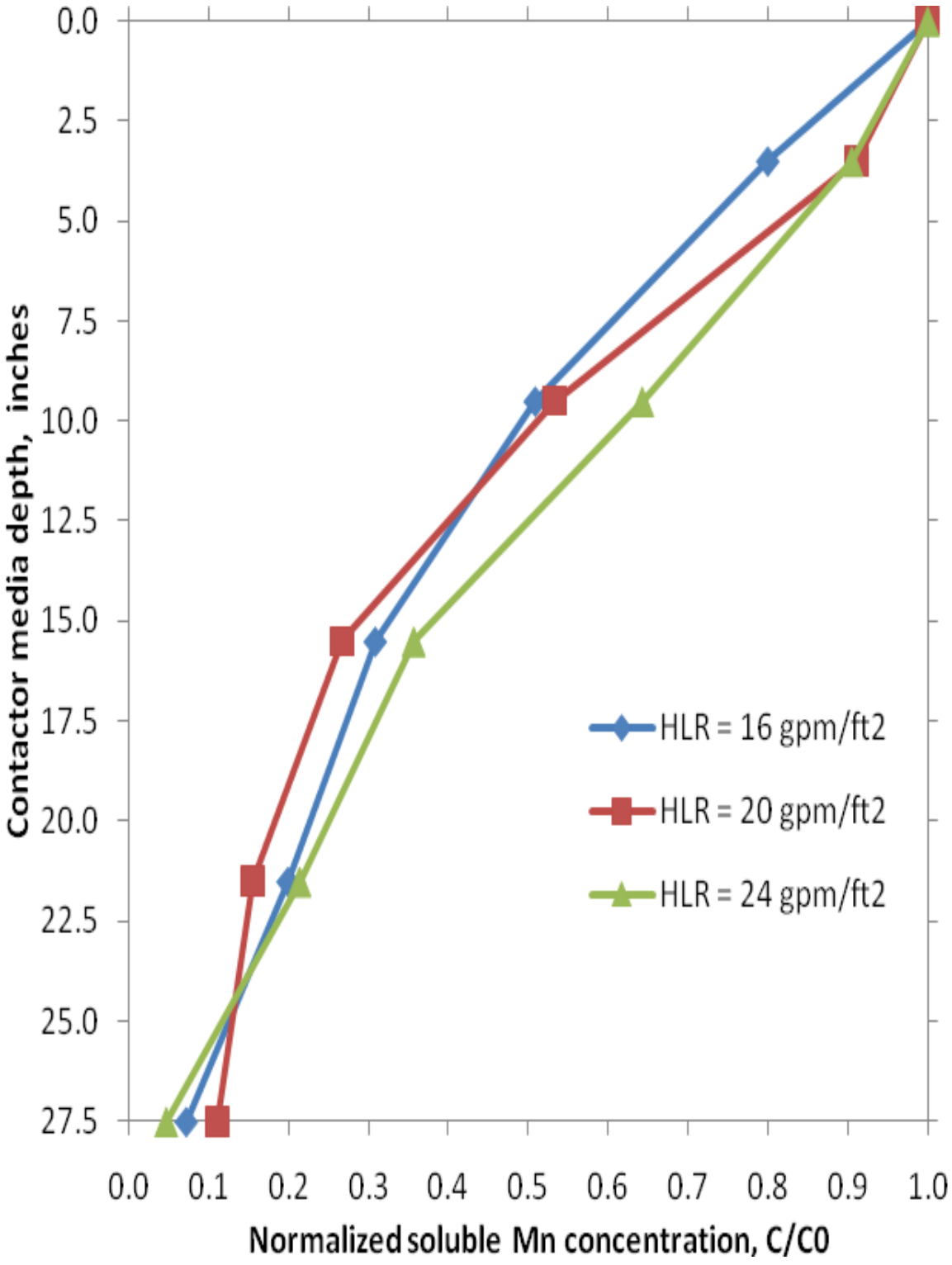

Figure A.5 Effect of HLR on Mn Uptake in contactor in terms of normalized Mn concentration, C/C_0

[Influent water: Mn^{2+}= 0.04-0.06 mg/L, pH = 6.5, Temp = 30^0C, free chlorine conc = 1.2-1.3 mg/L]

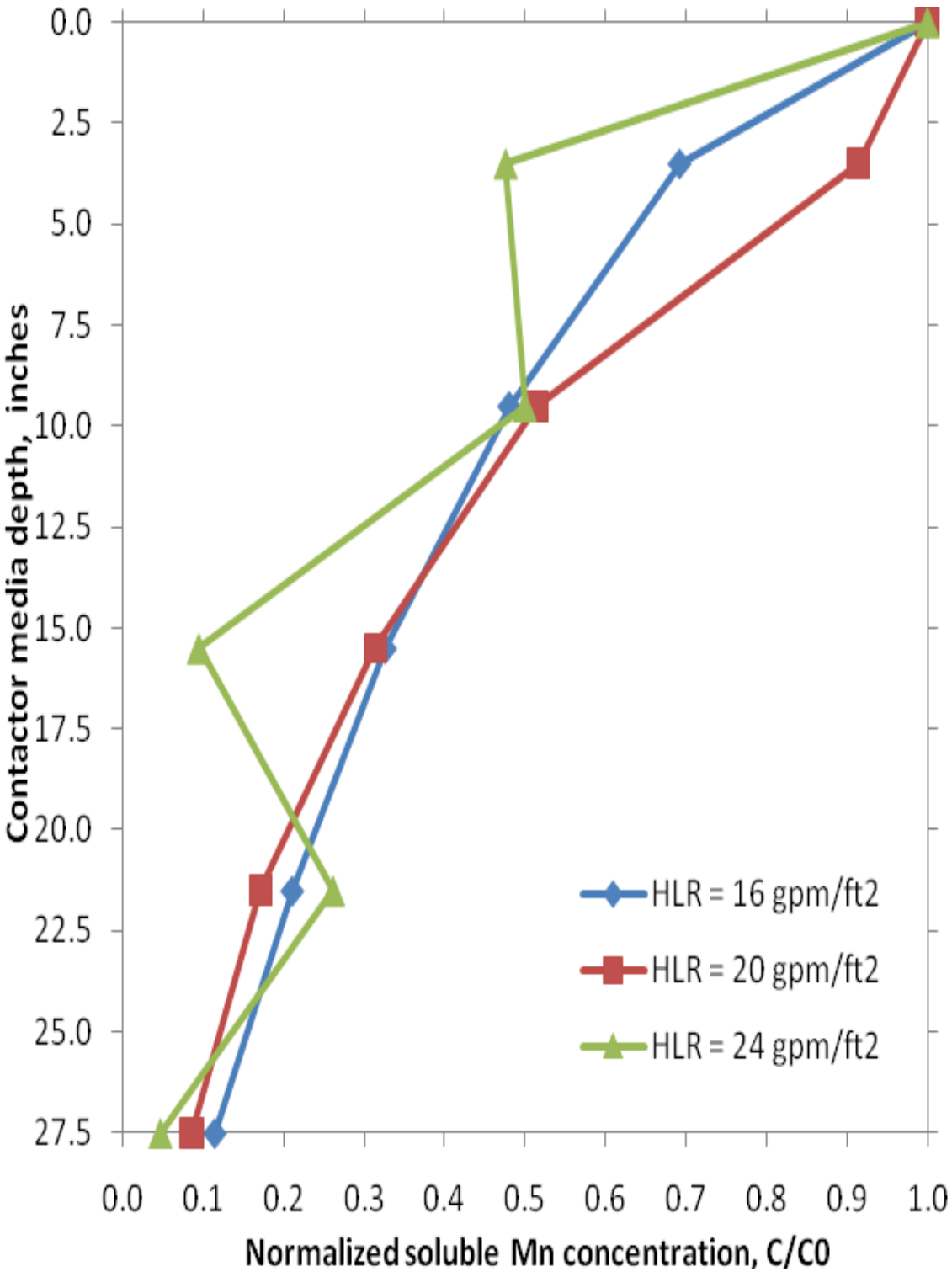

Figure A.6 Effect of HLR on Mn Uptake in contactor in terms of normalized Mn concentration, C/C_0

[Influent water: Mn^{2+}= 0.03-0.05 mg/L, pH = 7.5, Temp = 30^0C, free chlorine conc = 1.2-1.3 mg/L]

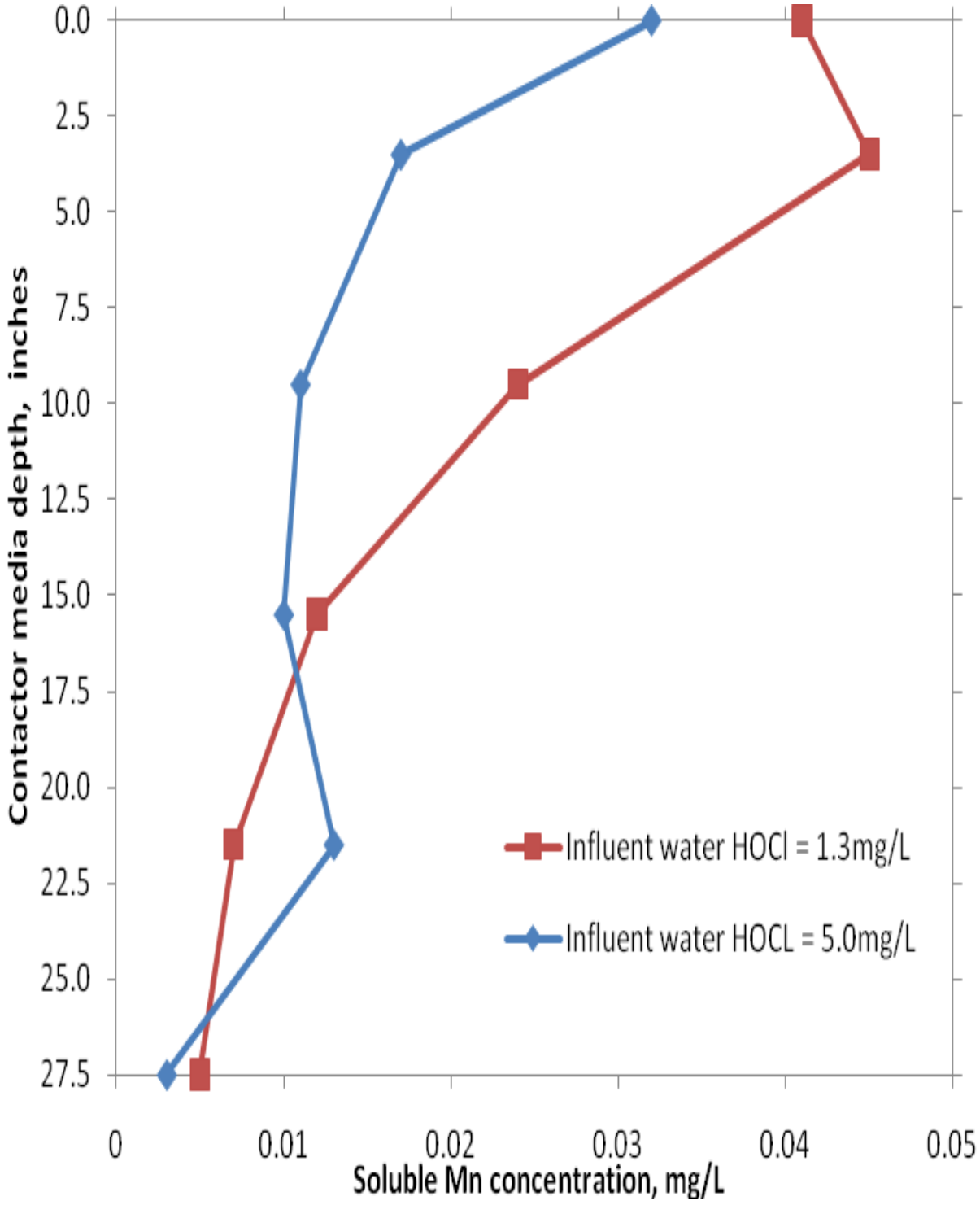

Figure A.7 Effect of free chlorine concentration on Mn Uptake in contactor in terms of normalized Mn concentration, C/C_0

[Influent water: Mn^{2+}= 0.03-0.04 mg/L, pH = 6.5, Temp = 30^0C, HLR = 20 gpm/ft^2]

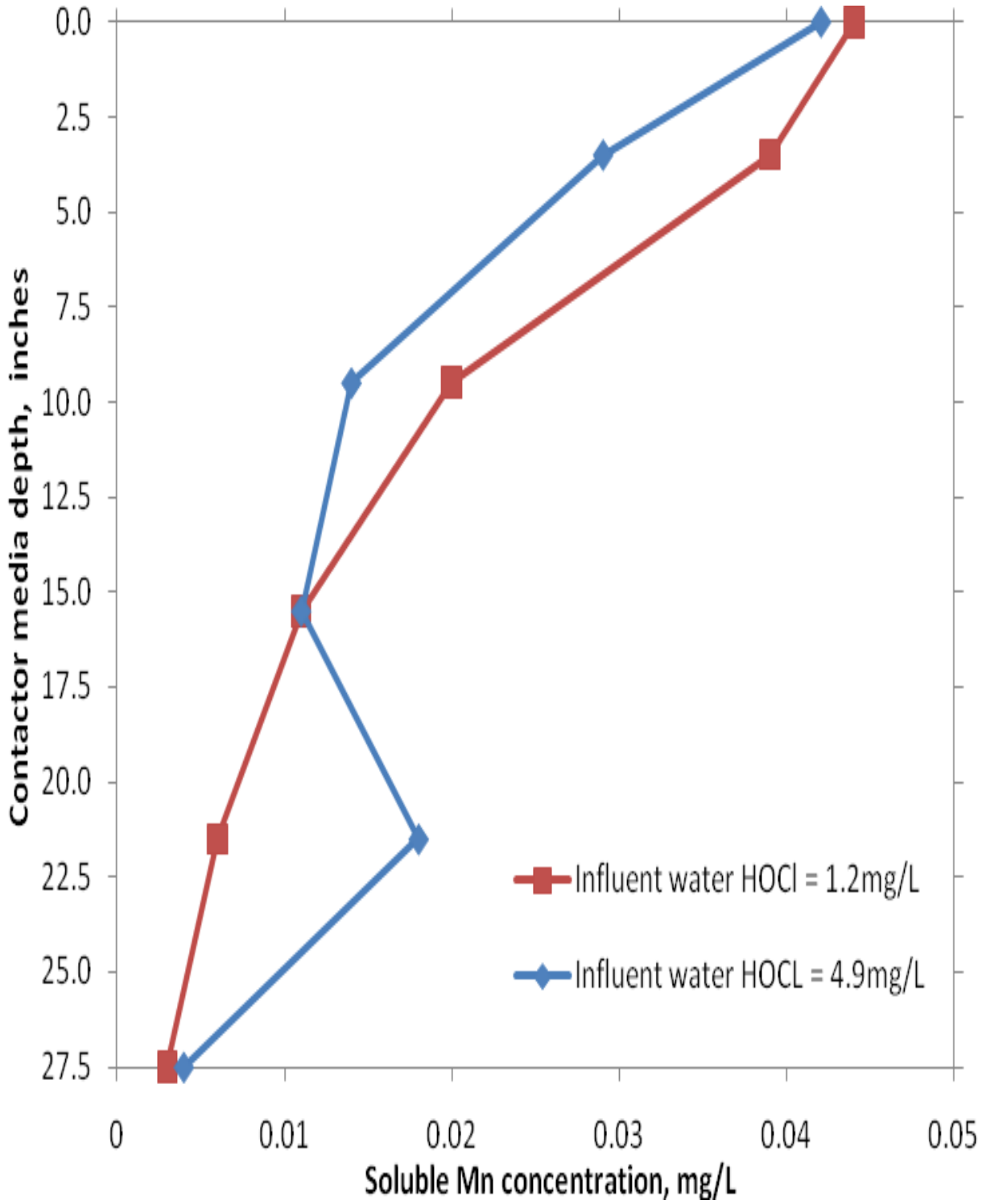

Figure A.8 Effect of free chlorine concentration on Mn Uptake in contactor in terms of normalized Mn concentration, C/C_0

[Influent water: Mn^{2+}= 0.04 mg/L, pH = 7.0, Temp = 30^0C, HLR = 20 gpm/ft^2]

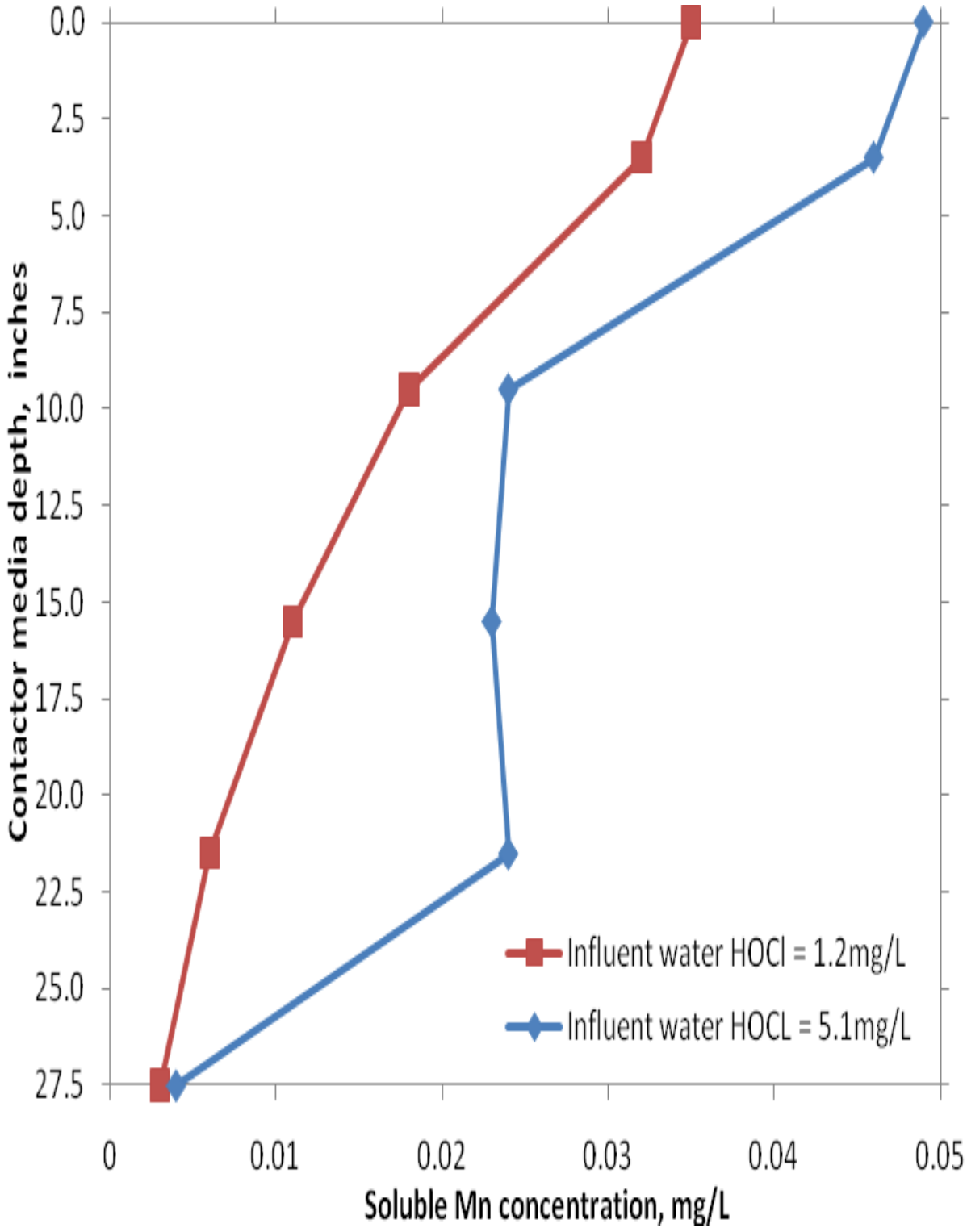

Figure A.9 Effect of free chlorine concentration on Mn Uptake in contactor in terms of normalized Mn concentration, C/C_0

[Influent water: Mn^{2+}= 0.03-0.05 mg/L, pH = 7.5, Temp = 30^0C, HLR = 20 gpm/ft^2]

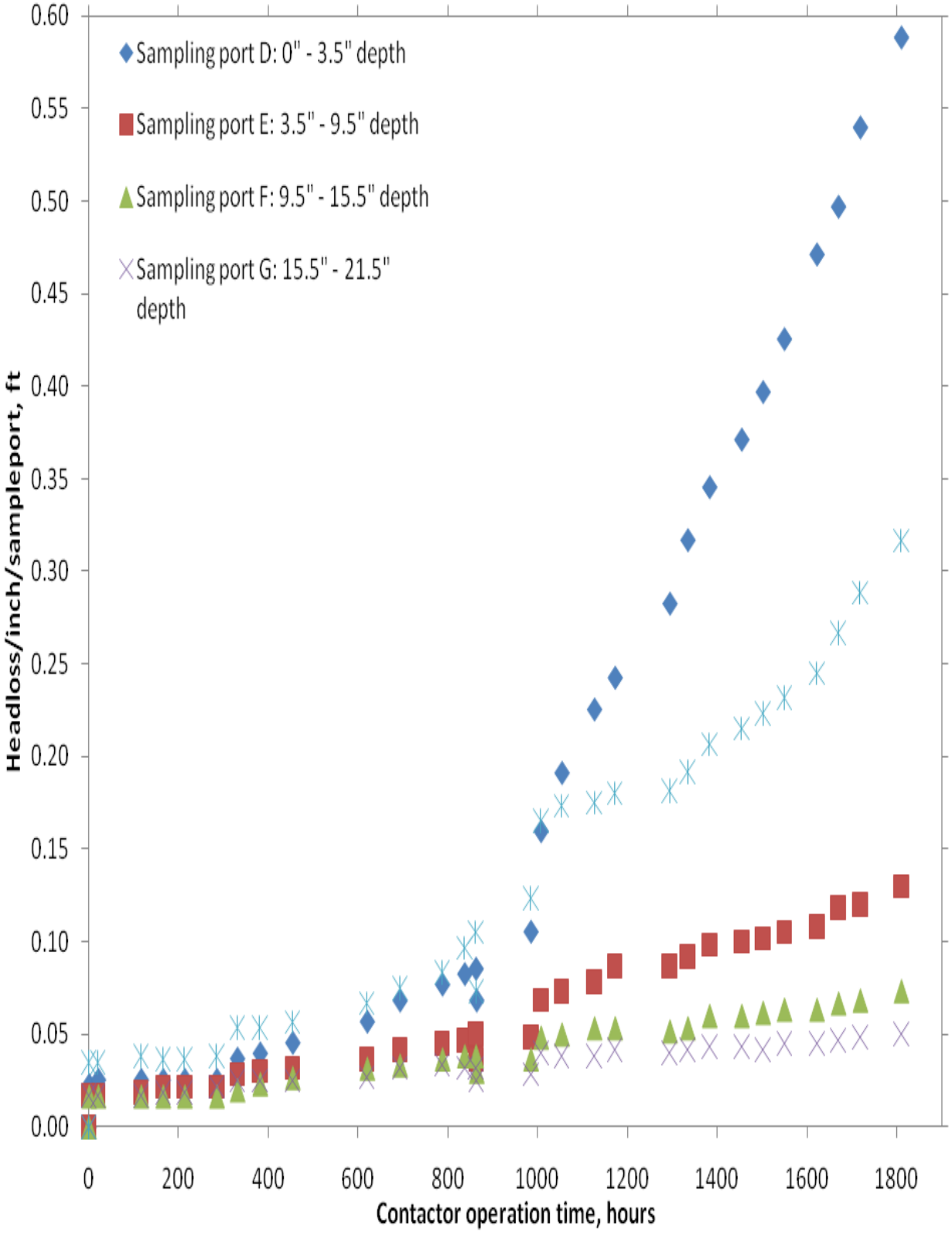

Figure A.10 Normalized headloss accumulation in contactor column as a function of the time period for which contactor was operated